

STABILITY AND THERMAL CONDUCTIVITY OF LOW
CONCENTRATION TITANIA NANOFLUIDS

AZADEH GHADIMI

THESIS SUBMITTED IN FULFILMENT OF THE REQUIREMENTS
FOR THE DEGREE OF DOCTOR OF PHILOSOPHY

FACULTY OF ENGINEERING
UNIVERSITY OF MALAYA
KUALA LUMPUR
2013

UNIVERSITY MALAYA
ORIGINAL LITERARY WORK DECLARATION

Name of Candidate: Azadeh Ghadimi

Registration/Matric No: KHA080060

Name of Degree: Doctor of Philosophy

Title of Project Paper/ Research Report/ Dissertation/ Thesis:

Stability and thermal conductivity of low concentration titania nanofluids

Field of Study: Mechanical Engineering

I do solemnly and sincerely declare that:

- (1) I am the sole author/writer of this Work;
- (2) This work is original;
- (3) Any use of any work in which copyright exists was done by way of fair dealing and for permitted purpose and any excerpt from, or reference to or reproduction of any copyright work has been disclose expressly and sufficiently and the title of the Work and its authorship have been acknowledge in this Work;
- (4) I do not have any actual knowledge nor do I ought reasonably to know that the making of this work constitutes an infringement of any copyright work;
- (5) I hereby assign all and every rights in the copyright to this work to the University of Malaya, who henceforth shall be owner of the copyright in this work and that any written consent of UM having been first had and obtained;
- (6) I am fully aware that if in the course of making this work I have infringed any copyright whether intentionally or otherwise, I am be subject to legal action or any other action as may be determined by UM.

Candidate's Signature

Date

Subscribed and solemnly declared before,

Witness's Signature

Date

Name:

Designation:

Abstract

Nanofluid as a new engineering medium is proved to be potential in many cooling processes in engineering applications. Nanofluid is prepared by dispersing nanoparticles or nanotubes in a host fluid. In this research, the “stability of nanofluids” is discussed as it has a major role in heat transfer enhancement for further possible applications. It also represents general stabilization methods as well as various types of instruments for stability inspection. Characterization, analytical models and measurement techniques of nanofluids after preparation by two-step method are studied.

Low concentration TiO_2 /Water nanofluid was prepared by Two-step method with the stability aiding tools of sodium Dodecyl Sulfate (SDS) as anionic surfactant, pH control and ultrasonic processes. The stability of prepared nanofluids was verified by TEM, UV-vis spectrophotometer, Dynamic Light Scattering (DLS), Zeta potential, sedimentation balance method and photo capturing. In addition, characteristic measurements including thermal conductivity were carried out to consider the effect of stability on enhancement of heat transfer.

The results showed that SDS addition to the nanosuspension will increasingly improve the stability of titania nanosuspension specifically for long term applications. The sedimentation rate decreases with the aid of ultrasonic processes.

Central composite design (CCD) and Box Behnken design (BBD) along with response surface method (RSM) were applied to model and optimize the stability of operating variables viz. SDS correspondingly. The stability and characteristics parameters were optimized by the statistical software of Design Expert (v.8). The appropriate measurement time for clear detection of the stability by UV-vis spectrophotometer were investigated in the intervals of one day, two days, one week and one month after preparation. The obtained results revealed that after one day this inspection is not convincing for stability measurement. It was found that homogeneous

nanosuspension for long term application located at surfactant loading equal to twice the amount of nanoparticle loading (0.09%wt.) for fully covering the particles at low pH value (=10).

Meanwhile, the nanofluid characteristic (thermal conductivity) was evaluated in accordance with stability measurement. Quadratic models have been developed for the four responses (zeta potential, particle size, UV absorption and thermal conductivity) indicated the optimum conditions is SDS dosage of 0.04%wt. at pH value of 11.4. The study demonstrated that high thermal conductivity obtained with almost stable nanofluid in low SDS concentration and high pH value. Besides, large particle size in the optimum point demonstrated that clustering theory could be the main reason to this phenomenon.

The influence of horn ultrasonic duration and power were studied by volume concentration increment. The results revealed that the optimum point which was evaluated by extra runs confirmed that the amplitude of 75% for ultrasonic horn, duration of 20 minutes and nanoparticle loading of 0.86 %vol. is the best combination of factors to reach the stable and high thermally conductive fluid.

In this thesis, the major factor for thermal conductivity enhancement in nanofluids was known as the formations of nano-clusters. Therefore, by optimizing the combination of factors with Design of Experiment software in nanofluid preparation, it is expected to provide better cooling solution than the conventional cooling fluids.

Abstrak

Nanofluid sebagai medium kejuruteraan baru dibuktikan untuk menjadi potensi dalam banyak proses penyejukan dalam aplikasi kejuruteraan. Nanofluid disediakan oleh bersurai nanopartikel atau nanotube di dalam bendalir pelbagai. Dalam kajian ini, "kestabilan nanofluids" dibincangkan kerana ia mempunyai peranan utama dalam peningkatan pemindahan haba bagi permohonan selanjutnya mungkin. Ia juga merupakan kaedah penstabilan umum serta pelbagai jenis instrumen untuk pemeriksaan kestabilan. Pencirian, model analitikal dan teknik pengukuran nanofluids selepas penyediaan dengan kaedah dua langkah dikaji.

Rendah kepekatan TiO_2 /Water nanofluid telah disediakan oleh kaedah Dua-langkah dengan kestabilan membantu alat natrium Dodecyl Sulfat (SDS) sebagai surfactant anionik, kawalan pH dan proses ultrasonik. Kestabilan nanofluids disediakan telah disahkan oleh TEM, UV-vis spectrophotometer, penyebaran Cahaya Dinamik (DLS), potensi Zeta, pemendapan kaedah kunci kira dan menangkap gambar. Di samping itu, pengukuran ciri-ciri termasuk kekonduksian terma dan kelikatan telah dijalankan untuk mempertimbangkan kesan kestabilan kepada peningkatan pemindahan haba.

Keputusan menunjukkan bahawa samping SDS untuk nanosuspension yang akan semakin meningkatkan kestabilan nanosuspension titania khusus untuk aplikasi jangka panjang. Kadar pemendapan berkurangan dengan bantuan proses ultrasonik.

Reka bentuk komposit Pusat (CCD) dan Box Behnken reka bentuk (BBD) bersama-sama dengan kaedah permukaan sambutan (RSM) telah digunakan untuk model dan mengoptimumkan kestabilan pembolehubah iaitu operasi. SDS sepadan. Parameter dan ciri-ciri kestabilan telah dioptimumkan oleh perisian statistik Pakar Rekabentuk (v.8). Masa pengukuran yang sesuai untuk pengesanan jelas kestabilan dengan spektrofotometer UV-vis telah disiasat di selang satu hari, dua hari, satu minggu

dan satu bulan selepas penyediaan. Keputusan yang diperolehi menunjukkan bahawa selepas satu hari pemeriksaan ini tidak meyakinkan untuk pengukuran kestabilan. Ia telah mendapati bahawa nanosuspension homogen untuk aplikasi jangka panjang terletak di loading surfactant bersamaan dengan dua kali ganda jumlah muatan nanopartikel (0.09% berat) untuk meliputi sepenuhnya zarah pada nilai pH yang rendah ($= 10$).

Sementara itu, ciri-ciri nanofluid (keberaliran haba) telah dinilai selaras dengan ukuran kestabilan. Kuadratik model telah dibangunkan untuk empat jawapan (zeta potensi, saiz zarah, penyerapan UV dan keberaliran haba) menunjukkan keadaan optimum adalah SDS dos 0.04% wt. pada nilai pH 11.4. Kajian ini menunjukkan bahawa kekonduksian haba yang tinggi diperolehi dengan nanofluid hampir stabil dalam kepekatan SDS yang rendah dan nilai pH yang tinggi. Selain itu, saiz zarah yang besar di titik optimum menunjukkan bahawa teori kelompok boleh menjadi sebab utama kepada fenomena ini.

Pengaruh tempoh tanduk ultrasonik dan kuasa telah dikaji oleh kepekatan jumlah kenaikan. Keputusan menunjukkan bahawa titik optimum yang telah dinilai oleh berjalan tambahan mengesahkan bahawa amplitud 75% untuk tanduk ultrasonik, tempoh 20 minit dan loading nanopartikel 0.86% vol. adalah kombinasi yang terbaik faktor untuk mencapai cecair yang stabil dan tinggi haba konduktif.

Dalam tesis ini, faktor utama bagi peningkatan kekonduksian terma dalam nanofluids dikenali sebagai pembentukan kelompok nano. Oleh itu, dengan mengoptimumkan gabungan faktor dengan Rekabentuk Eksperimen perisian dalam penyediaan nanofluid, ia dijangka untuk menyediakan penyelesaian yang lebih baik penyejukan daripada cecair penyejukan konvensional.

Acknowledgements

I would like to express my sincere gratitude to my supervisor Dr. Henk Metselaar for his guidance, encouragement and financial support throughout my work.

My special thanks to Babak Lotfizadeh Dehkordi for his kind cooperation along the project.

I am grateful to my friends, Masoud Kamali and Dr. Amir Hossein Afshari for helping me in editing thesis.

I wish to avail myself of this opportunity, express a sense of gratitude and love to my beloved parents for their manual support, strength, and help.

I am forever indebted to my husband and son (Danial) for their understanding, endless patience and encouragement when it was most required.

Also my sincere thanks go to the Energy Lab for their generosity in offering me the opportunity to use their equipment, in order to achieve the goals of my study.

I wish to acknowledge the Ministry of Higher Education of Malaysia and the University of Malaya, Kuala Lumpur, Malaysia for the financial support under UM.C/HIR/MOHE/ENG/21 (D000021-16001), UM.C/241/9 and also UM.TNC2/IPPP/UPGP/Geran (PPP)/PV005/2011B.

Table of content

Abstract	iii
Acknowledgements	vii
List of Figures	xiii
List of Tables.....	xviii
List of Symbols and Abbreviations	xx
Chapter 1: Introduction	2
1.1 Background	2
1.2 Statement of Research Objectives.....	4
1.3 Structure of thesis.....	5
Chapter 2: Literature review	7
2.1 Introduction	7
2.2 Nanofluid preparation methods.....	8
2.2.1 Two step technique	9
2.2.2 Single step technique.....	10
2.3 Importance of the stability of nanofluid.....	11
2.3.1 Surfactant or activator adding	13
2.3.2 pH control (surface chemical effect).....	15
2.3.3 Ultrasonic vibration.....	18
2.4 Stability inspection instruments	21
2.4.1 UV–vis spectrophotometer	22
2.4.2 Zeta potential test	24
2.4.3 Sediment photograph capturing	25
2.4.4 TEM (Transmission Electron Microscope) and SEM (Scanning Electron Microscope).....	26
2.4.5 Light scattering method.....	30

2.4.6	Sedimentation balance method	30
2.4.7	Three omega method.....	30
2.5	Characteristic measurements.....	30
2.5.1	Thermal conductivity	31
	Analytical model	37
	Measurement apparatus.....	39
2.6	Statistical software for optimization	42
2.6.1	Screening.....	42
2.6.2	Factorial.....	43
2.6.3	Response surface methodology (RSM).....	43
2.6.3.1	Central composite design (CCD)	44
2.6.3.2	Box-Behnken Design (BBD)	44
2.7	Summary	46
	Chapter 3: Methodology	50
3.1	Introduction	50
3.2	Materials.....	52
3.3	Applied apparatus.....	55
3.4	General Samples preparation	56
3.4.1	Absorbance measurement by UV-vis spectrophotometer.....	56
3.4.2	Zeta potential and particle size measurement	58
3.4.3	Sedimentation balance method and photo capturing techniques	58
3.4.4	TEM sample preparation method.....	58
3.5	Thermophysical properties.....	59
3.5.1	Thermal conductivity relations and calibration.....	59
3.6	Design of Experiment (DOE)	60
3.6.1	Data analysis	60

Chapter 4: Results and discussion.....	64
4.1 Effect of homogenization process on thermal conductivity and stability of low concentration titania nanofluid	64
4.1.1 Preliminary studies.....	64
4.1.1.1 The influence of surfactant addition on stability of titania nanofluid.....	64
4.1.1.2 The influence of surfactant and horn ultrasonic on the stability of titania nanofluid	65
4.1.1.3 The influence of surfactant and ultrasonic bath on stability of titania nanofluid	67
4.1.2 Monitoring results	69
4.1.2.1 TEM images	69
4.1.2.2 Sedimentation rate by UV-vis spectrophotometer	71
4.1.2.3 Particle size, zeta potential, thermal conductivity results	73
4.2 Effect of elapsed timing in stability measurement by UV-vis spectrophotometer.....	75
4.2.1 Central Composite Design (CCD)	75
4.2.2 Statistical Analysis	76
4.2.3 Graph Analysis.....	79
4.2.4 Optimization.....	81
4.2.4.1 Point Prediction Evaluation.....	83
4.3 Experimental design and optimization for the effect of pH value and surfactant concentration on the stability and thermal conductivity of titania nanofluid	84
4.3.1 Data analysis of the effect of pH control and surfactant addition on the stability and thermal conductivity.....	85

4.3.2	Influence of the parameters on responses	90
4.3.3	Nanofluid optimization for thermal conductivity, UV absorbance, zeta potential and particle size responses	93
4.3.3.1	Point Prediction Evaluation.....	96
4.4	Effect of nanoparticle volume concentration, duration and power of ultrasonic on the stability and thermal conductivity of nanofluid by Box Behnken method ...	96
4.4.1	Experimental design and statistical analysis	97
4.4.1.1	Thermal conductivity enhancement and stability evaluation by means of UV-vis spectrophotometer at short term and long term application.....	98
4.4.1.2	The influence of dispersion method on viscosity, thermal conductivity and stability by mean of zeta potential.....	104
4.4.1.3	Stability evaluation by sedimentation balance method at intervals of two days, one week and one month	110
4.4.2	Optimization.....	118
4.5	Comparison of thermal conductivity results	120
Chapter five: Conclusion.....		123
5-1	The influence of homogenization methods on stability and thermal conductivity of titania nanofluid.....	123
5.2	Suitability of UV-vis spectrophotometer for measuring stability in short and long term	124
5.3	The importance of nanofluid stability by means of zeta potential, UV absorbance and particle size on thermal conductivity enhancement of nanofluid.	124
5.4	The influence of nanoparticle volume concentration, duration and power of ultrasonic on the stability and thermal conductivity of nanofluid	125
5-5	Future works and recommendations	127
Appendix A		128

References	131
------------------	-----

List of Figures

Figure 2- 1	Ultrasonic-aided submerged arc nanoparticle synthesis system to produce TiO ₂ nanofluid (Chang, H. et al., 2007).....	11
Figure 2- 2	Schematic diagram of the high-pressure homogenizer for producing nanofluids (Chang, H. et al., 2007)	14
Figure 2- 3	Particle size distributions of nano-suspensions. (a) Al ₂ O ₃ –H ₂ O without SDBS, (b) Al ₂ O ₃ –H ₂ O with SDBS, (c) Cu–H ₂ O without SDBS and (d) Cu–H ₂ O with SDBS Concentration of nanoparticles and SDBS surfactant are 0.05% weight fraction, respectively (Wang, X.-j. et al., 2009)	14
Figure 2- 4	The interaction potentials at various pHs as a function of interparticle distance (Lee, D. et al., 2006)	18
Figure 2- 5	Variation of the nanofluids viscosity with pH and nanoparticles weight fraction at temperature 303 K: (a) the variation of the viscosity with pH, (b) the variation of the viscosity with nanoparticles concentration, (c) the sediment photograph of Al ₂ O ₃ -H ₂ O suspensions after depositing for seven days, (d) the sediment photograph of Cu-H ₂ O suspensions after depositing for seven days (Wang, H. & Sen, M., 2008) ..	25
Figure 2- 6	Octahedral-Cu ₂ O nanofluids 24 h after their preparation (CuSO ₄ molar concentration from 0.0025 mol/L to 0.002 mol/L)(Wei, X. et al., 2009)	26
Figure 2- 7	Spherical-Cu ₂ O nanofluids 24 h after their preparation (CuSO ₄ molar concentration from 0.01 mol/L to 0.05 mol/L)(Wei, X. et al., 2009)	26
Figure 2- 8	TEM pictures of (left) Cu nanofluids , (middle) CuO nanoparticles and (right) alkanethiol terminated AuPd colloidal particles (Kebblinski, P. et al., 2005).....	27
Figure 2- 9	SEM of carbon nanotube a) single-walled carbon nanotubes obtained by arc discharge and (b) multiwalled carbon nanotubes obtained by chemical vapor deposition growth (Kebblinski, P. et al., 2005).....	27

Figure 2- 10	TEM micrograph of nanoparticles (a) nano-alumina (b) nano-copper (Wang, X.-j. et al., 2009)	28
Figure 2- 11	TEM micrographs of ZnO aggregates prepared by two different methods as mixed suspensions (a, c) and the same suspensions ultrasonically agitated for 60 min (b,d) (Chung, S. J. et al., 2009)	28
Figure 2- 12	TEM image of dispersed TiO ₂ nanoparticles in water	29
Figure 2- 13	TEM photographs of Au, Al ₂ O ₃ , TiO ₂ and CuO particles and carbon nanofibers (Zhang, X. et al., 2007)	29
Figure 2- 14	Aggregation effect on the effective thermal conductivity (Wen, D. et al., 2009)	35
Figure 2- 15	Schematic modeling of a homogeneous suspension containing spherical mono-sized particle with resistance model (Meibodi, M. E. et al., 2010b)	39
Figure 2- 16	Three-factor full factorial design with center point	43
Figure 2- 17	Graphic representations of central composite, face-centered cube and Box–Behnken designs	45
Figure 3- 1	Schematic of well-dispersed aggregates (Prasher, Ravi et al., 2006)	52
Figure 3- 2	XRD of titanium (IV) oxide	53
Figure 3- 3	Adjusting of ξ –potential with pH for titania nanofluid (Penkavova, V. et al., 2011b)	54
Figure 3- 4	UV-vis spectrophotometer for TiO ₂ nanofluid with 25 nm average diameter	57
Figure 3- 5	Calibration curve at wavelength of 320 nm for titanium dioxide nanofluid (A.Ghadimi & Metselaar, H. S. C., 2011)	58
Figure 4- 1	Sedimentation rate of TiO ₂ /water nanofluid after one week without any ultrasonication: a) fresh low concentration of TiO ₂ nanofluid; b) same concentration as (a) with SDS; c) same suspension without SDS	65

Figure 4- 2	Particle size distribution by different horn ultrasonic processor timing (a)- without ultrasonic processing: (b)- after 6 min ultrasonic processing (c)- after 10 min ultrasonic processing (d)- after 15 min ultrasonic processing	66
Figure 4- 3	UV-vis spectrophotometer evaluation of ultrasonic process on the absorbance of TiO ₂ nanofluid (a),(b) and (c) 0.007%wt., 0.01%wt. and 0.012%wt. respectively before ultrasonication; (d),(e) and (f) 0.007%wt., 0.01%wt. and 0.012%wt. respectively after 15 minutes ultrasonic process.....	66
Figure 4- 4	Photo capturing of the effect of surfactant and horn ultrasonic on TiO ₂ nanofluid at five days after preparation; A) with surfactant without ultrasonic process, B) with surfactant and 15 minutes horn ultrasonic, C) without SDS with 15 minutes horn ultrasonic, D) without surfactant and ultrasonic process.....	67
Figure 4- 5	UV-vis spectrophotometer evaluation of titania nanofluid after one, two and three hours of ultrasonic bath	68
Figure 4- 6	The effect of three hours ultrasonic bath and surfactant addition on 0.1%wt. titania nanofluid; sample A: without SDS, sample B: with SDS; 1) three days after preparation; 2) four days after preparation; 3) one week after preparation; 4) one year after preparation	68
Figures 4- 7	TEM images (Scale 100 nm) of 0.1%wt. titania nanofluid with different preparation method; a) T1; b) T2; c) T3; d) T4; e) T5; f) T6.....	70
Figure 4- 8	Sedimentation rate for six prepared samples within seven days after preparation	73
Figure 4- 9	Predicted vs. actual values plot for the UV-vis spectrophotometer absorbance measurement: (a) after one day, (b) after two days, (c) after one week, and (d) after one month.....	78

Figure 4- 10 Two-dimensional contour plots for the UV-vis spectrophotometer absorbance measurement; (a) after one day (b) after two days, (c) after one week, and (d) after one month.....	79
Figure 4- 11 Response surface plot for the UV-vis spectrophotometer absorbance measurement; (a) after one day (b) after two days, (c) after one week, and (d) after one month	80
Figure 4- 12 a) 3D surface, b) Contour of desirability with consideration of all four responses for optimum stability area of titania nanofluid.....	82
Figure 4- 13 a) 3D surface, b) Contour of desirability of responses for optimum stability area of titania nanofluid without the first response	83
Figure 4- 14 A parity plot between actual experiment and predicted values using RSM for TiO ₂ nanofluid: (a) zeta potential, (b) particle size, (c) thermal conductivity, (d) UV absorbance. (The vertical and horizontal axes are predicted output and corresponding targets, respectively)	89
Figure 4- 15 2D representation of the responses for TiO ₂ nanofluid: (a) zeta potential, (b) particle size, (c) thermal conductivity, (d) UV absorbance. (Vertical and horizontal axes are the value of pH and the %wt. of surfactant, respectively)	91
Figure 4- 16 3D response surface plot for TiO ₂ nanofluid: (a) zeta potential, (b) particle size, (c) thermal conductivity, (d) UV absorbance.	92
Figure 4- 17 Desirability plot for TiO ₂ nanofluid: (a) 2D plot with contours, (b) 3D surface mesh	94
Figure 4- 18 Desirability plot for TiO ₂ nanofluid: (a) 3D surface mesh, (b) 2D plot with contours	95
Figure 4- 19 Actual versus predicted values for (a) UV absorbance after one week, (b) UV after one month and (c) thermal conductivity	100

Figure 4- 20	Contour plots showing the effect of time and power of sonication on UV measurements after one week; (a) 0.1, (b) 0.55, (c) 1 %vol., and after one month; (d) 0.1, (e) 0.55 and (f) 1 %vol.	101
Figure 4- 21	Contour plots showing the effect of time and power of sonication on thermal conductivity of TiO ₂ -water nanofluids at (a) 0.1 (b) 0.55 and (c) 1 %vol. concentration	104
Figure 4- 22	Actual versus predicted values for (a) thermal conductivity, (b) viscosity and (c) zeta potential	108
Figure 4- 23	Surface response plots presenting viscosity and zeta potential variation by altering power and volume concentration at different timing (t); (a and b) at t=2; (c and d) at t=11; and (e and f) at t=20 minutes	109
Figure 4- 24	Actual versus predicted plots for TiO ₂ nanofluid for the measurement of sedimentation rate: (a) after two days, (b) after one week, (c) after one month	113
Figure 4- 25	Two dimensional contour plots for sedimentation rate measurement of titania nanofluid at ultrasonic amplitude of 20%; a) after two days; b) after one week; c) after one month	114
Figure 4- 26	Two dimensional contour plots for sedimentation rate measurement of titania nanofluid at ultrasonic amplitude of 50%; a) after two days; b) after one week; c) after one month	116
Figure 4- 27	Two dimensional contour plots for sedimentation rate measurement of TiO ₂ nanosuspension at ultrasonic amplitude of 80%; a) after two days; b) after one week; c) after one month.....	117
Figure 4- 28	Desirability plot for TiO ₂ nanofluid: (a) 2D surface mesh, (b) 3D plot with contours	119

List of Tables

Table 2- 1	Particle size change of Al ₂ O ₃ /Distilled water nanofluids with two pH values (Lee, K. et al., 2009)	18
Table 2- 2	Actual values of pH _{pzc} of the TiO ₂ between 5 and 55 °C(Chou, J.-C. & Liao, L. P., 2005)	18
Table 2- 3	Summary of different ultrasonic processes	20
Table 2- 4	Summary of different nanofluids peak absorption measured by UV-vis spectrophotometer	23
Table 2- 5	Volumes of gold nanofluid in different synthesis conditions (Tsai, C. Y. et al., 2004)	23
Table 2- 6	Zeta potential and associated suspension stability (Vandsburger, L., 2009)	24
Table 2- 7	Summary of different tests that conduct to a theory	36
Table 2- 8	Equipment used for characteristic measurements	40
Table 2- 9	The α cond. of metal oxide nanofluids (Lee, J. H., 2009).....	41
Table 3- 1	Surfactant concentration for different nanofluid.....	54
Table 3- 2	Stability process and duration for different methods	55
Table 4- 1	Different homogenization method for preparing samples	69
Table 4- 2	Zeta potential, particle size, thermal conductivity and viscosity results for 0.1%wt. titania nanofluid	73
Table 4- 3	Variables and values used for CCD	75
Table 4- 4	The obtained experimental results based on the CCD method	76
Table 4- 5	The ANOVA results.....	76
Table 4- 6	The developed models of UV responses	77
Table 4- 7	Evaluation of experimental and predicted values at optimum condition	84

Table 4- 8	Factors and responses used for CCD in model optimization (coded values)	86
Table 4- 9	Statistical characteristics of optimum models and ANOVA results	87
Table 4- 10	P-Value of four responses	87
Table 4- 11	The developed models of characteristic and stability responses.....	88
Table 4- 12	Evaluation of experimental and predicted values at optimum condition	96
Table 4- 13	Independent variables and their levels used in the response surface design	97
Table 4- 14	Box-Behnken design matrix and experimental record responses	98
Table 4- 15	The developed models for stability and characteristic responses	99
Table 4- 16	ANOVA for response surface quadratic model	100
Table 4- 17	Experimental results based on the BBD method.....	105
Table 4- 18	ANOVA for response surface quadratic models.....	105
Table 4- 19	ANOVA for response surface method	106
Table 4- 20	The developed models of characteristic and stability responses.....	106
Table 4- 21	Box-Behnken design matrix and experimental record responses	110
Table 4- 22	The developed models of Ws responses	111
Table 4- 23	ANOVA for response surface quadratic models.....	111
Table 4- 24	ANOVA for response surface method for sedimentation balance method after intervals of two days, one week and one month	112
Table 4- 25	The goals and predicted point for nanofluid characteristics and stability evaluation	120
Table 4- 26	Models for the evaluation of thermal conductivity of titania nanofluid	121
Table A- 1	Specification of equipments in this research.....	150

List of Symbols and Abbreviations

AP	Adequate Precision
BBD	Box Behnken Design
C_p	specific heat
CCD	Central composite design
CV	Coefficient of Variance
D	Dimensional, day
e	random error
E	energy
El	electrostatic repulsion
g	acceleration velocity
K	thermal conductivity
k	constant rate of aggregation/ the number of factors
M	molecular weight, month
N	Avogadro's constant
Prob	probability value
PS	Particle Size
Q	electronic power
R	regression coefficient, particle radius
SDS	Sodium Dodecyl Sulfate
SDBS	Sodium Dodecyl Benzene Sulfonate
Std.Dev	Standard Deviation
T	temperature
THW	Transient Hot Wire
TNT	Titanate nanotube
TPS	Transient Plane Source

SSM	Steady state method
UDD	ultra dispersed diamond
UP	Ultrasonic Processor
UB	Ultrasonic Bath
V	Sedimentation velocity
vol.	Volume percentage
W	weight/stability coefficient, week
wt.	Weight percentage
x	interparticle surface-to-surface distance
y	predicted response
ZP	Zeta Potential

Greek symbols

α	collision efficiency
β	regression coefficient
λ	mean free path
ν	dynamic viscosity, Euler's constant
μ	viscosity
ρ	density
Φ	volume fraction
ω	surface potential
Ψ	zeta potential

Subscripts

A	van der Waals, attraction
Adj.	Adjusted
c	critical
cond.	conduction

d	particle
el	electrostatic repulsion
eff	effective
i	linear coefficient
j	quadratic coefficient
IEP	Iezo Electric Point,
m	maximum
nf	nanofluid
p	particle
pred.	predicted
PZC	Point of Zero Charge
s	nanoparticle
tot	sum, total

Introduction

Chapter 1: Introduction

1.1 Background

According to the historical evidences, the first people who used nanofluids were the medieval artisans. Most likely they weren't aware of their unique characteristics but prepared a suspension of gold nanoparticles to decorate their Cathedrals' windows with a deep red color. Later in the 15th century, Italian potters dispersed metallic nanoparticles in a liquid to make luster pottery. Finally the invention of a nanofluid with its unique properties came was officially announced by Choi in Argonne National Laboratory in 1995. He claimed that by dispersion of nanoparticles inside a base fluid, thermal conductivity of the fluid will surprisingly increase. Since then, many researchers worked on this new engineered fluid theory in which some approved Choi's theory and some rejected it (Hong, T. K. & Yang, H. S., 2005), (Kim, S. H. et al., 2007), (He, Y. et al., 2007), (Penkavova, V. et al., 2011a).

If the thermal transport properties of nanofluids can be utilized in industrial scales, this new engineered fluid may resolve many engineering dilemmas, which numerous manufacturers are facing in microelectronics, transportation and manufacturing. Advanced technologies such as microelectronic devices operating at high speeds, high power engines, and advanced optical devices require more efficient cooling systems as they undergo high thermal loads. The conventional method of increasing heat dissipation is to increasing the surface area exposed to conductive fluid. However, this method carries the disadvantage of bulky cooling systems; therefore, there is an urgent need for new and novel coolants with improved conductivity. The innovative concept of 'nanofluids' (heat transfer fluids comprised of suspended nanoparticles) was proposed as a solution to these challenges. There are also various potential advantages in nanofluids such as better long-term stability and thermal conductivity compared to millimeter or even micrometer sized particle suspensions and

less pressure drop and erosion particularly in microchannels. Though, there are major application prospects in advanced thermal applications, it still remained in the early stages of development. Nanofluid has a major obstacle in reaching the highest potential discharge which is nothing but stability of nanoparticles in the basefluid. This is a concern shows up mostly when nanofluid is prepared by two-step method (Meibodi, M. E. et al., 2010a) ,(Chen, L. & Xie, H., 2010) , (Nasiri, A. et al., 2011). To overcome this problem, some methods are recommended, such as physical or chemical treatment such as addition of surfactant, surface modification of the suspended particles or applying powerful forces on the clustered nanoparticles. Addition of surface-active agents has been used to modify hydrophobic characteristics of materials and to facilitate their dispersion in an aqueous solution (Jin, H. et al., 2009; Penkavova, V. et al., 2011b).

Generally nanofluids are called a type of colloidal dispersion, however there exist some major differences which show up the altered specifications including, basic processing steps, particle size, phase, major physical properties and main diversities in applications. Nano particles' dimension ranges between 1 and 100 nm, whereas colloids particle sizes are in the range of 10–1000 nm. Remarkable thermal phenomena can be observed merely with particles in size range smaller than 10 nm. Moreover colloidal dispersions can form a suspension, an emulsion, or a foam; while, a nanoparticle in nanofluids is a solid, which forms only a suspension. Furthermore, differences in preparation methods and applications prove these discrepancies.

Today's most challenging confronts of scientists are environmental issues including reduction of environmental pollution, improvement of the quality of life and elimination of impurities. Hence, researchers have started to develop the materials that can be combined with natural resources such as TiO_2 , vulcanized cadmium, zinc oxide and tungsten oxide. Within the scope of green materials, TiO_2 is the most stable and least toxic substance which is durable and cheap too, and these characteristics

encourage its extensive use in science and industries (Chang, H. et al., 2007). This substance in the form of nanoparticles can make new products for solar water heaters, micro-reactors, drug delivery and many other applications. Therefore, different tests were conducted to study the stability and heat transfer of the nano-suspensions in areas of refrigerants (Naphon, P. et al., 2009; Peng, H. et al., 2011), pool boiling (Kim, H. & Kim, M., 2009; Truong, B. et al., 2010), conduction (Nield, D. A. & Kuznetsov, A. V., 2010; Quaresma, J. o. N. N. et al., 2010) and convective heat transfer (Godson, L. et al., 2010; Ozerinc, S. et al., 2010). Recently, many researchers worked on titania nanoparticles for nanofluids preparation. He et al. (2007) stated that addition of TiO_2 into the base liquid enhances the thermal conduction and this effect increases with increasing particle concentration and decreasing particle (agglomerate) size. Increasing agglomerate size and particle concentration will directly increase the viscosity. In addition, results from (Kim, S. H. et al., 2007) showed the linear increment of effective thermal conductivity with decreasing the particle size, but no existing empirical or theoretical correlation can explain the behavior. It is also demonstrated that high-power laser irradiation can lead to substantial enhancement in the effective thermal conductivity although only a small fraction of the particles is fragmented. Yoo et al. (2007) claimed that titania nanofluid showed a large enhancement of thermal conductivity compared with their base fluids, which exceeds the theoretical expectation of a two-component mixture system. On the contrary, Zhang et al. (2007) could not correctly explain the unexpected enhancement of effective thermal conductivity TiO_2 nanofluid. Chung et al. (2009) worked on the stability of the ZnO /water nanofluid under various ultrasonic conditions. They proposed that the sedimentation behavior of nanofluids is proportional to the volume fraction and the ultrasonic power.

1.2 Statement of Research Objectives

This research is focused on the following objectives:

- (1) To examine the influence of homogenization methods on stability and thermal conductivity of titania nanofluid
- (2) To verify the suitability of UV-vis spectrophotometer for measuring stability in short and long term
- (3) To determine the stability of nanofluids by means of zeta potential, UV absorbance and particle size
- (4) To evaluate the influence of nanoparticle volume concentration, duration and power of ultrasonic on the stability and thermal conductivity of nanofluid using design of experiment

1.3 Structure of thesis

The dissertation is organized in the following manner. Chapter 2 introduces the nanofluid history, a complete review of literature on preparation methods, importance of the stability of nanofluid, various stabilization techniques, different stability monitoring equipments and titania nanofluid characteristics. Chapter 3 presents the experimental techniques for different stability inspection and characteristic measurement and a brief theory about the optimization software used to analyze the results. Chapter 4 discusses about the results of the experiments and responses of the Design of Experiment (DOE) software. Conclusions and recommendations for future works are stated in Chapter 5.

Literature review

Chapter 2: Literature review

2.1 Introduction

One of the most significant scientific challenges in the industrial area is cooling, which applies to many diverse productions, including microelectronics, transportation and manufacturing. Technological developments such as microelectronic devices operating at high speeds, high-power engines, and brighter optical devices producing high thermal loads, require advanced cooling systems.

Maxwell was the first presenter of a theoretical basis to predict a suspension's effective thermal conductivity about 140 years ago (1873) and his theory was applied from millimeter to micrometer sized particles suspensions. However, Choi and Eastman (1995) introduced the novel concept of nanofluids by presenting the unique properties of nanofluids in the annual meeting of American Society of Mechanical Engineering in 1995. Goldstein et al. added the condition that the particles must be in colloidal suspension. Choi and his colleagues carried out experiments on heat transport in systems with CuO nanoparticles in water, and Al₂O₃ particles in ethylene glycol and water. They found that the particles improve the heat transport by as much as 20%, and they interpreted their result in terms of an improved thermal conductivity (k/k_0), which they named it effective thermal conductivity (Goldstein, R. J. et al., 2000) .

A nanofluid is a fluid produced by dispersion of metallic or nonmetallic nanoparticles or nanofibers with a typical size of less than 100 nm in a liquid. Nanofluids have attracted huge interest lately because of their greatly enhanced thermal properties. For instance, experiments showed an increase in thermal conductivity by 40% and 150%, with dispersion of less than 1% volume fraction of Cu nanoparticles or carbon nanotubes in ethylene glycol or oil, respectively (Kebllinski, P. et al., 2005). During the past decade, some researchers have reported the heat transfer and flow characteristics of different nanofluids, namely: Trisaksri and Wongwises (2007), Beck

(2008), Wang and Mujumdar (2007), Duangthongsuk and Wongwises (2007), Godson et al. (2010), Li et al. (2009) and Wen et al. (2009), Leong et al. (2010). However, prior to utilizing nanofluids for heat transfer, significant knowledge about their thermophysical properties are required especially their thermal conductivity and viscosity. Many researchers have measured the thermophysical properties of nanofluids while many others used well-known predictive correlations. Their works have been both experimental and theoretical.

This project focuses on the stability of nanofluids and its influence on thermal conductivity and heat transfer enhancement, which is critical to eventual utilization of nanofluid in practice. This subject was put into consideration recently since different investigators reach different results with the same nanoparticles. Therefore, it was concluded that stability measurement and investigation for each nanofluid preparation may be leading to a standard way of preparation and unified data.

Theoretical attempts made to explain the associated characteristic mechanisms are also outlined. In addition to these, the measurement methods proposed for determination of stability are summarized; thermophysical property predictions of the models are compared with experimental findings, and significant discrepancies are specified (Duangthongsuk, W. & Wongwises, S., 2010a).

2.2 Nanofluid preparation methods

Preparing a stable and durable nanofluid is a prerequisite to optimizing its thermal properties. Therefore, many combinations of material might be used for particular applications, namely: nanoparticles of metals, oxides, nitrides, metal carbides, and other nonmetals with or without surfactant molecules which can be dispersed into fluids such as water, ethylene glycol, or oils (Kebllinski, P. et al., 2005). In the stationary state, the sedimentation velocity of small spherical particles in a liquid follows the Stokes law (Hiemenz, P. C. & Dekker, M., 1986):

$$V = \frac{2R^2}{9\mu}(\rho_P - \rho_L) \cdot g \quad (2-1)$$

where V is the particle's sedimentation velocity; R is the spherical particle's radius; μ is the liquid medium viscosity; ρ_P and ρ_L are the particle and the liquid medium density, respectively and g is the acceleration of gravity. This equation reveals a balance of the gravity, buoyancy force, and viscous drag that are acting on the suspended nanoparticles. According to Eq. (2-1), the following measures can be taken to decrease the speed of nanoparticles' sedimentation in nanofluids, and therefore to produce an improvement in the stability of the nanofluids: (1) reducing R , the nanoparticles size; (2) increasing μ , the base fluid viscosity and (3) lessening the difference of density between the nanoparticles and the base fluid ($\rho_P - \rho_L$). Clearly reducing the particle size should remarkably decrease the sedimentation speed of the nanoparticles and improve the stability of nanofluids, since V is proportional to the square of R . According to the theory in colloid chemistry, when the size of particle decreases to a critical size, R_c , no sedimentation will take place because of the Brownian motion of nanoparticles (diffusion). However, smaller nanoparticles have a higher surface energy, increasing the possibility of the nanoparticle aggregation. Thus, the stable nanofluids preparation strongly link up with applying smaller nanoparticles to prevent aggregation (Wu, D. et al., 2009).

Two different techniques can be applied to produce nanofluids namely: single-step and two-step method.

2.2.1 Two step technique

In this method, dry nanoparticles/nanotubes are first produced, and then they are dispersed in a suitable liquid host, but as nanoparticles have a high surface energy, aggregation and clustering are unavoidable and will appear easily. Afterward, the particles will clog and sediment at the bottom of the container. Thus, making a homogeneous dispersion by two step method remains a challenge. However, there exist

some techniques to minimize this problem, such as high shear and ultrasound. Therefore, we will discuss different methods of making a stable nanofluid in the next section. Nanofluids containing oxide particles and carbon nanotubes are produced by this method. This method works well for oxide nanoparticles and is especially attractive for the industry due to its simple preparation method. But its disadvantage due to quickly agglomerated particles brings about many challenges. If nanoparticles disperse only partially, dispersion is poor and sedimentation happens. Therefore, a high volume concentration is needed to increase the heat transfer (10 times of single step) (Das, S. K. et al., 2007) and accordingly the cost increase. The two-step method is useful for application with particle concentrations greater than 20 %vol. but it is less successful with metal nanoparticles. However, some surface treated nanoparticles showed excellent dispersion (Swanson, E. J. et al., 2008). The first materials tried for nanofluid preparation were oxide particles, mainly because they are easy to make and chemically stable in solution (Das, S. K. et al., 2006).

2.2.2 Single step technique

In this method nanoparticle manufacturing and nanofluid preparation are done concurrently. The single-step method is a process combining the preparation of nanoparticles with the synthesis of nanofluids, for which the nanoparticles are directly prepared by physical vapor deposition (PVD) technique or a liquid chemical method (condensing nanophase powders from the vapor phase directly into a flowing low-vapor-pressure fluid is called VEROS).

In this method drying, storage, transportation, and dispersion of nanoparticles are avoided, so the agglomeration of nanoparticles is minimized and the stability of the nanofluids is increased. A disadvantage of this method is that it is impossible to scale it up for great industrial functions and is applicable only for low vapor pressure host fluids. This limits the application of the method (Das, S. K. et al., 2007; Goldstein, R. J.

et al., 2000; Koblinski, P. et al., 2005; Li, Y. et al., 2009; Wang, X.-Q. & Mujumdar, A. S., 2007). Recently, Chang et al. (2007) prepared nanofluids of TiO₂ nanoparticles dispersed in water by a one-step chemical method using a high pressure homogenizer. This method is called modified magnetron sputtering. The schematic of the apparatus can be seen in Figure 2-1.

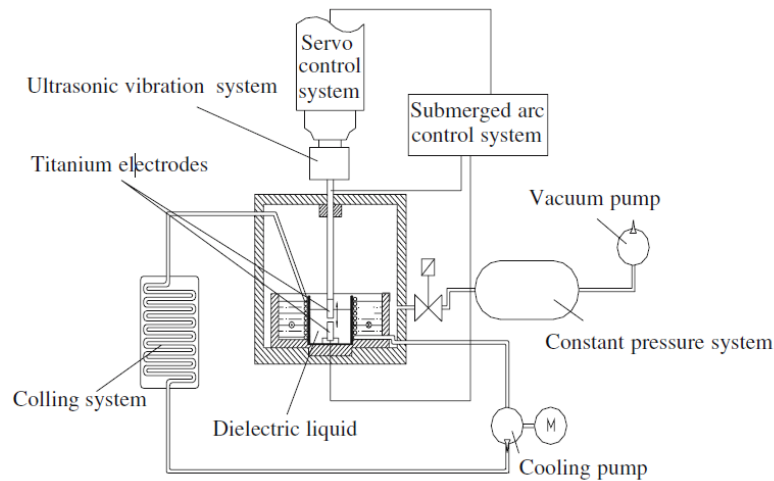


Figure 2- 1 Ultrasonic-aided submerged arc nanoparticle synthesis system to produce TiO₂ nanofluid (Chang, H. et al., 2007)

2.3 Importance of the stability of nanofluid

Preparing a homogeneous suspension is still a technical challenge as strong van der Waals interactions between nanoparticles always favors the formation of aggregates. To obtain stable nanofluids, some methods are recommended, such as physical or chemical treatment. They are listed as the addition of surfactant, surface modification of the suspended particles or application of high-power forces on the clustered nanoparticles. Spreading surface- active agents have been used to modify hydrophobic materials to enable dispersion in an aqueous solution (Hwang, Y. J. et al., 2006). Otherwise clogging, aggregation and sedimentation happen and cause deterioration of suspension characteristics like thermal conductivity, viscosity and increasing specific heat. There exists a theory that clustering and aggregation is one of the main features in

stability and extraordinary enhancement in thermal conductivity of nanofluids (Evans, W. et al., 2008), although this theory may be highly specific to the high aspect ratio nanoparticles, including single wall nanotubes. Philip et al. (2007) and Evans et al. (2008) claimed that the high aspect ratio structure of the fractal-like aggregates is a key factor allowing rapid heat flow over large distances. They also stated that well dispersed composites show low thermal conductivity enhancement but composites with fractal aggregates show significant enhancements, even with considerable interfacial resistance. Gharagozloo and Goodson (2010) also measured fractal dimensions for the 1%, 3% and 5% volume concentrations of Al_2O_3 in H_2O and concluded that aggregation is a more likely cause for the measured enhancements of nanofluid. On the contrary, another theory shows that agglomeration and clustering reduce stability and thermal conductivity improvement. Hong et al. (2006) claimed that ultrasonicated Fe nanofluids, due to their broken clusters, got enhancement in thermal conductivity although this enhancement reduced as a function of elapsed time after production. Therefore, for classification of the stability theory more experimental works are needed to clarify the role of aggregation in conductivity enhancement. But generally, to obtain a high quality suspension, small particles have to meet these two principles: (1) diffusion principle: particles are scattered by a liquid medium and dispersed into the liquid medium. (2) Zeta potential principle: the zeta potential absolute value among particles must be as large as possible, making a common repulsive force between the particles (Chang, H. et al., 2006).

According to the literature, there are three effective tactics used to manage stability of suspension against sedimentation of nanoparticles. Some of the researchers applied all of these methods to gain better stability (Pantzali, M. N., Kanaris, A. G., et al., 2009; Wang, X.-j. et al., 2009; Zhu, D. et al., 2009) but others just applied one (Chandrasekar, M. et al., 2010) or two techniques (Assael, M. J. et al., 2005; Meibodi,

M. E. et al., 2010a; Wei, X. et al., 2010) with satisfying results. There is no standard to recognize the superlative mix up of combining methods. This area requires more experiments to be clarified. Homogenization processes are summarized below.

2.3.1 Surfactant or activator adding

This is one of the general methods to avoid sedimentation of nanoparticles. Addition of surfactant can improve the stability of nanoparticles in aqueous suspensions. The reason is that the hydrophobic surfaces of nanoparticles/ nanotubes are modified to become hydrophilic and vice versa for non-aqueous liquids. A repulsion force between suspended particles is caused by the zeta potential which will rise due to the surface charge of the particles suspended in the base fluid (Hwang, Y. et al., 2007; Jin, H. et al., 2009). However, care should be taken to apply enough surfactant as inadequate surfactant cannot make a sufficient coating that will persuade electrostatic repulsion and compensate the van der Waals attractions (Jiang, L. et al., 2003). The effect of surfactant on aggregated particle size distribution can be demonstrated as shown in Figure 2-3. Popular surfactants that have been used in literature can be listed as sodium dodecyl sulfate (SDS) (Hwang, Y. et al., 2008; Hwang, Y. et al., 2007; Jiang, L. et al., 2003; Lee, K. et al., 2009; Wang, H. & Sen, M., 2008; Zhu, D. et al., 2009) Lee, 2009) , salt and Oleic Acid (Hwang, Y. et al., 2008; Yu, W. et al., 2010), cetyl trimethyl ammonium bromide (CTAB) (Assael, M. J. et al., 2005), Dodecyl trimethylammonium bromide (DTAB) and sodium octanoate (SOCT) (Madni, I. et al., 2010), hexadecyltrimethylammoniumbromide (HCTAB), polyvinylpyrrolidone (PVP) (Sato, M. et al., 2009; Zhu, H. et al., 2007) and Gum Arabic (Lee, K. et al., 2009). Choosing the right surfactant is the most important part of the procedure. Surfactants are categorized as anionic, cationic or non-ionic (Li, X. et al., 2007).

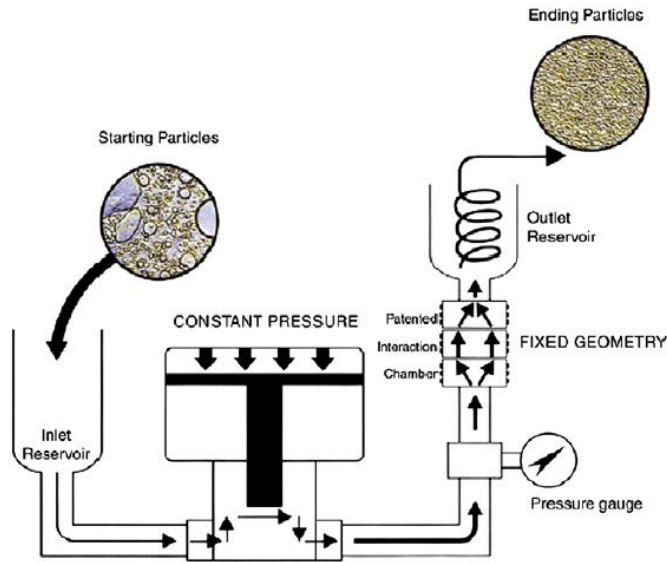


Figure 2- 2 Schematic diagram of the high-pressure homogenizer for producing nanofluids (Chang, H. et al., 2007)

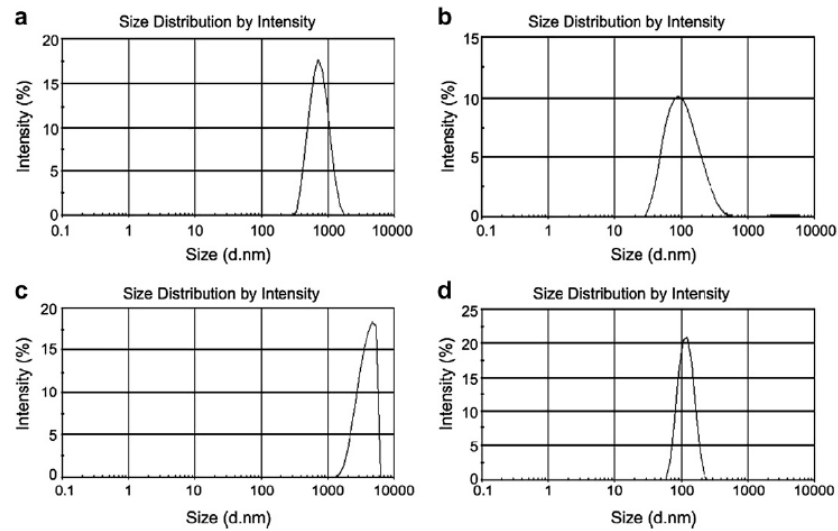


Figure 2- 3 Particle size distributions of nano-suspensions. (a) $\text{Al}_2\text{O}_3\text{--H}_2\text{O}$ without SDBS, (b) $\text{Al}_2\text{O}_3\text{--H}_2\text{O}$ with SDBS, (c) $\text{Cu--H}_2\text{O}$ without SDBS and (d) $\text{Cu--H}_2\text{O}$ with SDBS Concentration of nanoparticles and SDBS surfactant are 0.05% weight fraction, respectively (Wang, X.-j. et al., 2009)

The disadvantage of addition of surfactants is the fact that the bonds between nanoparticles and surfactant may get damaged/break in temperatures above 60°C (Assael, M. J. et al., 2005; Wen, D. et al., 2009; Wu, D. et al., 2009),(Murshed, S.M.S.

et al., 2008). Consequently, the nanofluid will lose its stability and the sedimentation of nanoparticles will occur (Wang, X.-Q. & Mujumdar, A. S., 2007).

2.3.2 pH control (surface chemical effect)

The stability of an aqueous nanofluid directly links to its electrokinetic properties. Through a high surface charge density, strong repulsive forces can stabilize a well-dispersed suspension (Chang, H. et al., 2006; Chou, J.-C. & Liao, L. P., 2005; Fovet, Y. et al., 2001; Hwang, K. S. et al., 2009; Zhu, D. et al., 2009). Xie et al. (2003) showed that by simple acid treatment a carbon nanotube suspension in water gained a good stability. This was caused by a hydrophobic-to-hydrophilic conversion of the surface nature due to the generation of a hydroxyl group. The isoelectric point (IEP) is the concentration of potential controlling ions at which the zeta potential is zero. Thus, at the IEP, the surface charge density equals the charge density, which is the start point of the diffuse layer. Therefore, the charge density in this layer is zero. Critical to nanoparticle nucleation and stabilization in solution is that the repulsive energy is smaller for small particles, so a larger zeta potential is required for suspension stability (Chang, H. et al., 2007). As the pH of the solution departs from the IEP of particles the colloidal particles get more stable and ultimately the thermal conductivity of the fluid improves. The surface charge state is a basic feature which is mainly responsible for increasing thermal conductivity of the nanofluids (Jin, H. et al., 2009; Lee, D. et al., 2006). But in some experiments it has been shown that the particles' shape can be changed by varying the pH (Hadjov, K. B., 2009; Wei, X. et al., 2009). In a liquid suspension, particles attract or repel each other. This interaction depends on the distance between particles and the total interface energy E_{tot} that is the sum of the van der Waals attraction E_A and the electrostatic repulsion E_{el} between them. The E_{el} among two charged particles with the surface potentials Ψ_{d1} and Ψ_{d2} is approximated by the DLVO theory:

$$E_{el} = \frac{\epsilon_0 \epsilon_1 r_1 r_2}{r_1 + r_2} \left\{ 2\Psi_{d1} \Psi_{d2} \ln \left[\frac{1 + \exp(-kx)}{1 - \exp(-kx)} \right] + (\Psi_{d1}^2 + \Psi_{d2}^2) \ln[1 - \exp(-2kx)] \right\} \quad (2-2)$$

where r is the radius of particles, x is a interparticle surface-to-surface distance, and the other symbols have their conventional meanings.

It is noticeable that higher potentials (Ψ_d or ζ) lead to a bigger potential barrier for agglomeration. At the 0.3 %vol. dose of CuO nanoparticles in distilled water, which the pH for the Point of Zero Charge (PZC) is about pH 8.5-9.5, the interparticle distance is about 100 nm for mobility-equivalent spherical particles. In this condition, the second term in the bracket of above equation is negligible compared to the first. Thus, the repulsion energy of the same-sized particles increases approximately in proportion to ζ^2 .

The attraction energy between the same particles is given by the Hamaker equation: $E_A = -A_{132}r/(12x)$. The Hamaker constant A_{132} of metal oxide is typically on the order of 10^{-20} J. With the above equation, the Hamaker equation, and the estimated Ψ_d , E_{tot} is calculated as a function of x at different pHs as shown in Figure 2-4. In this condition, the repulsion barrier gets larger than the attraction as pH moves from PZC, which makes the colloids more stable. At pH 8 or 10 when Ψ is small, the repulsion barrier disappears, and particles get subjected only to attraction; Strong particle agglomeration is expected in that case. Here, we need to quantify the suspension stability in terms of collision efficiency α that is responsible for colloidal particle growth. The α , a reciprocal value of stability coefficient, W , is related to constant rate of aggregation, $k = \alpha k_{diff} = k_{diff} / W$.

The k_{diff} represents the rate constant of the coagulation between uncharged particles. Then a general relation of stability coefficient W to total interaction energy E_{tot} can be derived (Lee, D. et al., 2006).

$$W = 2r \int_0^\infty \exp\left(\frac{E_{tot}}{k_b T}\right) \frac{dx}{(2r+x)^2} \quad (2-3)$$

For example, as the pH of the nanofluid goes far from the isoelectric point, the surface charge increases by applying SDBS surfactant in Cu-H₂O nanofluid. Since

more frequent attacks occur to the surface hydroxyl and phenyl sulfonic group by potential-determining ions (H^+ , OH^- and phenyl sulfonic group), zeta potential and the colloidal particles increase. Subsequently, the suspension gets more stable and eventually changes the thermal conductivity of the fluid (Li, X. F. et al., 2008).

Lee et al. (2009) also worked on different pH of Al_2O_3 nanofluids. The experiments indicated that when the nanofluid had a pH of 1.7, the agglomerated particle size was reduced by 18% and when the nanofluid had a pH of 7.66, the agglomeration size was increased by 51%. More particles aggregated in pH of 7.66 because of reduction in electric repulsion force. When Al_2O_3 particles are immersed in water, hydroxyl groups ($-OH$) form at the surface of the Al_2O_3 particle. The relevant reactions depend on the solution pH. When the pH of the solution is lower than the PZC, the hydroxyl groups react with (H^+) from water which leads to a positively charged surface. Alternatively, when the pH of the solution is higher than the PZC, the hydroxyl groups react with ($-OH$) from water and create a negatively charged surface (Peterson, G. P. & Li, C. H., 2006). In addition, as it is demonstrated in Table 2-1, the particle sizes differ when the pH of nano-suspensions change (Lee, K. et al., 2009).

The Optimized pH is different for different nanoparticles. For example, the proper pH for alumina is around 8 while for copper and graphite nanoparticles are 9.5 (Wang, X.-j. et al., 2009) and about 2.0 respectively. The pH for the point of zero charge also changes by temperature modification as it is illustrated in Table 2-2 (Chou, J.-C. & Liao, L. P., 2005).

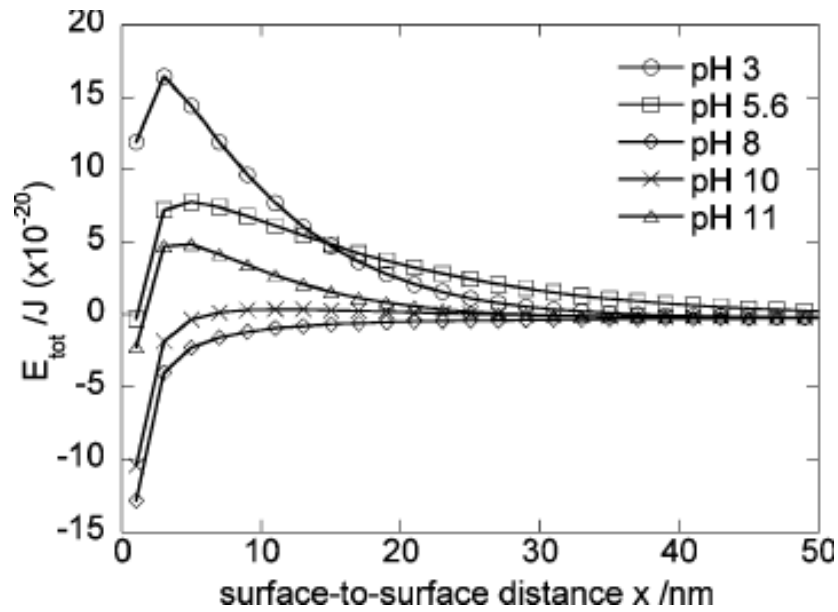


Figure 2- 4 The interaction potentials at various pHs as a function of interparticle distance (Lee, D. et al., 2006)

Table 2- 1 Particle size change of Al₂O₃/Distilled water nanofluids with two pH values (Lee, K. et al., 2009)

Nanofluid	Al ₂ O ₃ /DI	Al ₂ O ₃ /DI/PBS*/HCl	Al ₂ O ₃ /DI/PBS
pH		pH = 1.7	pH = 7.66
Mean particle size(nm)	170	139	1033

*Phosphate Buffered Saline contains sodium chloride, sodium phosphate and potassium phosphate and helps to maintain a constant pH

Table 2- 2 Actual values of pH_{pzc} of the TiO₂ between 5 and 55 °C (Chou, J.-C. & Liao, L. P., 2005)

Temperature (°C)	PH _{PZC}
5	6.62
15	6.39
25	6.17
35	5.97
45	5.78
55	5.61

2.3.3 Ultrasonic vibration

All the mentioned techniques are aimed to change the surface properties of suspended nanoparticles and to suppress particle cluster formation, with the purpose of

attaining stable suspensions. Ultrasonic bath, processor and homogenizer are powerful tools for breaking down the agglomerations in comparison with the others tools like magnetic and high shear stirrer as experienced by some researchers (Hwang, Y. et al., 2008). However, occasionally after passing the optimized duration of the process, it will cause more serious problems in agglomeration and clogging resulting in fast sedimentation. Furthermore, there is a new method to get stable suspensions proposed by Hwang et al. (2008) which consists of two micro-channels, dividing a liquid stream into two streams. Both divided liquid streams are then recombined in a reacting chamber. Breaking the clusters of nanoparticles was studied using the high energy of cavitations (Munson, B. R. et al., 1998). This work was conducted for Carbon Black with water and silver with silicon oil nanofluids. When the suspension contacts with the interior walls of the interaction chamber, it will flow through the microchannel. Therefore, the flow velocity of the suspension through the microchannel should be increased according to Bernoulli's theorem, and concurrently cavitations extensively occur. In this fast flow region, particle clusters must be broken down due to a combination of various mechanisms, including (i) strong and irregular shock on the wall inside the interaction chamber, (ii) microbubbles formed by cavitations'-induced exploding energy, and (iii) high shear rate of flow. This leads to desired homogeneous suspensions with fewer aggregated particles at high-pressure. This procedure can be repeated three times to achieve the desired homogeneous nanoparticle distribution in the base fluids. An ultrasonic disruptor is a more generally accessible apparatus than the one prepared by Hwang et al. (2008). Many researchers used this technique to obtain a stable nanosuspension. In some cases, they mixed different methods of stabilization to fine-tune the results. A summary of investigators who reached diverse duration of stability by using ultrasonic methods is given in Table 2-3. It is noticeable that typically it is rare to maintain nanofluids (synthesized by the traditional one-step and two-step

methods) in a stable homogeneous state for more than 24 h (Peterson, G. P. & Li, C. H., 2006) we gathered.

Table 2- 3 Summary of different ultrasonic processes

Investigator	nanoparticle	Base fluid	Concentration	Stability process	Duration	Sedimentation
(Oh, D.-W. et al., 2008)	Al ₂ O ₃ (45nm)	DW EG	1-5.5 % vol. 1-8 % vol.	Ultrasonic cleaner	15 Hrs	Minutes after preparation
(Patel, H. et al., 2005)	Al ₂ O ₃ (11nm)	DW	0.8 % vol.	Ultrasonic	6 Hrs	N/A
(Das, K. et al., 2003)	Al ₂ O ₃ (38.4nm) CuO (28.6nm)	DW	1-4 % vol. 1-4 % vol.	Ultrasonic	11 Hrs	After 12 hours
(Asirvatham, L. G. et al., 2009)	CuO (10nm)	DI	0.003% vol.	Ultrasonic	2–7 Hrs	N/A
(Hwang, Y. et al., 2007)	MWCNT (10-50×10-30nm) Fullerene (10nm)	DI+SDS Oil+SDS DI+SDS Oil+SDS	0-1.6% vol. 0-1.6% vol.	N/A N/A	N/A N/A	N/A N/A
	Mixed Fullerene (10nm) C ₇₀ and C ₆₀ CuO (33nm) SiO ₂ (12nm)	EG+SDS Oil+SDS DI+SDS EG+SDS DI+SDS DI+SDS	0-1.6% vol. 0-1.6% vol. 0-1.6% vol.	N/A N/A N/A	N/A N/A N/A	N/A N/A N/A
(Wang, X.-j. et al., 2009)	Al ₂ O ₃ (25nm) Cu (25nm)	DW+SDBS DW DW+SDBS DW	0-0.08 (N.P)% wt. 0-0.14% wt (SDBS)	Ultrasonic, pH control and Surfactant adding	15 min 1 Hr 15 min 1 Hr	N/A
(Duangthongsuk, W. & Wongwises, S.)	TiO ₂ (21nm)	DW	0-1.2% vol	Ultrasonic	2Hrs	N/A

Continued Table 2- 3 Summary of different ultrasonic processes

(Chen, H. et al., 2009)	TNT (10×100nm)	EG	(0.5-8) % wt	Ultrasonic bath	48 Hrs	More than 2 months stability
(Hong, K. S. et al., 2006)	Fe (10nm)	EG	(0.2-0.55)% vol.	Ultrasonic cell disrupter	10 to 70 min	Optimized 30 min
(Lee, D. et al., 2006)	CuO (25nm)	DW	0.3% vol.	N/A		N/A
(Li, X. F. et al., 2008)	CuO (25nm)	DW+SDBS	0.1% wt.	Ultrasonic vibrator , pH control and Surfactant addition	1Hr	N/A
(Zhu, H. et al., 2007)	Graphite (nm)	DW+PVP	0.5% wt.	Ultrasonic vibration	30 min	N/A
(Yu, W. et al., 2010)	Fe ₃ O ₄ (15nm)	Kerosene+ oleic acid ammonium	0-1.2% vol.	Ultrasonic	0-80 min	stable
(Chung, S. J. et al., 2009)	ZnO (20nm) (40-100nm)	poly methacrylate +DI	0.02% vol.	Horn Ultrasonic	0-60 min	Stable over 10000 h
(Lee, K. et al., 2009)	Al ₂ O ₃ (40-50nm)	DW	1% vol.	Horn Ultrasonic Ultrasonic Bath	0-30 min 8Hrs	Particle size reduction
	MWCNT (10-30nm×10-50µm)	DW+SDS				Surfactant adding avoid entanglement
(Hwang, Y. J. et al., 2006)	SiO ₂ (7nm)	DW	0-1% vol.	Ultrasonic disruptor	2Hrs	Stable
	CuO (35.4nm)	DW EG				Stable
	CuO (35.4nm)					Stable

2.4 Stability inspection instruments

There are some instruments and methods that can rank the relative stability of nanosuspension. The list includes UV–vis spectrophotometer, zeta potential, sediment photograph capturing, TEM (Transmission Electron Microscopy) and SEM (Scanning Electron Microscope), light scattering, three omega and sedimentation balance method.

Therefore, the rate or percentage of sedimentation will be determined by analyzing gathered data.

2.4.1 UV–vis spectrophotometer

Even though the stability of a nanofluid is the key issue for its application, there are limited studies on estimating the stability of a suspension. Ultra Violet–visible spectrophotometer (UV–vis) measurements have been used to quantitatively characterize colloidal stability of the dispersions. One of the most striking features of this apparatus is its applicability for all base fluids, whereas zeta potential analysis has restrictions for the viscosity of the host fluid. A UV–vis spectrophotometer exploits the fact that the intensity of the light changes due to absorption and scattering of the light beamed through a fluid. At 200–900 nm wavelengths, the UV–vis spectrophotometer measures the absorption by liquid and is used to analyze various dispersions in the fluid (Lee, K. et al., 2009). Typically, suspension stability is determined by measuring the sediment volume versus the sedimentation time. However, this method is unsuitable for nanofluid dispersions with a high concentration and especially for CNT solutions. These dispersions are too dark to differentiate the sediment visibly. Jiang et al. (2003) were the first investigators who proposed sedimentation estimation using UV–vis spectrophotometer for nano suspensions. In this method, first step is to find the peak absorbance of the dispersed nanoparticles at very dilute suspension by scanning. As the concentration of suspension has a linear relation with absorbance, preparing a standard to fit a linear relation to at least three different dilute concentrations (0.01–0.03%wt.) will be the next step in this method. Relative stability measurement will be followed by preparing the desired concentration of nanofluid and put aside for a couple of days. Whenever it is needed to check the relative stability, the supernatant concentration will be measured by UV–vis spectrophotometer and the concentration can be plotted against time. This method was used by Refs. (Hwang, Y. et al., 2007; Kim, S. H. et al., 2007;

Lee, K. et al., 2009; Li, X. F. et al., 2006). Table 2-4 presents a summary of different nanofluid peak absorptions by UV-vis spectrophotometer.

Table 2- 4 Summary of different nanofluids peak absorption measured by UV-vis spectrophotometer

Nanoparticle	Base fluid	Peak wavelength	Investigator
MWCNT and Fullerene	Oil	397	(Hwang, Y. et al., 2007)
Aligned CNT	DW	210	(Liu, Z.-Q. et al., 2008)
CNT	DW	253	(Jiang, L. et al., 2003)
TiO ₂	DW	280-400nm	(Chang, H. et al., 2007)
Cu	DW	270	(Chang, H. et al., 2006)
CuO	DW	268	(Chang, H. et al., 2006)
Ag	DW	410	(Sato, M. et al., 2009)

According to Mie's theory (Kreibig, U. & Genzel, L., 1985), the surface plasmon absorption and the plasmon bandwidth depend on the size of the metallic particles in the solution. Consequently, the peak value represents the most populated nanoparticle size in the solution. Additionally, by increasing the particle size especially, those which are smaller than 20 nm, the bandwidth decreases. Contrariwise, the bandwidth of the surface Plasmon for the particles larger than 20 nm, increases with the particle size (Kreibig, U. & Vollmer, M., 1995; Link, S. & El-Sayed, M. A., 2003).

Table 2- 5 Volumes of gold nanofluid in different synthesis conditions (Tsai, C. Y. et al., 2004)

Condition	Basefluid	Na ₃ citrate (ml)	Tannic acid (ml)	HAuCl ₄ (ml)	Particle size (nm)	Peak wavelength
A	DW	0.2	2.5	3	21.3	528
B	DW	0.2	5	6	43.7	530.5
C	DW	3	0.1	1	8	568.5
E	DW	3	2.5	6	9.3	647
G	DW	3	0.1	3	15.6	721.5

The local peak in the UV-vis spectra shifts towards longer wavelength as the particle size increases (Tsai, C. Y. et al., 2004). Tsai et al. (2004) have conducted a series of tests on this theory. The sizes of Au nanoparticles from different preparation methods measured by TEM and peak wavelength are summarized in Table 2-5.

2.4.2 Zeta potential test

Zeta potential measurement is one of the most critical tests to validate the quality of nanofluids' stability by studying their electrophoretic behavior (Lee, D. et al., 2006; Vadasz, P., 2006). According to the electrostatic stabilization theory, the electrostatic repulsions between the particles increase if there exists a high absolute value of zeta potential, which then leads to highly stable suspensions (Zhu, H. et al., 2007).

Table 2- 6 Zeta potential and associated suspension stability (Vandsburger, L., 2009)

Zeta potential (absolute value [mV])	Stability
0	Little or no stability
15	Some stability but settling lightly
30	Moderate stability
45	Good stability, possible settling
60	Very good stability, little settling likely

The experiments are conducted by using a 0.05% weight fraction of nanosuspension to measure zeta potential and particle size (Wang, X.-j. et al., 2009). The relationship between suspension stability and zeta-potential arises from the mutual repulsion that occurs between similarly charged particles. For this reason, particles with a high surface charge tend not to agglomerate, since contact is opposed. Typically accepted zeta-potential values are summarized in Table 2-6. Generally, a suspension with a measured zeta-potential above 30 mV (absolute value) is considered to have

good stability (Lee, J.-H. et al., 2008a; Vandsburger, L., 2009), this is one of the most common methods among the researchers to determine the stability as mentioned above.

2.4.3 Sediment photograph capturing

A primary method to examine sedimentation of nanofluids is photo capturing. After preparation, a portion of the suspension is put aside to capture photos in certain time intervals. By comparing these photos of nano suspensions, sedimentation of suspension will be determined. Different sets of nanofluid preparation for the photo capturing are illustrated in Figs.2-5 to Fig. 2-7. Clearly variable pH, viscosity and weight fractions for Al_2O_3 and Cu and Cu_2O were investigated after seven days and 24h by photo capturing.

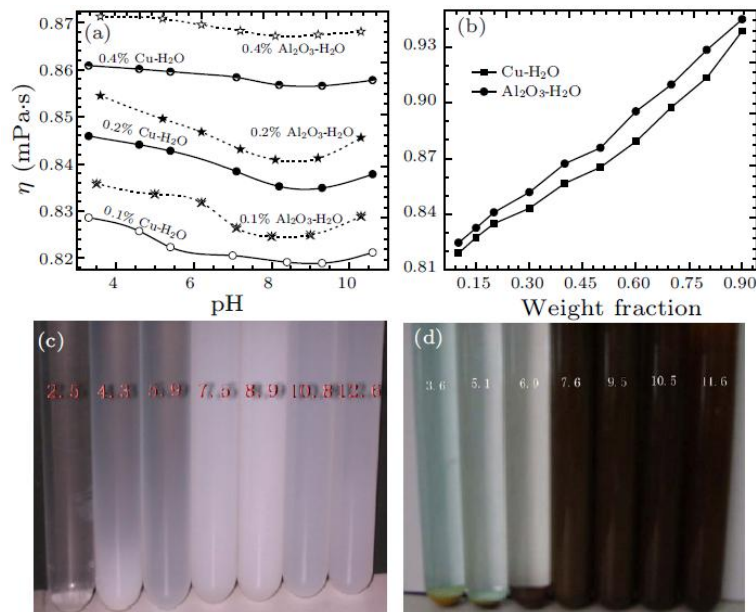


Figure 2- 5 Variation of the nanofluids viscosity with pH and nanoparticles weight fraction at temperature 303 K: (a) the variation of the viscosity with pH, (b) the variation of the viscosity with nanoparticles concentration, (c) the sediment photograph of $\text{Al}_2\text{O}_3\text{-H}_2\text{O}$ suspensions after depositing for seven days, (d) the sediment photograph of $\text{Cu-H}_2\text{O}$ suspensions after depositing for seven days (Wang, H. & Sen, M., 2008)

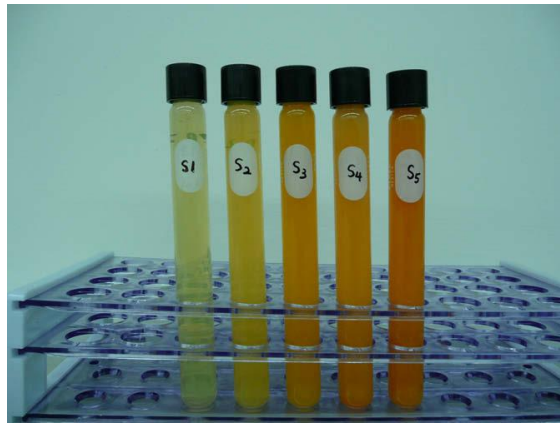


Figure 2- 6 Octahedral-Cu₂O nanofluids 24 h after their preparation (CuSO₄ molar concentration from 0.0025 mol/L to 0.002 mol/L)(Wei, X. et al., 2009)

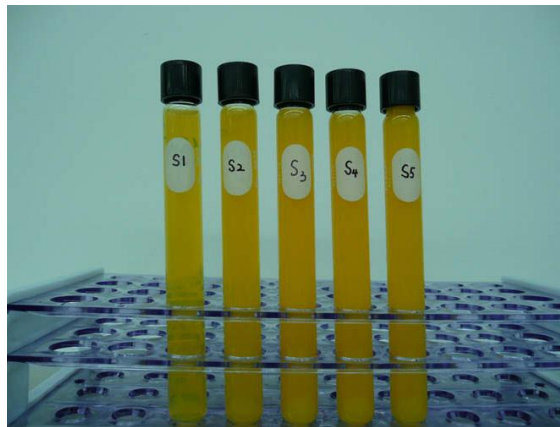


Figure 2- 7 Spherical-Cu₂O nanofluids 24 h after their preparation (CuSO₄ molar concentration from 0.01 mol/L to 0.05 mol/L)(Wei, X. et al., 2009)

2.4.4 TEM (Transmission Electron Microscope) and SEM (Scanning Electron Microscope)

TEM and SEM are very useful tools to distinguish the shape, size and distribution of nanoparticles. Nevertheless, it cannot present the real situation of nanoparticles in nanofluids when dried samples are needed. Cryogenic electron microscopy (Cryo-TEM, Cryo-SEM) might provide a method to resolve this problem if the microstructure of nanofluids is not changed during cryoation. Nanoparticles aggregation structure in nanofluids could be directly monitored by this instrument as well (Wu, D. et al., 2009).

The following procedure is attributed to the standard SEM/TEM micrographs of nanoparticles (Liu, M. S. et al., 2006):

- (1) Obtain stable nanofluid in solution form.
- (2) Place one drop of the solution on sticky tape of top surface of the SEM specimen holder (carbon grid in the case of TEM).
- (3) Heat in the vacuum oven to dry the liquid drop or leave to dry naturally.
- (4) Obtain solid particle.
- (5) Place the sample in the vacuum chamber of SEM/TEM for electron microscopy.

The stable nanofluids have different shapes after preparation as are shown in TEM and SEM images in Figs. 2-8 until 2-13.

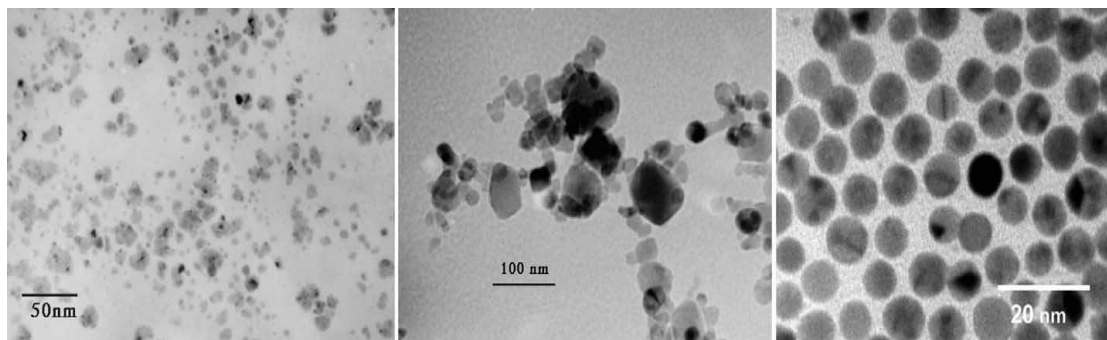


Figure 2- 8 TEM pictures of (left) Cu nanofluids , (middle) CuO nanoparticles and (right) alkanethiol terminated AuPd colloidal particles (Kebinski, P. et al., 2005)

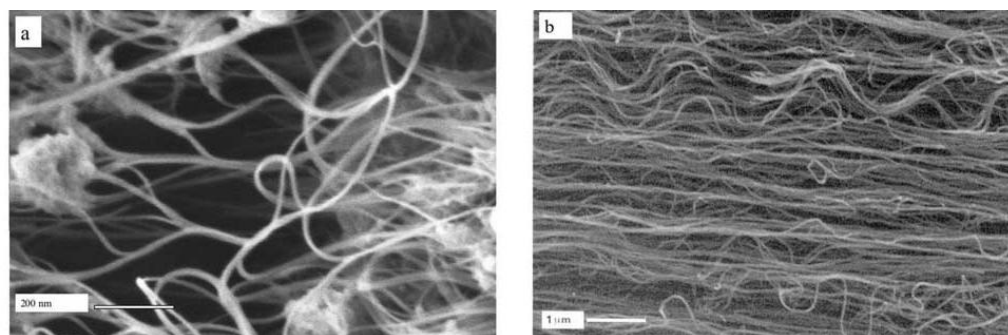


Figure 2- 9 SEM of carbon nanotube a) single-walled carbon nanotubes obtained by arc discharge and (b) multiwalled carbon nanotubes obtained by chemical vapor deposition growth (Kebinski, P. et al., 2005)

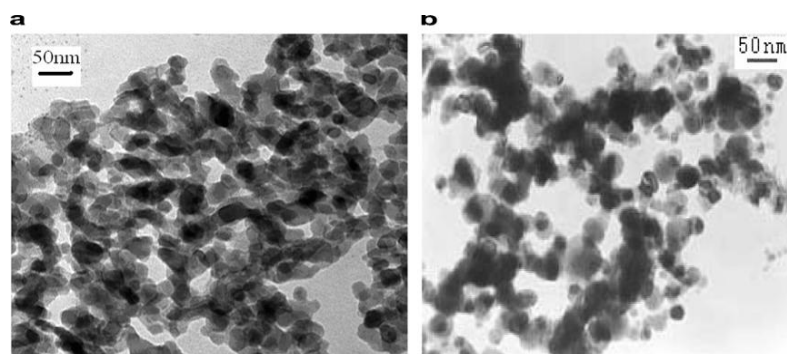


Figure 2- 10 TEM micrograph of nanoparticles (a) nano-alumina (b) nano-copper
(Wang, X.-j. et al., 2009)

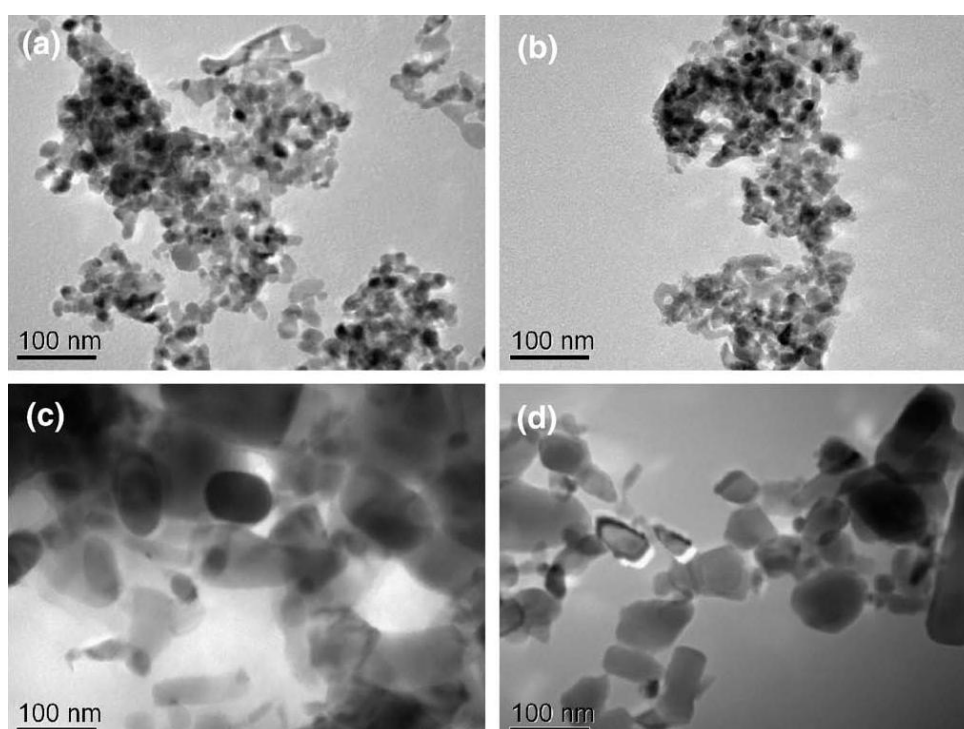


Figure 2- 11 TEM micrographs of ZnO aggregates prepared by two different methods
as mixed suspensions (a, c) and the same suspensions ultrasonically agitated for 60 min
(b,d) (Chung, S. J. et al., 2009)

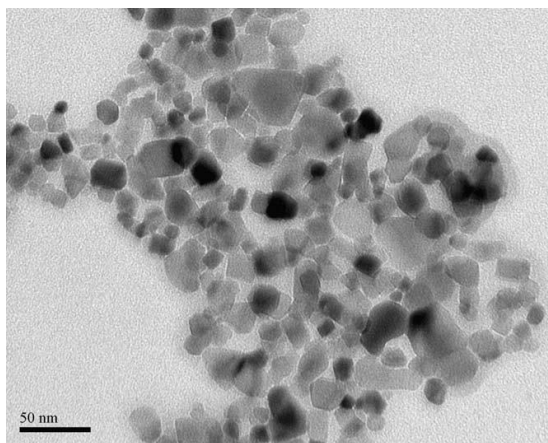


Figure 2- 12 TEM image of dispersed TiO_2 nanoparticles in water

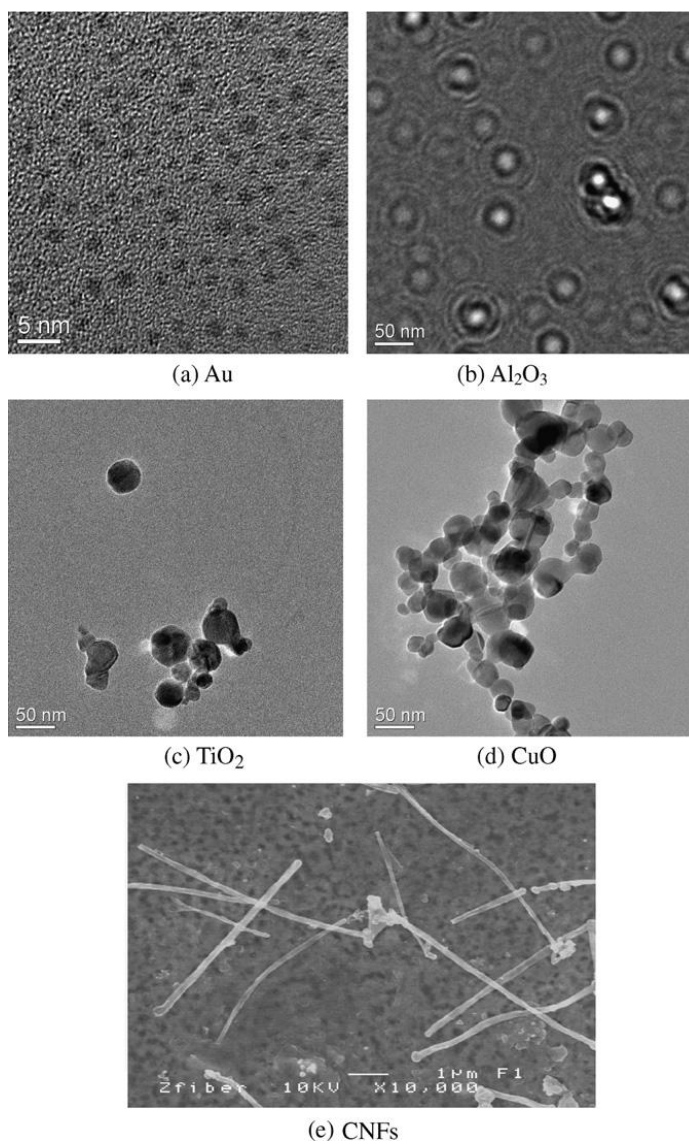


Figure 2- 13 TEM photographs of Au, Al_2O_3 , TiO_2 and CuO particles and carbon nanofibers (Zhang, X. et al., 2007)

2.4.5 Light scattering method

The single-particle analysis from which the light scattering theory can be approached has been used to visualize polymer molecule structure in solutions or colloidal particles in suspension. The intensity of scattered light for a single particle is related to the particle volume. While the interaction of electromagnetic radiation with a small particle is weak in light scattering, most of the incident light is transmitted and only a little amount of light is distributed. In one study, the average size of the clusters was obtained every five minutes after the sonication stopped (Hong, K. S. et al., 2006).

2.4.6 Sedimentation balance method

The stability of the nano-suspension can be also measured by another method named a sedimentation balance. The tray of a sedimentation balance is immersed in the fresh nano-suspension. The weight of sediment nanoparticles during a certain period of time is measured. The suspension fraction (F_s) of nanoparticles at an accepted time is calculated by the formula $F_s = (W_0 - W)/W_0$ in which W_0 is the total weight of all nanoparticles in the measured space, and W is the weight of the sediment nanoparticles at a certain time (Zhu, H. et al., 2007).

2.4.7 Three omega method

The colloidal stability of nanofluid can also be determined by the three omega method. It can be evaluated by detecting the thermal conductivity growth caused by the nanoparticle sedimentation in a wide nanoparticle volume fraction range. There are a few stability measurements attributed to this method in the literature (Oh, D.-W. et al., 2006, 2008).

2.5 Characteristic measurements

There are four major thermophysical properties that their values change due to nanoparticle addition to a host fluid which are thermal conductivity, viscosity, density

and specific heat; however, in this study I focused on thermal conductivity and viscosity of nanofluid. Different investigators have dissimilar ideas about the effect of nanoparticle dispersion. Typically, these nanofluid parameters will increase except for the specific heat which decreases. The percentage of increment will vary as the function of dispersion, volume concentration, temperature, base fluid. There is not a standard protocol for preparation of nanofluid since then it would be obvious if the data will vary from time to time.

2.5.1 Thermal conductivity

Thermal conductivity is the most important factor that can be investigated to prove the heat transfer enhancement of a prepared nanofluid. Reviewing available literature explains that the rise in thermal conductivity of the nanofluids is considerable. Addition of only a small volume percent of solids produces a dramatic enhancement in thermal conductivity (Murshed, S.M.S. et al., 2008; Paul, G. et al., 2010; Trisaksri, V. & Wongwises, S., 2007; Wang, X.-Q. & Mujumdar, A. S., 2007).

Four mechanisms have been identified in the literature as being responsible for heat transfer enhancement in nanofluids under stationary conditions, namely, (i) molecular-level layering of the liquid at the liquid/particle interface, (ii) the nature of heat transport inside the nanoparticles, (iii) aggregation and clustering, and (iv) the Brownian motion of nanoparticles within the base fluid. Henderson and Swol (Henderson, J. R. & van Swol, F., 1984) were the first who proposed that liquid molecules close to a solid surface form a layered structure. Keblinski and co-workers (2002) showed that the atomic structure of this liquid layer is more ordered than that of the base liquid. Yu and Choi (2003) proposed that the main reason of improved thermal conductivity of nanofluid is that liquid nanolayer act as a thermal bridge between a nanoparticle and base fluid.

Following the pioneering work of Yu and Choi many other studies (Chandrasekar, M. & Suresh, S., 2009; Wang, B.-X. et al., 2003; Xue, Q. & Xu, W.-M., 2005; Yu, W. & Choi, S. U. S., 2003) were conducted on various aspects of nanolayering and its effects on thermal conductivity enhancement of the nanofluids. Leong's model in particular highly agreed with experimental data. This led many to believe that the nanolayering phenomenon alone is responsible for extraordinary enhancements in thermal conductivity of nanofluids. Another important mechanism that comes into play when the particles get smaller is the nature of heat transport inside the nanoparticle. While for large particles the heat conduction expressed by the Fourier Law adequately explains the nature of heat transfer, the ballistic heat transport becomes important when the temperature gradient becomes large or sample size is smaller than the mean free path of the phonons. In the case of conductive heat transport phonons go through the material in random directions while in the case of the ballistic heat transport all phonons jump directly from lower surface to the upper surface. According to the Debye theory, the mean free path of the phonon is given by structure of this liquid layer is more ordered than that of the base.

Brownian motion, interfacial layer and aggregation of particles have been discussed about comprehensively (Amrollahi, A. & et al., 2008; Keblinski, P. et al., 2002; Li, L. et al., 2008; Tillman, P. & Hill, J. M., 2007; Wang, B.-X. et al., 2003; Wang, X. et al., 1999; Xie, H. et al., 2005; Xuan, Y. et al., 2003; Xue, Q. & Xu, W.-M., 2005; Yajie, R. & et al., 2005). Some researchers described a nanofluid as a two-phase flow mixture and utilized theories of a two-phase mixture or properties of nanofluid, such as Maxwell's theory (Maxwell, C. & Thompson, J. R., 1904) and the Hamilton and Crosser approach (1962). These models are based on an effective medium theory that presumes well dispersed particles in a fluid medium. If aggregated particles in the fluid form particle chains or clusters, the predicted thermal conductivity would be

significantly higher as was observed by many researchers (Sommers, A. & Yerkes, K., 2009; Wen, D. et al., 2009) ,which might highly be related to the aggregates dimension and the radius of gyration of the aggregates. This result is based on the three-level homogenization theory, validated by MC (Monte Carlo) simulation of heat conduction on model fractal aggregates (Evans, W. et al., 2008; Gharagozloo, P. E. et al., 2008; Gharagozloo, P. E. & Goodson, K. E., 2010). As it can be seen in Fig. 2-14, they related the enhancement of thermal conductivity to nanoparticle aggregation. It is seen that there should be an optimized aggregation structure for achieving maximum thermal conductivity, which is far beyond the prediction from homogeneous dispersions. Such an argument eliminates thermal conductivity as an intrinsic physical characteristic. Possible influence of particle aggregation on conduction highlights the colloid chemistry's significant role in optimizing this property of nanofluids. Meanwhile, there exists another theory of lowering thermal conductivity of aggregation formation as found by Hong et al. (2006) from experiments by light scattering of Fe nanoparticles aggregate. The effective thermal conductivity increment may also depend on the shape of nanoparticles as discussed by Zhou and Gao (Gao, L. & Zhou, X. F., 2006; Zhou, X. F. & Gao, L., 2006). They proposed a differential effective medium theory based on Bruggeman's model to approximate the effective thermal conductivity of nano-dispersion with nonspherical solid nanoparticles with consideration of the interfacial thermal resistance across the solid particles and the host fluids. They found that a high enhancement of effective thermal conductivity can be gained if the shape of nanoparticles deviates greatly from spherical. Many of the researchers suggested altogether new mechanisms for the transport of thermal energy. There is another idea proposed by Koblinski et al. (2002) of an ordered liquid layer at particle interfaces and 'tunneling' of heat-carrying phonons from one particle to another. The subsequent simulation work from the same group of investigators concludes that these mechanisms

do not contribute considerably to heat transfer. Koo and Kleinstreuer (2005) found that the role of Brownian motion is much more significant than the thermophoretic and osmo-phoretic motions. In conclusion, some investigators believe that nanoparticle aggregation plays an important role in thermal transport due to their chain shape (Evans, W. et al., 2008; Karthikeyan, N. R. et al., 2008; Zhu, H. et al., 2006) but some others believe that the time-dependent thermal conductivity in the nanofluids proves the reduction of thermal conductivity by passing time due to clustering of nanoparticles with time (Karthikeyan, N. R. et al., 2008).

Vadasz (2006) showed that heat transfer enhancement may be caused by a transient heat conduction process in nanofluids. Experiments demonstrate that a nanofluids thermal conductivity depends on a great number of parameters, such as the chemical composition of the solid particle and the base fluid, surfactants, particle shape, size, concentration, polydispersity, etc., though the exact variation trend of the conductivity with these factors has not yet been found. Additionally, the temperature influences the thermal conductivity of a nanofluid as shown in several studies that have been carried out to see that effect on CuO, Al₂O₃, TiO₂, ZnO dispersed nanofluids by Mintsa et al. (2009), Duangthongsuk and Wongwises (2009), Vajjha and Das (2009), Murshed et al. (2008), Yu et al. (2009) and Karthikeyan et al. (2008). A temperature increase improves the thermal conductivity of the nanofluids. However, the actual mechanism of this increment has not been revealed yet. A deficiency of reliable data for the conductivity of nanofluid is the major problem of non-commercialization for this product. The other influencing factor for the thermal conductivity increase of nanosuspension is the volume fraction which has been directly proportional with this characteristic (Chandrasekar, M. et al., 2010), although this relationship is generally nonlinear for nanoparticles with a high aspect ratio (Zhu, H. et al., 2006). Thermal conductivity increment data for DI (De- Ionized) water based suspensions were

investigated by Wang et al. (1999), which showed a high rise in comparison with the results of Lee et al. (1999) and Das et al. (2003). Moreover, experiments conducted by Oh et al. (2008) for EG based nanofluids data showed relatively low thermal conductivity values compared to those of Lee et al. (1999) and Wang et al. (1999).

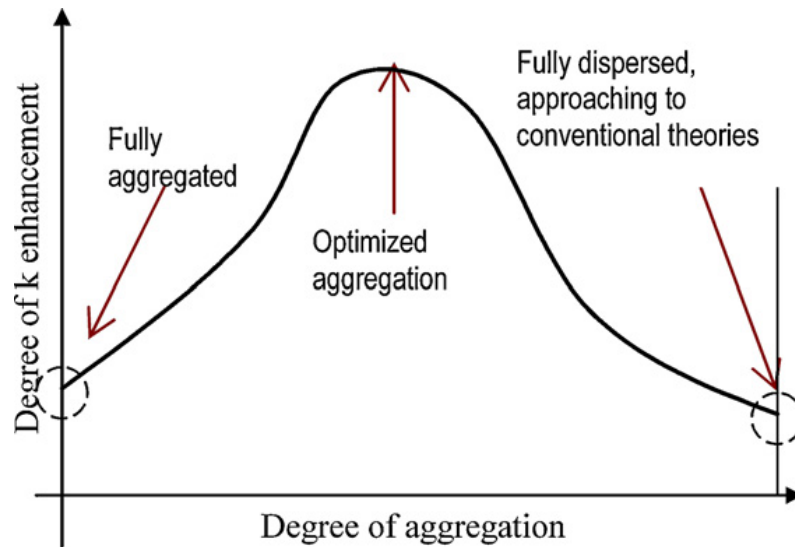


Figure 2- 14 Aggregation effect on the effective thermal conductivity (Wen, D. et al., 2009)

It has been found that the thermal conductivity of a base fluid is nearly constant at different doses of surfactant or base. Hence it seems that this property improvement is related only to the particles when dispersing the nanoparticles into water. The general behavior of the particle-water interaction depends on the properties of the particle surface. Addition of surfactant may cause high or low pH value, which result in a lower surface charge and a weaker repulsion between particles. Therefore, this action leads to a stronger coagulation (Wang, X.-j. et al., 2009).

Xuan et al. (2003) developed a classic theory of Brownian motion and the Diffusion Limited Aggregation (DLA) model for random movement of suspended nanoparticles. This theory does not describe the experimentally determined thermal conductivity satisfactorily; however, the dependence of this characteristic on temperature is also mentioned in their work. The effect of particle surface charge and

IEP is also exposed in varying thermal conductivity experiment sets conducted by Lee et al. (2006). They proved that the colloidal particles get more stable and enhance thermal conductivity of nanofluid when the pH of the solution goes far from the IEP of particles. Moreover, research, demonstrated that there is a priority factor in controlling nanofluid aggregation by surface charge. They proposed a new interpretation of the charged sites and ion densities in the diffuse layer as the number and efficiency of channels for phonon transport, respectively. The same theory was accepted by Wang et al. (Li, X. F. et al., 2008; Wang, X.-J. & Li, X.-F., 2009; Wang, X.-j. et al., 2009).

In conclusion, understanding the mechanism and magnitude of effective thermal conductivity (k_{eff}) of nano-scale colloidal suspensions still continues to be an active research area. A summary of experiments and proposed theories is given in Table 2-7.

Table 2- 7 Summary of different tests that conduct to a theory

Investigator	Nanofluid type	Concentration (%)	Thermal conductivity enhancement	Theory
(Karthikeyan, N. R. et al., 2008)	CuO (8 nm)+DW +EG	1% vol.	31.6% 54%	nanoparticle size, polydispersity, particle clustering and the volume fraction of particles
(Kwak, K. & Kim, C., 2005)	CuO (10-30nm)+EG	<0.002% vol.	N/A	Thermal conductivity enhancement due to viscosity increase
(Lee, D. et al., 2006)	CuO (25nm)+DW	0.3% vol.	3 times increasing pH from 3 to 8	Setting pH far from isoelectric point getting 3 times effective thermal conductivity and better dispersion
(Wang, X.-J. & Li, X.-F., 2009)	Al ₂ O ₃ (15-50nm)+DW Cu(25-60nm)+DW	0.4% wt.	13% 15%	pH control and adding surfactant far from isoelectric point
(Li, X. F. et al., 2008)	Cu+DW	0.1% wt.	10.7%	pH control and adding surfactant far from isoelectric point
(Zhu, H. et al., 2007)	Graphite (106nm)+DW	2.0% vol.	34%	pH control and adding surfactant far from isoelectric point
(Wei, X. et al., 2009)	Cu ₂ O (200.5nm)+DW	0.01-0.05 % vol.	24%	thermal conductivity can be controlled by either the synthesis parameters or its temperature

Analytical model

Even though many models have been developed to predict the nanofluid thermal conductivity, all presented models can be classified into two general groups, as follows:

Static models such as those of Maxwell and Hamilton–Crosser, which presume immobile nanoparticles in the host fluid in which conduction-based models predict the thermal transport properties, and Dynamic models, which are based on the idea that nanoparticles have sideways, arbitrary movement in the fluid. The particle motion is believed to be responsible for energy transport directly through collision between nanoparticles or indirectly through micro liquid convection that enhances the thermal energy transfer.

A simple relationship suggested by Weber (1880) shows the thermal conductivity of liquids with accuracy usually within 15% and the equation is:

$$k = 3.59 \times 10^{-9} C_P \rho \left(\frac{\rho}{M} \right)^{\frac{1}{3}} \quad (2-4)$$

This formula has been developed previously to calculate the thermal conductivity of nanofluids, as:

$$k_{nf} = 3.59 \times 10^{-9} C_{P,nf} \rho_{nf} \left(\frac{\rho_{nf}}{M_{nf}} \right)^{\frac{1}{3}} \quad (2-5)$$

By supposing well dispersed nanoparticles, the thermo-physical properties of the particle fluid mixture can be evaluated using Eqs. (2-6)–(2-8). Properties with subscript ‘‘s’’ are for nanoparticles while without subscripts are for base fluid

$$\rho_{nf} = (1 - \phi) \rho + \phi \rho_s \quad (2-6)$$

$$(\rho C_P)_{nf} = (1 - \phi) \rho C_P + \phi \rho_s C_{p,s} \quad (2-7)$$

$$M_{nf} = (1 - \phi) M + \phi M_s \quad (2-8)$$

The effective thermal conductivity is defined as the ratio of the thermal conductivity of nanofluid to that of the base fluid. Therefore, from Equations (2-4) and (2-5), the generalized form of relative thermal conductivity can be given as:

$$\frac{k_{nf}}{k} = \left(\frac{C_{p,nf}}{C_p} \right)^a \left(\frac{\rho_{nf}}{\rho} \right)^b \left(\frac{M}{M_{nf}} \right)^c \quad (2-9)$$

In which a, b and c should be defined from experiments and are equal to -0.023, 1.358 and 0.126, respectively for Al₂O₃/water nanofluids. Xuan et al. (2003) proposed a formula for the effective thermal conductivity in conjugate with Brownian motion and DLA theory as follows:

$$\frac{k_{eff}}{k_f} = \frac{k_p + 2k_f - 2\phi(k_f - k_p)}{k_p + 2k_f + \phi(k_f - k_p)} + \frac{\rho_p \phi C_p}{2k_f} \sqrt{\frac{k_B T}{3\pi r_c \eta}} \quad (2-10)$$

where k_f , k_p , ρ , C_p , T , μ , ϕ and r_c are the actual thermal conductivity of the base liquid and the nanoparticle, density, specific heat, temperature (K), viscosity, volume concentration and the radius of the cluster, respectively.

Meibodi et al. (2010b) described the model of thermal barrier resistance and claimed that the most important factor for thermal conductivity enhancement of nanofluids might be MFP (Mean Free Path), the distance between particles that can be calculated by Brownian approach for very low nanoparticle volume fractions and by effective diameter for micro-particles and/or high particle volume fractions (Meibodi, M. E. et al., 2010b). The schematic of this model is presented in Fig. 2-15. Likewise, Hadjov (2009) assumed a flux jump and a discontinuity between the inclusion and the matrix as well which is called the thermal conductive interface. This assumption conflicts with the previous model. They stated that the thermal conductivity depends strongly on the morphology via the kind of particle packing.

The thermal conductivity of nanofluids increases linearly as a function of the particle volume concentration. For the simple representation of the thermal conductivity increase, Joo Hyun Lee (2009) developed the augmentation factor, α_{cond} , which is defined as:

$$k_{nf} = k_{bf}(1 + \alpha_{cond} \phi) \quad (2-11)$$

The application of this formula for the same nanoparticles with various measurements method stated different as described in the next section.

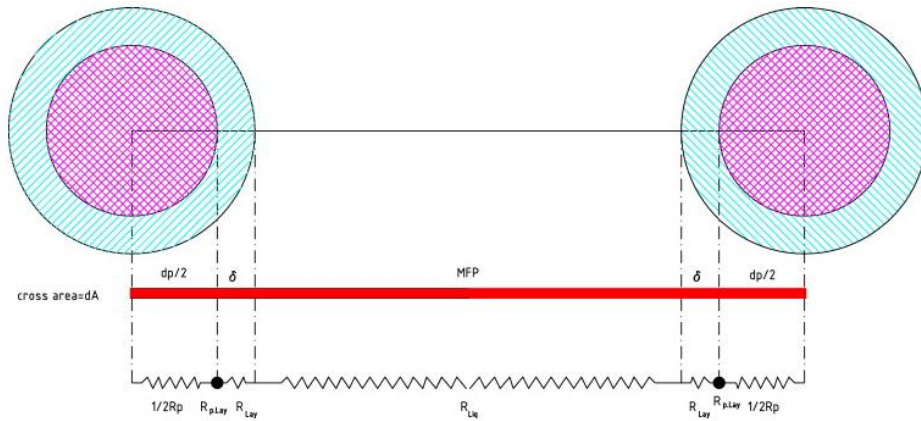


Figure 2- 15 Schematic modeling of a homogeneous suspension containing spherical mono-sized particle with resistance model (Meibodi, M. E. et al., 2010b)

Measurement apparatus

The measurement of thermal conductivity of liquids is a challenging task. In general, Fourier's law of heat conduction is exploited for the measurement of thermal conductivity. The thermal conductivity of nanofluids can be measured by different methods, including transient hot-wire (THW, also called transient line heat source method) which is further categorized into a basic transient hot-wire method, insulated wire method and liquid metal wire method (Beck, M. P., 2008; Das, S. K. et al., 2007; Eastman, J. A. et al., 2004; Peterson, G. P. & Li, C. H., 2006; Tavman, S. & Tavman, I. H., 1998; Vadasz, P., 2006; Vadász, P., 2008). A detailed explanation of the transient hot wire method in measuring the thermal conductivity of nanofluids is given by Lee et al. (1999). Also, a summary of the apparatus utilized for thermophysical properties by different investigators is given in Table 2-8.

Among the stated techniques, the steady state parallel plate method used by Wang et al. (1999) seems to be least affected by the particle sedimentation as their

thickness of the loaded sample fluid is less than one mm. The sedimentation of nanofluids can affect the THW method used by Lee et al. (1999).

Table 2- 8 Equipment used for characteristic measurements

Investigator	nanofluid	Thermal conductivity	Viscosity
(Pantzali, M. N., Mouza, A. A., et al., 2009)	CuO+CTAB Al ₂ O ₃ CNT TiO ₂	THW(Assael et al., 2004)	Rheometer with coaxial cylinders(HaakeRheostress RS600)
(Chandrasekar, M. et al., 2010)	Al ₂ O ₃ +DW	KD2 Pro (Decagon Devices, Inc., USA)	Brookfield cone and plate viscometer (LVDV-I PRIME C/P)
(Duangthongsuk, W. & Wongwises, S., 2010b)	TiO ₂ +DW	THW	Bohlin rotational rheometer
(Wang, X.-J. & Li, X.-F., 2009)	Al ₂ O ₃ +DW Cu+DW	TPS	capillary viscometer
(Wei, X. et al., 2009)	Cu ₂ O+DW	KD2 system	N/A
(Duangthongsuk, Weerapun & Wongwises, Somchai, 2009)	N/A	KD2 system	Bohlin CVO rheometer
(Timofeeva, E. V. et al., 2007)	N/A	KD2 Pro	Ubbelohde capillary viscometer (Fisher Scientific)

An increment of the temperature gradient within the vertical hot wire may be caused by non-homogeneous nanoparticle concentration which might be a source of measurement errors. This is also true for the temperature oscillation technique by Das et al. (2003) where the thermocouple that measures the fluid temperature oscillation lies in the upper half of the nanofluid chamber (Oh, D.-W. et al., 2008). The 3 omega method

is exploited by a small number of investigators; a thin film heater is powered by an AC power source so there is an oscillating heat transfer rate through the material, whose thermal conductivity is to be measured. The three omega wire method may be suitable to measure temperature-dependent thermal conductivity (Murshed, S.M.S. et al., 2008).

Table 2- 9 The $\alpha_{cond.}$ of metal oxide nanofluids (Lee, J. H., 2009)

Particle Material	Particle Size(nm)	Base fluid Material	$\alpha_{cond.}$	Measurement Techniques	References
CuO	36	Water	12	THW	Eastman, J. A. et al., 1996)
CuO	33	Water	3	THW	(Zhang, X. et al., 2006)
CuO	28.6	Water	3.8	3-Omega Method	(Das, K. et al., 2003)
CuO	23	Water	3.8	SSM	(Wang, X. et al., 1999)
CuO	18.6	Water	4	THW	(Lee, S. et al., 1999)
TiO ₂	15	Water	6	THW	(Murshed, S. M. S. et al., 2005)
TiO ₂	40	Water	2.4	THW	(Zhang, X. et al., 2006)
Al ₂ O ₃	47	Water	5	SSM	(Li, C. H. & Peterson, G. P., 2007)
Al ₂ O ₃	47	Water	6	THW	(Chon, C. H. et al., 2005)
Al ₂ O ₃	38.4	Water	2.5	3-Omega Method	(Das, K. et al., 2003)
Al ₂ O ₃	36	Water	6	SSM	(Li, C. H. & Peterson, G. P., 2007)
Al ₂ O ₃	28	Water	4	SSM	(Wang, X. et al., 1999)
Al ₂ O ₃	20	Water	1.3	THW	(Zhang, X. et al., 2007)

Regard to the thermal conductivity of nanofluid, $\alpha_{cond.}$ was calculated by formula (2-11). Table 2.9 was achieved by Lee (2009). In this Table, controlling parameters affecting $\alpha_{cond.}$ are not detected significantly when the available information such as the particle size and preparation method are compared. Therefore, the main reason of these discrepancies among identical nanoparticles is not defined yet and it may be accredited to the diverse preparation methods and the lack of a proper standard in step by step homogenization methods.

2.6 Statistical software for optimization

Statistically designed experiments are a powerful tool for improving the efficiency of experimentation. Through an iterative process, they allow us to gain knowledge about the system being studied with a minimum number of experiments. Inclusion of replicate test conditions allows the estimation of random, experimental variation. Statistical analysis of data generated from the experiment clearly establishes the relationship between the measured parameter of interest (response) and the process parameters (input factors or factors) being studied. The factors may have individual, simple effects on the response (referred to as main effects) or may have effects that are interdependent (referred to as interaction effects). Since the designed experiments are generated on the basis of statistical theory, confidence in the results obtained and conclusions drawn are clearly defined.

Different types of designs are available; their choice is determined by the objectives of the experiment and the current state of knowledge about the experimental environment. They can be categorized as follows:

- Screening
- Fractional & full factorial
- Response surface

2.6.1 Screening

If there would be little data about the target, screening designs can be applied for exploring the experimental space. In this design, information of each factor can be derived, but interactions cannot be interpreted. The factors are run at two levels with only high and low levels as defined by the range of each factor. The number of factors can be as high as 15.

2.6.2 Factorial

Factional designs are used when there is former information about which factors are significant. If a complicated design would be selected, the main effects and their interactions could be distinguished more precise. Two to six factors can be selected in this design in which two-level designs with variation of low and high level appears. Replicate experiments in the center (where all factors are simultaneously held at their midlevel) can detect the behavior of nonlinear factor.

Meanwhile, another design of this series, fractional factorial, exist which can detect the interactions and significant factors by less number of experiments without losing a lot of information (see Figure 2-16).

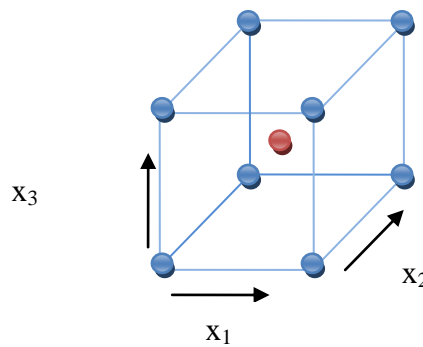


Figure 2- 16 Three-factor full factorial design with center point

2.6.3 Response surface methodology (RSM)

Response surface designs are applied to gain accurate information about factor effects including magnitude and direction. Like factorial design, normally two to six factors with three levels design can be selected to estimate linear, two-factor interaction and nonlinear effects of all factors under study. If there would be a prior indication of nonlinear behavior or when a set of preliminary (factorial) experiments shows nonlinear behavior, selection of this method would be thoughtful. They provide precise prediction of responses within the experimental region and are useful in identifying optimum

conditions. Assay optimization in particular produces responses that are nonlinear. Fig.2-17 shows various response surface designs using three factors for illustration.

2.6.3.1 Central composite design (CCD)

The first approach in RSM is central composite design (CCD) where experiments are added to the factorial design after nonlinear behavior is detected (see Fig.2-17). The next method is a modified CCD, called a face-centered cube design, where the added experiments lie on the faces of the space formed by the factorial design.

Recently, Low et al. (2011) applied RSM in the optimization of the thermophysical properties of composite materials. Furthermore, Ghafari et al. (2009) employed RSM with CCD to optimize the operating variables versus coagulant dosage and pH value. Zabeti et al.(2009) applied the same method to optimize the activity of $\text{CaO}/\text{Al}_2\text{O}_3$ solid catalysts for the production of biodiesel. Nosrati et al. (2011b) applied this technique to find out the effect of parameters such as pH, stirring speed and the concentration of stripping agent on phenol removal.

2.6.3.2 Box-Behnken Design (BBD)

BBD is used to further study the quadratic effect of factors after identifying the significant factors using screening factorial experiments. The Box-Behnken design is an independent quadratic design in that it does not contain an embedded factorial or fractional factorial design. In this design the treatment combinations are at the midpoints of edges of the process space and at the center. These designs are rotatable (or near rotatable) and require 3 levels of each factor. The designs have limited capability for orthogonal blocking compared to the central composite designs.

Box-Behnken designs do not contain any points at the vertices of the experimental region. This could be advantageous when the points on the corners of the

cube represent factor-level combinations that are prohibitively expensive or impossible to test because of physical process constraints.

A Box–Behnken design is run when there is prior information about the existence of nonlinear effects. The experiments are located on the edges of the experimental space. Box–Behnken and CCDs involving up to 10 numerical and 1–3 categorical factors are fast becoming popular because of nonlinear responses common in assay development (Altekar , M. et al., 2006).

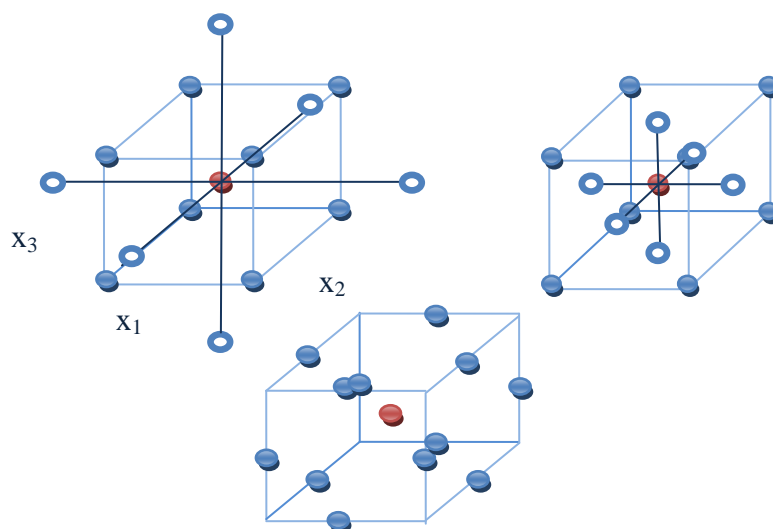


Figure 2- 17 Graphic representations of central composite, face-centered cube and Box–Behnken designs

The effect of different parameters such as concentration of the surfactant, the ratio of organic phase to internal phase in the membrane and membrane to external phase ratio on process parameters were studied using Box-Behnken design and response surface method by Nosrati et al. (2011a). Analysis of variance (ANOVA) provides the statistical results and diagnostic checking tests which enables researchers to evaluate adequacy of the models (Ghafari, S. et al., 2009; Nosrati, S. et al., 2011a).

2.7 Summary

Nanofluid preparation with a single and two-step method would definitely affect the stability as the two-step method needs a higher nanoparticle concentration to equalize the heat transfer enhancement reached by single step. A higher concentration causes more sedimentation. However, unfortunately, the single step method is not industrialized in a wide range so experiments are mostly conducted by two-step method. Therefore, higher costs and lower stability are inevitable.

Major factors influencing the extraordinary enhancement of heat transfer are listed as chemical composition of the solid particle and the base fluid, particle source and concentration, particle shape and size, surfactants, temperature, pH value (surface charge), mono-dispersity, IEP and elapsed time.

Comparing several studies in the literature, some discrepancies appear among the results. At this moment, it cannot be clearly explained why incongruities take place among the measurements of the nanofluid characteristics such as thermal conductivity and viscosity. However, at least we are able to mention that different sources of measurement uncertainties such as sedimentation and aggregation of nanoparticle, lack of a standard for nanofluid preparation, different source of nanoparticle manufacturing, various stabilization methods, and time duration between the nanofluids preparation and measurement in which cause the aggregate to grow with time, could be the most important reasons for the dispersed data. Furthermore, the timing for the ultrasonic processes such as horn processor or ultrasonic bath is not optimized properly with respect to different nanoparticles and base fluids.

There is also another important result regarding stability and thermal conductivity that more stable nanofluid does not necessarily have more enhanced characteristics.

Three methods of homogenization are used by researchers and bring about various results. It can be mentioned that different nanoparticles need their own stability method. Sometimes, these methods have to be combined together while in other cases just one method would be adequate to obtain the preferred stability.

Surfactant selection in nanofluid preparation has an important role in improving heat transfer. Temperature is considered as a restricted factor in case of nanofluid application for exploiting at the high temperatures. Likewise, the optimum percentage of surfactant should be considered as a factor in stable nanofluid preparation as well.

Ultrasonication method, particularly the more effective one named horn ultrasonic, attracts much attention for its short timing preparation among the other homogenization techniques. It has to be considered that if a critical time is exceeded, it may have an inverse effect and cause agglomeration and speedy sedimentation of nanoparticles.

The pH control, which has an important role in stability control, places the IEP of the suspension, far from the PZC in order to avoid coagulation and instability. It should be taking into account that acidic or alkaline pH is corrosive to metals. Therefore, it can lead to damage to the piping and instrumentation in long term applications.

In support of stability measurement, it is better to examine at least three different tests with the different stability measurement apparatus to come out with a reasonable result regarding stability. Furthermore, reproducibility is important in experiments so the samples have to be run at least three times to meet the requirements of uncertainties.

Among the characteristics discussed in the literature, thermal conductivity and viscosity have a major role in nanofluid characterization. To reach the best hypothesis for thermal conductivity enhancement, different theories were discussed such as

Brownian motion, interfacial layer and aggregation of particles. Additionally, some researchers discussed nanofluid as a two-phase flow mixture and utilized certain formulas of two-phase mixtures for properties of nanofluid. However, still none of the proposed theories can exactly predict the improvement of thermal conductivity of nanofluid. Although there are some results regarding the viscosity of nanofluids, none is usable across a wide range of volume fractions of nano particles so further experiments are required.

Systematic experiments are needed that will show the effect of the stability on heat transfer mechanism and characteristics enhancement in stationary condition. Refer to other thermophysical properties, including, specific heat and density, a few researchers conducted tests as the correlations satisfied the result of experiments.

Methodology

Chapter 3: Methodology

3.1 Introduction

This section explains about the chemicals used, the sample preparation methods for different tests and apparatus employed for the experimental investigation of the stability, thermal conductivity and viscosity of nanofluids.

Recently, many researchers worked on the preparation of titania nanofluids. He et al. (2007) stated that, addition of TiO_2 into the base liquid enhances the thermal conduction and the enhancement increases with increasing particle concentration and decreasing particle (agglomerate) size. Increasing agglomerate size and particle concentration will directly increase viscosity. In addition, results from Kim et al. (2007) showed the linear increment of effective thermal conductivity with decreasing the particle size but no existing empirical or theoretical correlation can explain the behavior. Yoo et al. (2007) claimed that, titania nanofluid showed a large enhancement of thermal conductivity compared with their base fluids, which exceeds the theoretical expectation of a two-component mixture system. Additionally, Zhang et al. (2007) could not correctly explain the unexpected enhancement of effective thermal conductivity TiO_2 nanofluid.

Jiang et al. (2003) studied the effect of SDS on stability of CNT. They concluded that the zeta potential for the SDS-CNTs nanofluids was higher than that of the bare CNTs. They suggested that the electrostatic repulsion between the negatively charged cluster surfaces played an essential role in the stabilization of the CNT. In addition, Wang et al. (2008) observed that SDS significantly influences the absolute value of zeta potential in titania and alumina nanofluids by the mass fraction of 0.01 and 0.05% correspondingly.

Chung et al. (2009) worked on the stability of ZnO/water nanofluid under various ultrasonic conditions. They proposed that, the sedimentation behavior of nanofluids is proportional to the volume fraction and the ultrasonic power.

Moreover, the theory of thermal conductivity enhancement is not quite clear after about two decades of experimental and analytical works on nanofluids. Keblinski et al. (2002) elaborated on four potential mechanisms of heat transfer enhancement in nanofluids including Brownian motion, molecular-liquid layering, diffusive propagation of heat in both particles and liquid, and clustering of nanoparticles. At that time they found out that clustering may have a negative effect on heat transfer enhancement. In addition, Xuan et al. (2003) revealed that nanoparticle aggregation reduces the efficiency of the energy transport enhancement of the suspended nanoparticles. However, in 2006, Prasher et al. (2006) boosted up the probability of two of the theories and showed that (1) micro-convection caused by the BM (Brownian motion) of the nanoparticles and (2) clustering aggregation of the nanoparticles leading to local percolation behavior are the most appropriate theories among all due to the experimental and simulation works done in the period of 1993-2005. They finally proved that optimized aggregation size in low volume concentration nanofluids (less than 1%) explains the surprising improvements in thermal conductivity of nanofluids (see Fig. 3-1). Therefore, the reason of scattered data among the investigators may be resulted from not reaching the optimized size for the agglomerates.

In the current research we study the influence of SDS dispersant and ultrasonication on stability of TiO₂-Water nanofluid. Furthermore, the theory of thermal conductivity enhancement in stationary condition will be discussed regard to the clustering and agglomeration theory proposed by Prasher et al. (2006). Stability of prepared nanofluids was verified by TEM, UV-vis spectrophotometer, Dynamic Light Scattering (DLS),

Zeta potential and photo capturing methods. Stability of nanofluid has recently been comprehensively revised by Ghadimi et al. (2011)

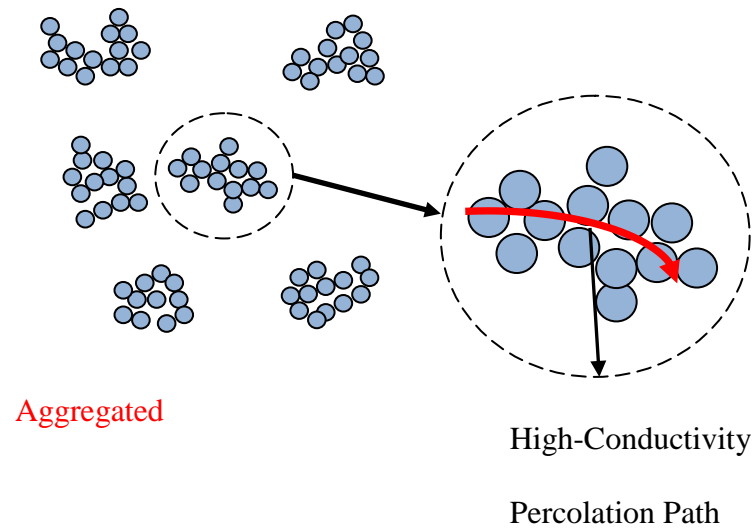


Figure 3- 1 Schematic of well-dispersed aggregates (Prasher, Ravi et al., 2006)

3.2 Materials

Titania (TiO_2) has excellent chemical and physical stability and is a cheap and commercially available mineral product which yet has not been used widely in nanofluid area. Therefore, the experiments were conducted using low concentration titania nanoparticles (Anatase crystallography) up to 1 %vol. with an average diameter of 25 nm and a specific surface area of 45-55 m^2/g dispersed in distilled water. Titania (IV) nanopowder with 99.7% metal basis from Sigma Aldrich Company (USA) was used in this study. The XRD of titanium dioxide that inspects the structure of powder is shown in Figure 3-2 which is exactly the same as the one prepared by the supplier. An anionic surfactant, SDS in chemical grade, from Sigma Aldrich (USA), was used to stabilize the suspension. In this research, the value of pH was controlled by adding NaOH and HCl.

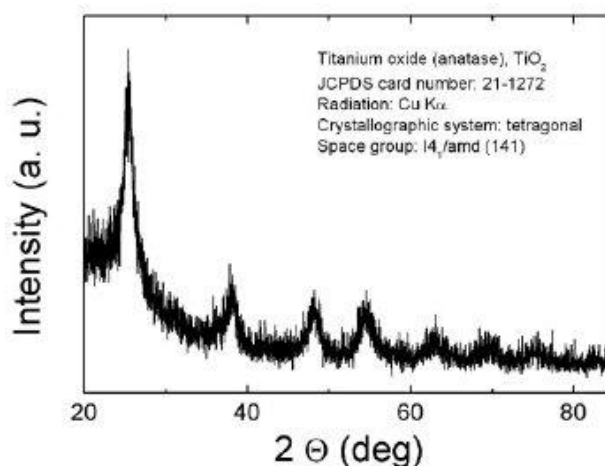


Figure 3- 2 XRD of titanium (IV) oxide

The reason we focused on these two variables is that the reported optimum value in the previous studies is very much variant and controversial. The pH value of aqueous TiO_2 nanofluid for the particle volume fraction of 0.001-0.02 is between 6.2 and 6.8 which show that the nanofluid was nearly neutral. The pH value decreases with increasing particle volume fraction. In fact, this pH range is the Isoelectric point (IEP) of TiO_2 from which the prepared Titania nanosuspension should be far away to be stable. Therefore, adjusting pH for the prepared nanosuspension would be a necessity in order to have a stable nanofluid as can be seen in Figure 3-3 by Penkavova (2011b).

As demonstrated in Table 3-1, the surfactant-nanoparticle concentration ratio is different among various researchers. Moreover, we can see a different pH value for the stability of titanium dioxide nanofluid in the literature as shown in Table 3-2. Therefore, neither any specific pH value nor an optimum ratio of surfactant to nanoparticle concentration has been found in the literature.

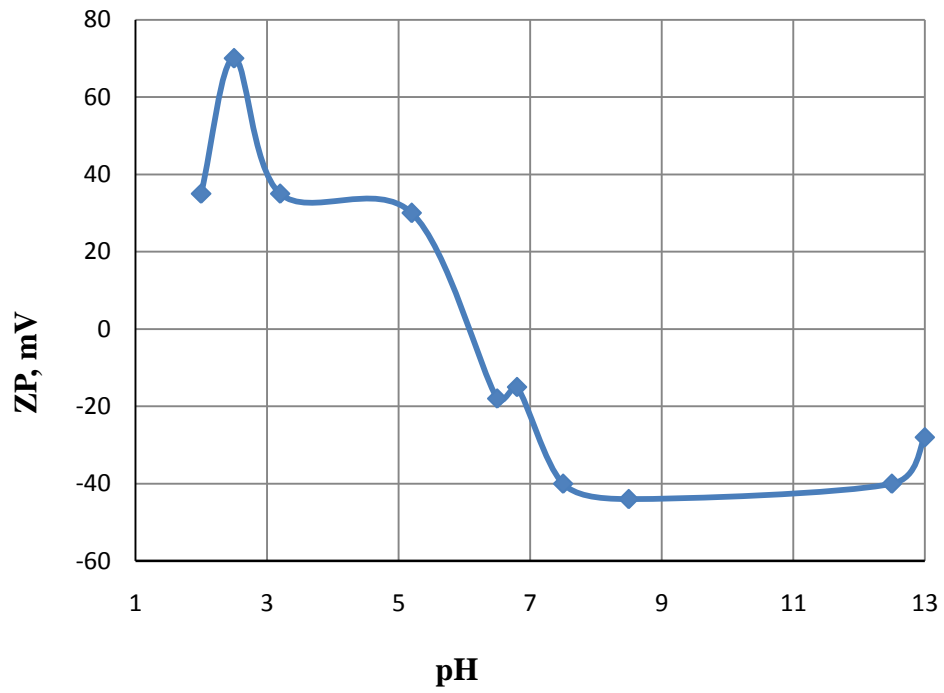


Figure 3- 3 Adjusting of ξ –potential with pH for titania nanofluid (Penkavova, V. et al., 2011b)

Table 3- 1 Surfactant concentration for different nanofluid

Reference	Nanofluid composition	Surfactant to nanoparticle concentration ratio
(Duangthongsuk, W. & Wongwises, S., 2008)	TiO ₂ +CTAB	0.1
(Murshed, S. M. S. et al., 2005)	TiO ₂ +CTAB	
(Kumar, R. & Milanova, D., 2009)	CNT+ NaDBS	0.25
(Wang, X.-j. et al., 2009)	Al ₂ O ₃ +SDBS	1
	Cu+SDBS	
	CB+SDS	
(Hwang, Y. et al., 2008)	Ag+Oleic Acid	2

Table 3- 2 Stability process and duration for different methods

TiO ₂ Nanofluid	Stability process	Surfactant concentration	Stability duration
		%vol.	
(Wen, D. & Ding, Y., 2005)	pH=3.0	0.19-0.57	Several weeks
	ultrasonication and high shear mixing pH=10.0		
(Pak, B. C. & Cho, Y. I., 1998)	mixing(10000 rpm)	1-10	More than 6 days
(Murshed, S. M. S. et al., 2005)	2 hours CTAB	0.5-5	Some clusters
	ultrasonication 8-10 hours pH =11.0		
(Chen, H. et al., 2008)	high shear homogenizer	N/A	stable for at least two weeks

3.3 Applied apparatus

A Zeta size analyzer Malvern in nano series was applied for measuring the particle size distribution and Zeta potential value of nanofluid. The X-ray diffraction (XRD) was employed for inspecting the structure of powder and the UV-visible absorption spectrum Varian Cary 50 probe for inspecting the light absorption strength and absorbance of the nanoparticles in the nanosuspension. An ultrasonic bath (Branson 3210) and a horn processor (Sonic Vibra cell) were utilized for preparing a homogeneous dispersion. PH value was adjusted by a pH meter (Eutech). Thermal conductivity and viscosity of nanofluids were determined by a KD2 Pro (Decago) and an A&D viscometer correspondingly.

3.4 General Samples preparation

A two-step method, which is the most practical method based on the literature survey, was employed to prepare the nanosuspension. Following steps were pursued in preparing samples by the preliminary experiments. Weighing the desired amount of nanoparticles and the container were followed by pouring the distilled water via volumetric flux into the container. In the case of dispersant addition, initially, SDS should be added to the water, stirred completely via a magnetic stirrer for almost 1.5 hours to have a suitable dispersion. Secondly, the weights of nanoparticles were measured and added to the solution. In order to apply an ultrasonic process, there exist two methods of ultrasonication regard to the objectives. The aim of the first objective is to differentiate the outcomes of these two methods including ultrasonic processing by the aid of horn (15 minutes) and bath (3 hours) with and without surfactant addition with the same concentration of 0.1%wt. Second and third objectives were achieved by three hour ultrasonic bath, SDS addition which was nominated as the best result of the first objective. In addition, pH control was added as a factor to monitor the stability and its influence on thermal conductivity. Therefore, the suspension pH value was adjusted before and after nanoparticle addition. The last objective was achieved by sonication with a horn processor for different duration at different percentage of its amplitude.

Various tests were conducted to investigate the effects of homogenization methods on minimizing the agglomeration and improving the stability of nanofluid, including UV-vis spectrophotometer, zeta potential and particle size measurement, TEM, sedimentation balance method and photo capturing. The specification of applied apparatus is presented in appendix Table A-1.

3.4.1 Absorbance measurement by UV-vis spectrophotometer

UV-vis spectrophotometer absorption measurement which was tested by Varian, Cary 50 probe, initially conducted with a scan of the nanofluid to extract the peak. The

peak of titania samples was almost 320nm as shown in Figure 3-4. Afterward, the calibration graph was obtained versus absorbance for three different concentrations which was supposed to be between 0.01 and 0.02 wt.% (Jiang, L. et al., 2003).

The standard graph is demonstrated in Fig. 3-5 in which the concentration of the nanofluid is linearly related to the absorbance. In order to measure the concentration and absorbance of the nanofluid, different samples were examined by this standard graph. The experiments were repeated three times and in order to prevent incidental errors, the results were averaged.

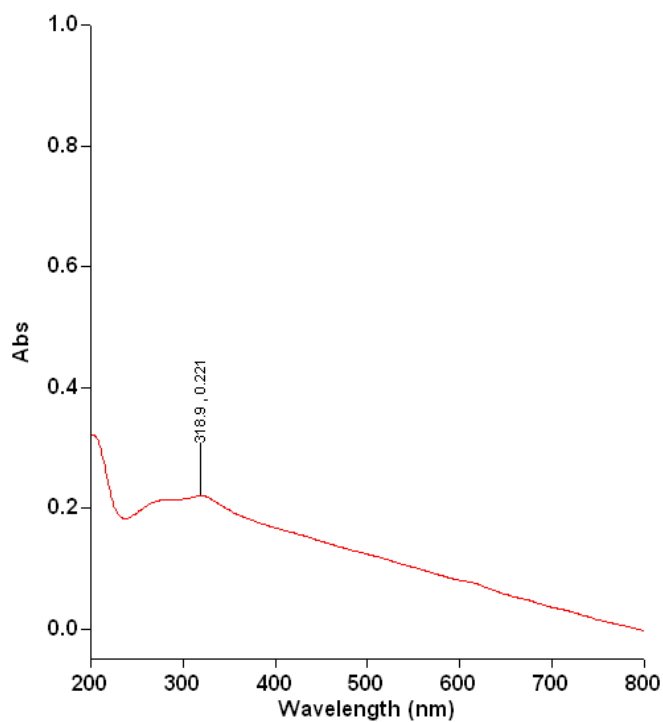


Figure 3- 4 UV-vis spectrophotometer for TiO₂ nanofluid with 25 nm average diameter

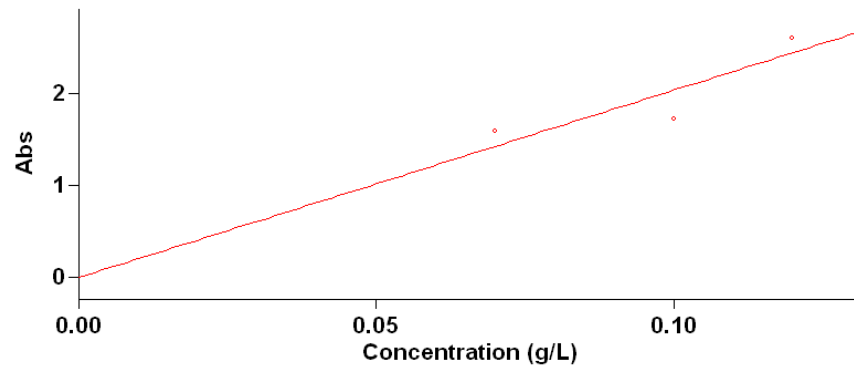


Figure 3- 5 Calibration curve at wavelength of 320 nm for titanium dioxide nanofluid (A.Ghadimi & Metselaar, H. S. C., 2011)

3.4.2 Zeta potential and particle size measurement

In order to measure the zeta potential and particle size result, the suspension was stirred and sonicated for about 15 minutes. Concentrated suspensions are not suitable for particle size and zeta potential measurements. Consequently, transparent suspensions are needed. If our prepared nanofluid was not clear enough for this purpose, the samples were diluted by the ratio of 1:7 with distilled water. Each experiment was repeated minimum three times to calculate the mean value of the experimental data.

3.4.3 Sedimentation balance method and photo capturing techniques

With the purpose of stability analysis by photo capturing method, the fresh nanofluid was poured into vials or gradient cylinders of 10 ml, 50 ml or 100 ml. Subsequently, a digital camera was applied to take the pictures within certain intervals. Meanwhile, Sedimentation rate was calculated in the light of abovementioned formula in section 2-4-6.

3.4.4 TEM sample preparation method

A drop of the fresh nanofluid was placed on a carbon grid with 250 mesh by a pipette. The sample should be rested for 3-5 days to get dry completely. Afterward, the

sample was checked by a transmission electron microscope to detect the agglomeration size, and shape.

3.5 Thermophysical properties

3.5.1 Thermal conductivity relations and calibration

Transient Hot Wire method (THW) is a well-established, most accurate and reliable technique for the thermal conductivity measurement of nanofluids, which was applied successfully by different researchers (Abareshi, M. et al., 2010; Mints, H. A. et al., 2009; Moosavi, M. et al., 2010; Wen, D. & Ding, Y., 2004; Yeganeh, M. et al., 2010). Therefore, thermal conductivity measurements in this work were done based on THW method. This thermal analyzer device has 5% uncertainty over the 5°C to 40°C temperature range. The device was calibrated by glycerin and distilled water in which the measurements were within the above-mentioned accuracy. Hagen correlation (Hagen, 1999) for distilled water, which was compared with experimental data, is shown in appendix 1 Figure A-1. Thermal conductivity of fresh nanofluid was measured right after preparation.

KD2 pro reaches the thermal conductivity from the temperature response of a thermocouple by using THW system. The temperature change and the subsequent thermal conductivity can be calculated by following relation:

$$T(t) - T_{ref} = \frac{q}{4\pi k} \left[\ln(t) - \gamma - \ln\left(\frac{a^2}{4\alpha}\right) \right] \quad (3-1)$$

where $T(t)$ is the temperature at time t , T_{ref} a reference temperature, q the electric power applied to the hot-wire, k the thermal conductivity, γ the Euler's constant, a the wire radius, and α is the thermal diffusivity of the test fluid. This shows that $\Delta T = T - T_{ref}$ and $\ln(t)$ are linearly related with a slope $m = q/4\pi k$. Linearly regressing ΔT on $\ln(t)$ yields a slope that, after rearranging, gives the thermal conductivity as:

$$k = \frac{q}{4\pi m} \quad (3-2)$$

where q is known from the supplied power (Wei, X. et al., 2009).

The uncertainty of measurement was tested by Hong et al (2011). They stated that it takes a limited time for the heat flux on the wire surface to reach steady state. In addition, the temperature data during the transient phase should not be included in the temperature data to estimate the thermal conductivity. Therefore, the start-time of the selected temperature data range should be set after the transient phase which for the case of the 50 μm diameter platinum wire in THW is about 1 s.

3.6 Design of Experiment (DOE)

Design of Experiments is a set of techniques that revolve around the study of the influence of different variables on the outcome of a controlled experiment applied in this study (Version 8.0). Generally, the first step is to identify the independent variables or factors that affect the product or process, and then study their effects on a dependent variable or response. The experimental designs employed in this research were consisted of two design sets of experiments. The primary design is a five level two factor CCD for optimizing the influence of homogenization method by means of surfactant addition and pH control. It has 11 runs with three replicates at the center to verify reproducibility.

The subsequent design is a three level three factors BBD to optimize the influence of ultrasonication by means of time and power with increasing nanoparticle volume fraction. This study includes 17 run with 5 replicates in the center.

3.6.1 Data analysis

The quadratic equation model for predicting the optimal conditions can be expressed according to Eq. (3-4):

$$Y = \beta_0 + \sum_{i=1}^k \beta_{0i} \cdot X_i + \sum_{i=1}^k \beta_{ii} \cdot X_i^2 + \sum_{i \leq j}^k \sum_{j=1}^k \beta_{ij} \cdot X_i \cdot X_j + \dots + e \quad (3-4)$$

where i is the linear coefficient, j is the quadratic coefficient, β is the regression coefficient, k is the number of factors studied and optimized in the experiment, e , is the random error and Y is the predicted response. The response surface plots are obtained by a statistical process that is described in the design and the modeled CCD data. The relationships between the parameter and the responses are graphically illustrated by RSM to get the exact optimum. Meanwhile, we can use the analysis of variance (ANOVA) and least squares techniques to evaluate the statistical specification of the constructed models. The ANOVA consists of determining which factor significantly affects the response, using a Fisher's statistical test (F-test). The significance and the magnitude of the estimated coefficients of each variable and all their possible interactions on the response variable are determined. Such coefficients for each variable represents the improvement in the response, that is, to expect as the variable setting is changed from low to high. Effects with a confidence level less than 95% (effects with a p-value higher than 0.05) were discarded and pooled into the error term and a new analysis of variance was performed for the reduced model. The p-value represents a decreasing index of the reliability of a result. The fitness of the model can be recognized by the regression coefficient (R). However, the adjusted regression coefficient (R_{adj}) and the prediction regression coefficient (R_{pred}) are better criteria than the absolute regression coefficient. In statistical modeling the R_{adj} , shows the number of regression variables and the R_{pred} , indicates the predictive power of the model. Hence, R , R_{adj} and R_{pred} together are very convenient to get a quick impression of the overall fit and the prediction power of a constructed model.

The “Lack of Fit Tests” table compares residual error with “Pure Error” from replicated design points. If there is significant lack of fit, as can be also shown by a low probability value (“Prob>F”), then we have to be careful about using the model as a response predictor. In this case, the linear model definitely can be ruled out, because it’s

Prob > F falls below 0.05. The quadratic model, identified earlier as the likely model, does not show significant lack of fit.

Adequate precision (AP) compares the range of the predicted values at the design points to the average prediction error. Ratios greater than 4 indicate adequate model discrimination.

The coefficient of variance (CV) as the ratio of the standard error of estimate to the mean value of the observed response defines reproducibility of the model. A model normally can be considered reproducible if its CV is not greater than 10% (Chang, H. et al., 2007; Ghafari, S. et al., 2009; Liu, S. et al., 2010; Nosrati, S. et al., 2011a, 2011b).

Result and discussion

Chapter 4: Results and discussion

In this chapter, results of the performed experiments are discussed to observe the influence of nanofluid dispersion methods on nanofluid characteristics. The characteristics assessed were thermal conductivity and viscosity along with the stability parameters like zeta potential, particle size, TEM, sediment photo capturing, sedimentation balance method and UV absorbance. The homogenization methods included ultrasonication (bath and horn processor), surfactant addition and pH control. Evaluation of stability inspection by UV-vis spectrophotometer was investigated in relation to elapsed time. In addition, duration and power of horn ultrasonication were also investigated as independent factors for modeling and optimization of homogenization process and their influence on the stability and thermal conductivity of prepared nanofluid.

4.1 Effect of homogenization process on thermal conductivity and stability of low concentration titania nanofluid

4.1.1 Preliminary studies

Some preliminary experiments were carried out to observe the effect of different homogenization methods on the stability of titania nanofluid including surfactant addition and ultrasonic bath and horn. The samples were monitored by photo capturing and UV-vis spectrophotometer scans.

4.1.1.1 The influence of surfactant addition on stability of titania nanofluid

Three low concentration samples of titania nanofluid (0.007-0.012%wt.) were prepared to investigate the effect of surfactant in sedimentation rate of nanoparticles. As can be seen in Figure 4-1, sample (a) shows fresh nanofluids, whereas samples (b) and (c) display the same concentrations after the period of one week with SDS and without SDS, respectively. The suspensions demonstrated that after an interval of one week, the

nanofluids with surfactant would have an increasing rate of precipitation compared to the nanofluids without surfactant. Since nanofluid is prepared by a simple mixture of nanoparticles and distilled water, the accelerated sedimentation rate in surfactant treated group should not be adopted as a general rule. Therefore, some more experiments are required to observe the effect of ultrasonication on surfactant treated nanofluid.

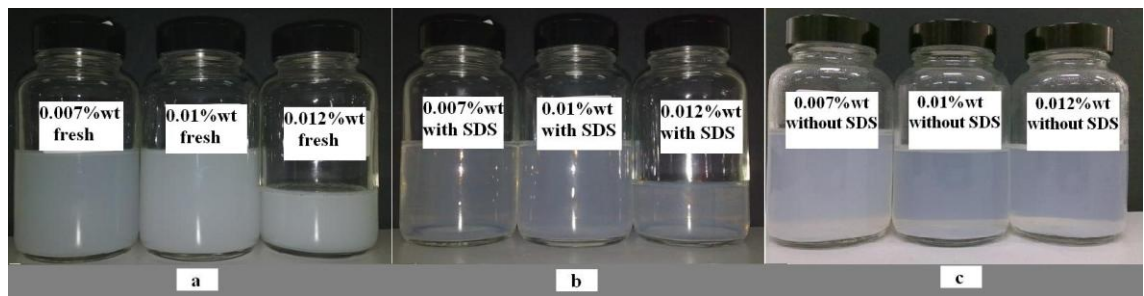


Figure 4- 1 Sedimentation rate of TiO_2 /water nanofluid after one week without any ultrasonication: a) fresh low concentration of TiO_2 nanofluid; b) same concentration as (a) with SDS; c) same suspension without SDS

4.1.1.2 The influence of surfactant and horn ultrasonic on the stability of titania nanofluid

Determining the processing time for horn ultrasonic is important because durations longer than optimum will cause agglomeration (Garg, P. et al., 2009; Lee, J. H. et al., 2008). The effect of different timing of ultrasonic horn in terms of particle size can be seen in Figure 4-2. Based on the results presented in this Figure, increasing the horn ultrasonic time would change the particle size distribution and breaks down the agglomeration into smaller sizes. Moreover, Figure 4-3 shows that increasing the ultrasonic time will improve the absorbance of low concentration nanofluid which is linearly related to concentration of the samples (see calibration curve, Figure 3-5). In addition, Figure 4-4, which shows photo capturing of the samples, reveals that 15 minutes ultrasonic horn will decrease the sedimentation rate especially if it would is

accompanied by surfactant addition. Therefore, SDS addition and horn ultrasonic improve the stability of titania nanofluid.

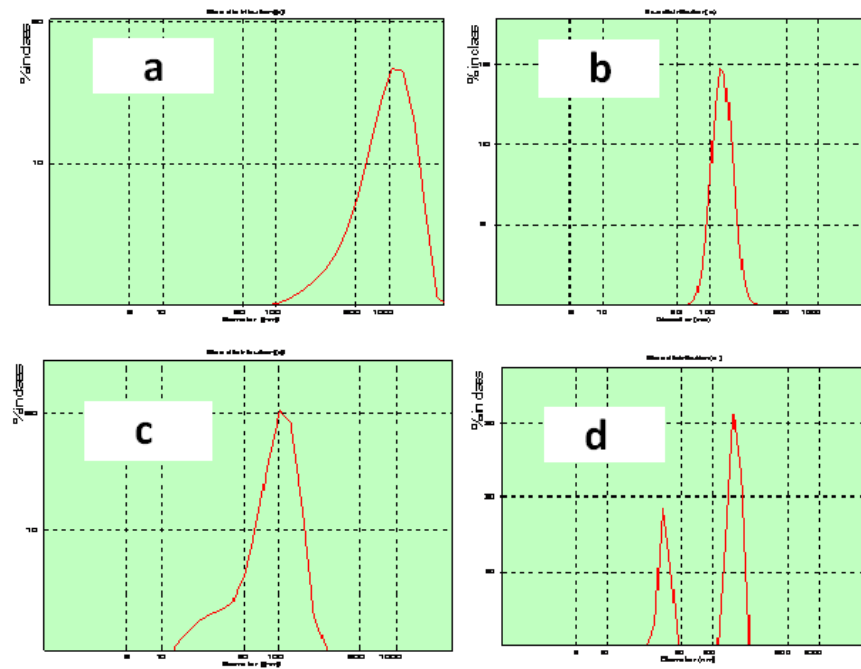


Figure 4- 2 Particle size distribution by different horn ultrasonic processor timing
(a)- without ultrasonic processing: (b)- after 6 min ultrasonic processing (c)- after 10 min ultrasonic processing (d)- after 15 min ultrasonic processing

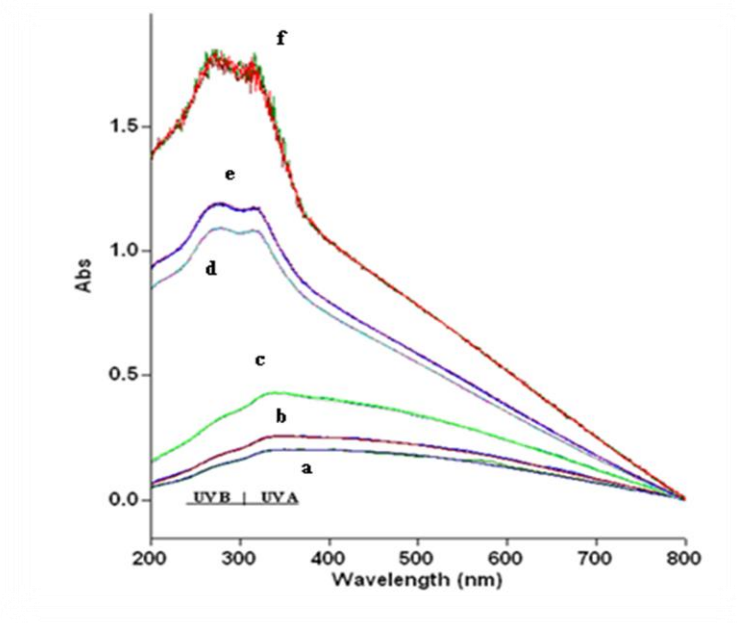


Figure 4- 3 UV-vis spectrophotometer evaluation of ultrasonic process on the absorbance of TiO_2 nanofluid (a),(b) and (c) 0.007% wt., 0.01% wt. and 0.012% wt.

respectively before ultrasonication; (d),(e) and (f) 0.007% wt., 0.01% wt. and 0.012% wt.
respectively after 15 minutes ultrasonic process

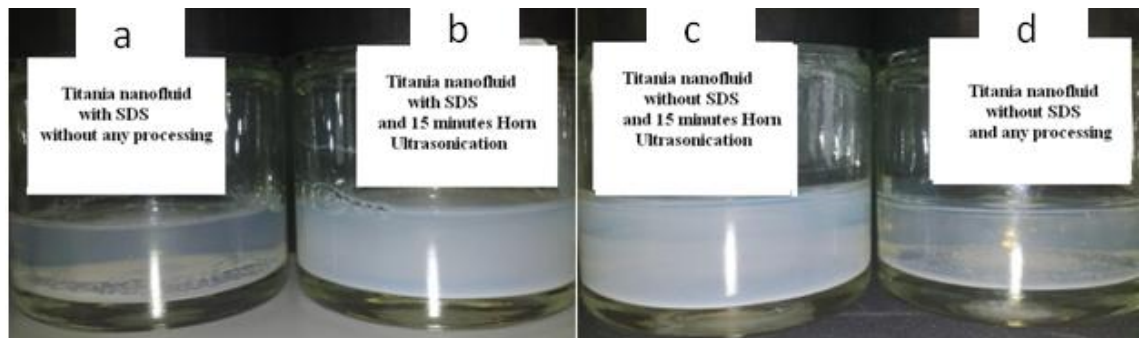


Figure 4- 4 Photo capturing of the effect of surfactant and horn ultrasonic on TiO_2 nanofluid at five days after preparation; a) with surfactant without ultrasonic process, b) with surfactant and 15 minutes horn ultrasonic, c) without SDS with 15 minutes horn ultrasonic, d) without surfactant and ultrasonic process

4.1.1.3 The influence of surfactant and ultrasonic bath on stability of titania nanofluid

Figure 4-5 shows the influence of ultrasonic bath on the concentration of nanofluid. This parameter, which has a linear relation with absorbance, can be detected through the absorbance measurement of UV-vis spectrophotometer. Changing the processing time from one to three hours shows an enhancement in the absorbance of UV as illustrated in Figure 4-5 and this incident proves better stability achievement. The result confirms that longer ultrasonication leads to more homogenized suspension. Moreover, in Figure 4-6 we can observe the impact of surfactant on dispersion of titania nanoparticles by ultrasonic bath. Samples (a) and (b) were prepared by dispersion of 0.1 %wt. titania with three hours ultrasonic bath. However, sample (b) contains the same weight concentration of SDS in its recipe. It revealed that the precipitation rate is faster in the surfactant-free sample (a) and supernatant part clears more promptly ($L_1 > L_2$ in Figure 4-6 (1), (2) and (3)). However, after one year sample (b) is surprisingly clear but sample (a) is still opaque and contains nanoparticles. Consequently, surfactant addition

coupled with three hours ultrasonic bath improves the stability merely for short term application but in the case of long term, it is not effective and requires more experiments.

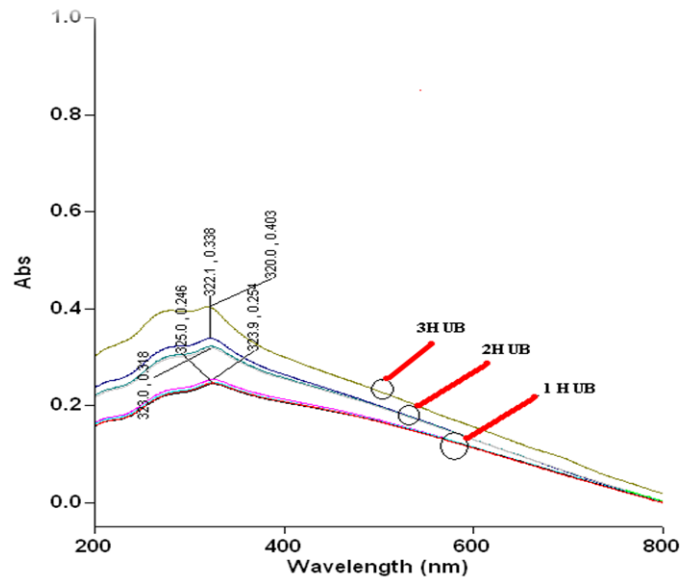


Figure 4- 5 UV-vis spectrophotometer evaluation of titania nanofluid after one, two and three hours of ultrasonic bath

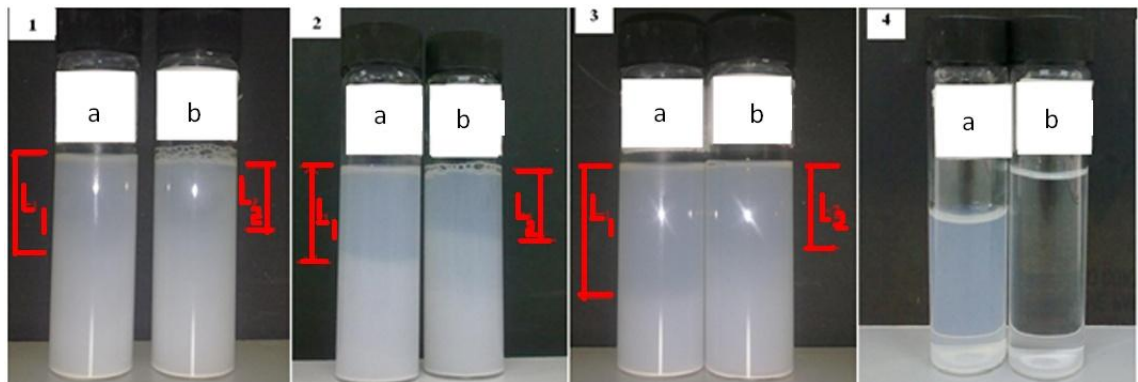


Figure 4- 6 The effect of three hours ultrasonic bath and surfactant addition on 0.1% wt. titania nanofluid; sample (a): without SDS, sample (b): with SDS; 1) three days after preparation; 2) four days after preparation; 3) one week after preparation; 4) one year after preparation

4.1.2 Monitoring results

By preliminary studies, it was found that agglomerations of nanoparticles with 0.1 %wt. concentration are broken down when sonicated for fifteen minutes by ultrasonic horn or three hours by ultrasonic bath. But in order to compare the results and choose an optimal timing of ultrasonication, six different samples of 0.1% wt. were prepared by simple mixture, ultrasonic bath and ultrasonic horn, with and without addition of SDS. The homogenization methods for the six samples are presented at Table 4-1. Subsequently, four different methods including TEM, zeta potential, particle size and UV-vis absorbance were appointed to monitor the homogeneity of nano-suspensions. In addition, thermal conductivity and viscosity of the samples were measured to characterize the nanofluids. Measurements were carried out immediately after preparation.

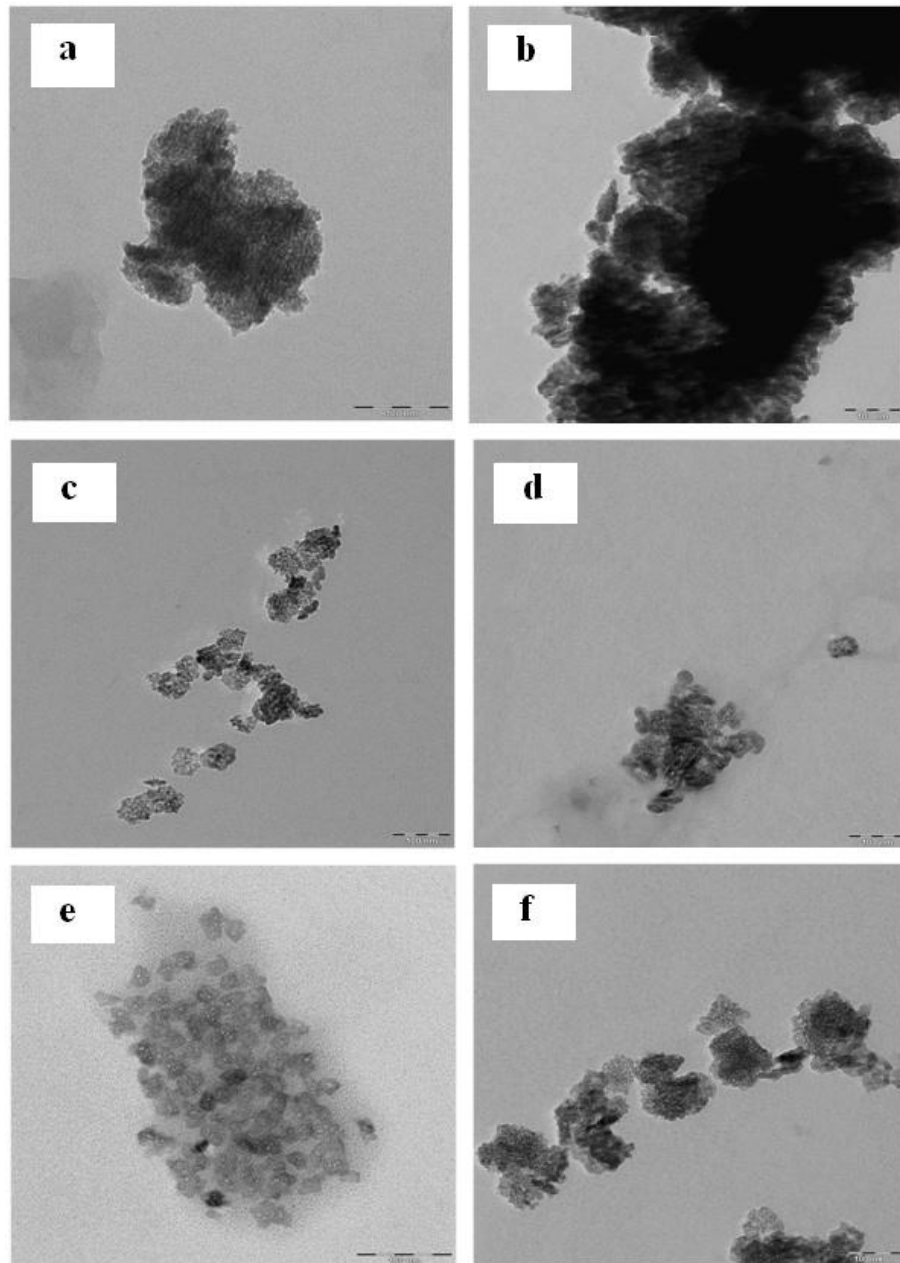
Table 4- 1 Different homogenization method for preparing samples

Sample	Homogenization technique
T1	0.1% wt. TiO_2 , a simple mixture
T2	0.1% wt. SDS and TiO_2 , a simple mixture
T3	0.1% wt. TiO_2 prepared by 15 minutes ultrasonic horn
T4	0.1% wt. TiO_2 and SDS prepared by 15 minutes ultrasonic horn
T5	0.1% wt. TiO_2 prepared by 3 hours ultrasonic bath
T6	0.1% wt. TiO_2 and SDS prepared by 3 hours ultrasonic bath

4.1.2.1 TEM images

After preparation of nanofluids, a drop of each suspension was placed on top of a carbon grid (250 mesh) to be scanned with TEM. Subsequently, the samples were dried for three to five days. Figs 4-7 show TEM images of six samples prepared to monitor their aggregation and level of dispersion. In essence, the particles are near-spherical. Figs. 4-7 (a and b) represent simple mixtures of titania nanofluid with and without SDS, correspondingly. We noticed black agglomerations in Figs. 4-7.a and 4-7.b in which surfactant treated nanofluid contains quite large agglomeration. This means

that surfactant addition should be accompanied by a sort of processing in order to function properly within suspension. It is noticeable in Fig. 4-7.c that ultrasonic horn processor can affect the nanofluid by clustering around the small agglomerations. In this case, based on Evans et al.(2008) and Wang et al. (2003), I could expect an enhancement on thermal conductivity of this sample which will be discussed further in section 4-2-3.



Figures 4- 7 TEM images (Scale 100 nm) of 0.1% wt. titania nanofluid with different preparation method; a) T1; b) T2; c) T3; d) T4; e) T5; f) T6

By adding surfactant and applying ultrasonic horn, clustering will be more evident (Figure 4-7.d).

Figs. 4-7.e and 4-7.f depict the results of three-hour ultrasonic bath on nanofluids with and without surfactant; this process was found to be more effective on SDS added suspension. Clustering and less agglomeration can be seen in Fig. 4-7.f. This suggests three hours ultrasonic bath with SDS added surfactant as an optimum condition to have a good stability. Although, this kind of preparation condition should be checked with other means of inspections in parallel, concerning the clustering theory proposed by Koblinski et al. (2002).

4.1.2.2 Sedimentation rate by UV-vis spectrophotometer

Figure 3-4 shows that two different peaks appeared by scanning the diluted suspension of nanofluids around 280 nm and 320 nm. It was found that the first peak is related to size scattering of the nanoparticles, but the second peak remained even after imposing different processes. Therefore, the focus of this research is based on the second peak of 320 nm wavelength. Stability measurement of nanofluids with UV-vis spectrophotometer was first proposed by Jiang et al. (2003) as an extension of the sediment time method. Peak scanning and standard preparation of nanofluid are the most important issues that need to be taken into account as reported by (Hwang, Y. et al., 2007; Hwang, Y. et al., 2006; Jiang, L. et al., 2003).

Literature review showed that a standard preparation method should be a diluted suspension of around (0.01-0.02 %wt.) so that UV-vis spectrophotometer can detect the wavelengths (Habibzadeh, S. et al., 2010). Finally, our research came out with diluted concentrations of titanium dioxide between 0.007% and 0.012%.wt. The concentration (standard) graph is presented in Figure 3-5.

The six prepared samples were monitored by UV-vis sediment method in Figure 4-8. This graph demonstrates the relative concentrations of the six samples (see Table 4-1) in the elapsed time of seven days.

Nanofluid sample without ultrasonic processing and surfactant would sediment the fastest (T1 and T2). As can be seen in Figure 4-8, the measurement after two days shows very little concentration which confirms the unstable condition of this simple mixture. Although this method has the lowest rate of precipitation, its low concentration makes it unappealing. Comparing T1, T3 and T5, reveals that (Figure 4-8) 15 minutes ultrasonic horn would not have a proper influence on absorbance as it has the lowest concentration rate due to the UV-vis spectrophotometer results. Conversely, suspensions with surfactant had better concentration and relative stability. But it is evident that the impact of 15 minutes ultrasonic horn is more than an unprocessed nanofluid.

The best relative concentration of nanofluid comparing with the fresh one is for T6, although the slope of the sedimentation rate is steep and it is possible to have a clear nanofluid after one month. As a result, surfactant addition to the nanofluid shows a very effective influence on the stability of nanofluid.

The rate of sedimentation is different among these 6 samples as different techniques are imposed. This rate is changing as lowest precipitation rate appears from 17% by first sample (T1) to the highest of 56% by the third one (T3). These results show that different homogenization methods affect the rate of sedimentation as well as properties which agrees well with the results of the previous studies (Hwang, Y. et al., 2008).

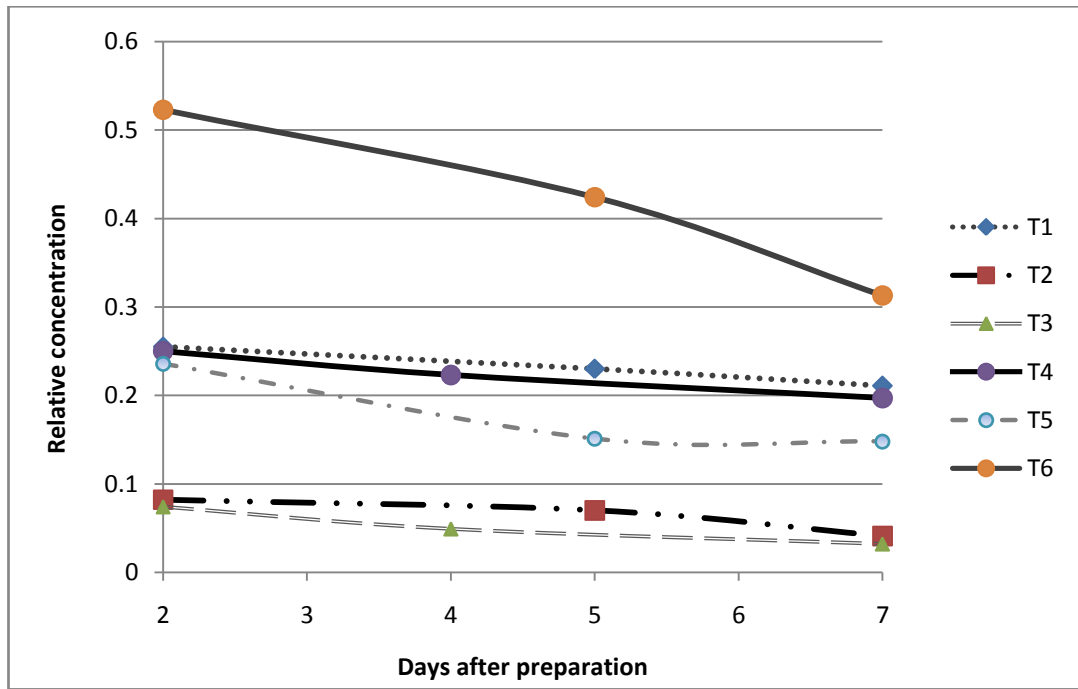


Figure 4- 8 Sedimentation rate for six prepared samples within seven days after preparation

4.1.2.3 Particle size, zeta potential, thermal conductivity results

The six prepared nano-suspensions were tested for stability and characterized by means of zeta potential, particle size, thermal conductivity and viscosity. Each experiment was repeated at least three times to calculate the mean value of the experimental data. The results are presented in Table 4-2.

Table 4- 2 Zeta potential, particle size and thermal conductivity results for 0.1% wt. titania nanofluid

SAMPL E	Zeta potential (mV)	Particle size (nm)	Relative thermal conductivity K_{nf}/K_{bf}
T1	-33.1	250.4	1
T2	-44	276.75	1.008
T3	-31.1	188.2	1.009
T4	-47.9	176.9	1.01
T5	-33.3	212	1.008
T6	-55	237.65	1.01

It is confirmed that, firstly, all the samples are moderately stable according to the criteria presented by Vandsburger (2009) on his thesis presented at Table 2- 6. Secondly, T6 is the most stable suspension; however, the particle size is not the smallest among all. Potentially large enhancements of thermal conductivity can occur in stabilized solutions if aggregates are less dense and small enough to stay in solution (Gharagozloo , P. & Goodson, K. E., 2010). Therefore, it is suspected that this size will lead to an agglomeration in time evolution and cause sedimentation due to the homogenization theory. On the other hand, the optimized agglomeration theory proposed by Prasher et al. (2006), may prove that this size is not the smallest but it can be the optimized agglomeration size and lead to the enhanced thermal conductivity with chain like aggregates. The second most stable suspension is T4. Proper results appeared for the suspension by adding the surfactant (over 40 mV) in comparison with surfactant free nano suspensions. From the particle size point of view, 15 min ultrasonic process got the best homogeneity among all and smallest coagulation will be reached by this method. However, an overall conclusion cannot be made since it has to be confirmed by other characterization instruments due to the errors and uncertainty of equipment and human.

Thermal conductivity of nanofluid got the most enhancements in surfactant-added nanofluid by imposing either 15 minutes ultrasonic horn or three hours ultrasonic bath. As a result, adding proper surfactant to the nanofluid increases stability and thermal conductivity if it is accompanied by ultrasonication. Otherwise, this would not help the dispersion and enhancement of thermal conductivity. The thermal conductivity has been shown to increase with aggregation, but decrease if the aggregates become dense and large causing settling (Gharagozloo , P. & Goodson, K. E., 2010). However, this finding may corroborate the evaluation of the work has done by Meibodi et al.

(2010a) that the more stable nanofluid doesn't have higher value of thermal conductivity.

4.2 Effect of elapsed timing in stability measurement by UV-vis spectrophotometer

Since there is limited attention to nanofluid stability and optimizing preparation method by UV-vis spectrophotometer, I consider it as a critical necessity to conduct some experiments in order to evaluate this method. In this section, based on the preliminary studies and reviewing literature we focused on the effect of pH values (between 10 and 12) and SDS surfactant concentration from one-tenth to twice the amount of nanoparticle concentration (ranging 0.01-0.2%wt.) on the stability of 0.1 %wt. titania nanofluid. The absorbance measurements using UV-vis spectrophotometer were taken as the stability responses in the periods of one day, two days, one week (168hrs) and one month (720 hrs) after preparation. The results obtained from the nanofluid, were imported to DOE for optimizing these two factors separately and simultaneously.

In this study, the appropriate measurement time for a clear detection of the stability of nanofluid by the UV-vis spectrophotometer is discussed. Furthermore, the optimum stable combination of SDS %wt. and pH value is determined.

4.2.1 Central Composite Design (CCD)

The experimental conditions were optimized using Central Composite Design (CCD). SDS concentration and pH value, as the two independent factors, were studied at five levels with three repeats at the central point.

Table 4- 3 Variables and values used for CCD

Variable	Name	-1	-0.5	0	+0.5	+1
A	SDS (wt. %)	0.01	0.0575	0.105	0.1525	0.2
B	pH	10	10.5	11	11.5	12

Table 4- 4 The obtained experimental results based on the CCD method

Run	SDS wt. %	pH	coded value A	coded value B	UV after 1 M	UV after 1 W	UV after 2 D	UV after 1 D
1	0.105	10.5	(0)	(-0.5)	0.23	0.231	0.422	0.436
2	0.2	10	(+1)	(-1)	0.193	0.198	0.243	0.325
3a	0.105	11	(0)	(0)	0.209	0.215	0.415	0.345
4	0.2	12	(+1)	(+1)	0.015	0.055	0.25	0.513
5	0.01	10	(-1)	(-1)	0.038	0.216	0.348	0.338
6	0.1525	11	(+0.5)	(0)	0.111	0.133	0.334	0.417
7a	0.105	11	(0)	(0)	0.122	0.154	0.436	0.42
8	0.0575	11	(-0.5)	(0)	0.116	0.175	0.419	0.411
9	0.01	12	(-1)	(+1)	0.165	0.214	0.513	0.513
10	0.105	11.5	(0)	(+0.5)	0.106	0.14	0.412	0.431
11a	0.105	11	(0)	(0)	0.084	0.127	0.426	0.408

a: indicates 3 repeats at center point, M:month, W:week, D:day

For each of the studied variables, high (coded value: +1) and low (coded value: -1) set points were selected as shown in Table 4-3. In addition, Table 4-4 shows the coded and real values of the designed experiments based on the CCD methodology in DOE software.

4.2.2 Statistical Analysis

The design of experiment aimed to achieve the optimum range of SDS dosage and pH value to have the best stability based on the UV-vis spectrophotometer measurement for short term and long term application of 0.1%wt. titania nanofluid.

Table 4- 5 The ANOVA results

Model	P	R ²	Adj. R ²	Pred. R ²	AP	C.V	Std.Dev
1	0.0085	0.866	0.777	0.664	9.37	7.10	0.029
2	0.001	0.987	0.967	0.702	22.68	3.87	0.015
3	0.001	0.88	0.84	0.603	13.99	7.28	0.17
4	0.0002	0.964	0.94	0.751	20.12	12.77	0.44

The relationship between the two variables and the four stability responses of the UV-vis spectrophotometer absorbance measurement (after one day, two days, one week,

and one month) was analyzed using RSM. A total number of eleven experiments including three replicates at the centre were carried out. The tested variable combinations and experimental results are tabulated in Table 4-4. The responses were gathered from the UV- absorbance measurement of mixed distilled water and SDS as base fluid. The sedimentations were investigated by comparing the measured absorbance.

The effect of SDS concentration and pH value on UV absorbance was evaluated using a regression model based on the equations shown in Table 4-6. The statistical analysis indicated that the whole regression model is significant (p-value less than 0.05); however, as can be seen in Table 4-6, some of the terms are missing in the predicted model, such as term AB in the first equation. The reason is that, the p-values for those terms are well above 0.05 (See Table 4-5). Removing these terms and performing regression again resulted in the equations of Table 4-6.

Table 4- 6 The developed models of UV responses

UV response after preparation	Final equation in terms of coded factors
1 day	$0.41 - 0.0022 - 0.037B + 0.018B^2 + 0.13B^3$
2 days	$0.42 - 0.091A - 0.010B - 0.039AB - 0.12 A^2 + 0.042B^2 + 0.053 A^2B$
1 week	$2.32 + 0.36A + 0.35B + 0.33 AB$
1 month	$2.68 + 0.64A + 0.83B + 2.14AB + 1.81A^2$

Besides, terms with a higher degree or a combination of coded values in the models like A^2B (in the 2nd model) or B^3 (in the 1st model) were added to the model for better regression. In this table (Table 4-6), the influence of coded factors of A and B are very little in the first model. Besides, regression coefficient and predicted R^2 of the model have the lowest amount. The absorbance could not be reliably measured due to the strongly fluctuating readings. Therefore, the calculated parameters and measured UV were chaotic after one day. The highest R^2 and lowest standard deviation were achieved

by model 2 (after two days). The equation denotes the short term stability of nanofluid after 48 hours. Likewise, UV absorbance after one month which is considered as long term stability characteristic of nanofluid has a fairly high regression coefficient. In this model both of the factors and their interactions have a considerable influence on the long term stability.

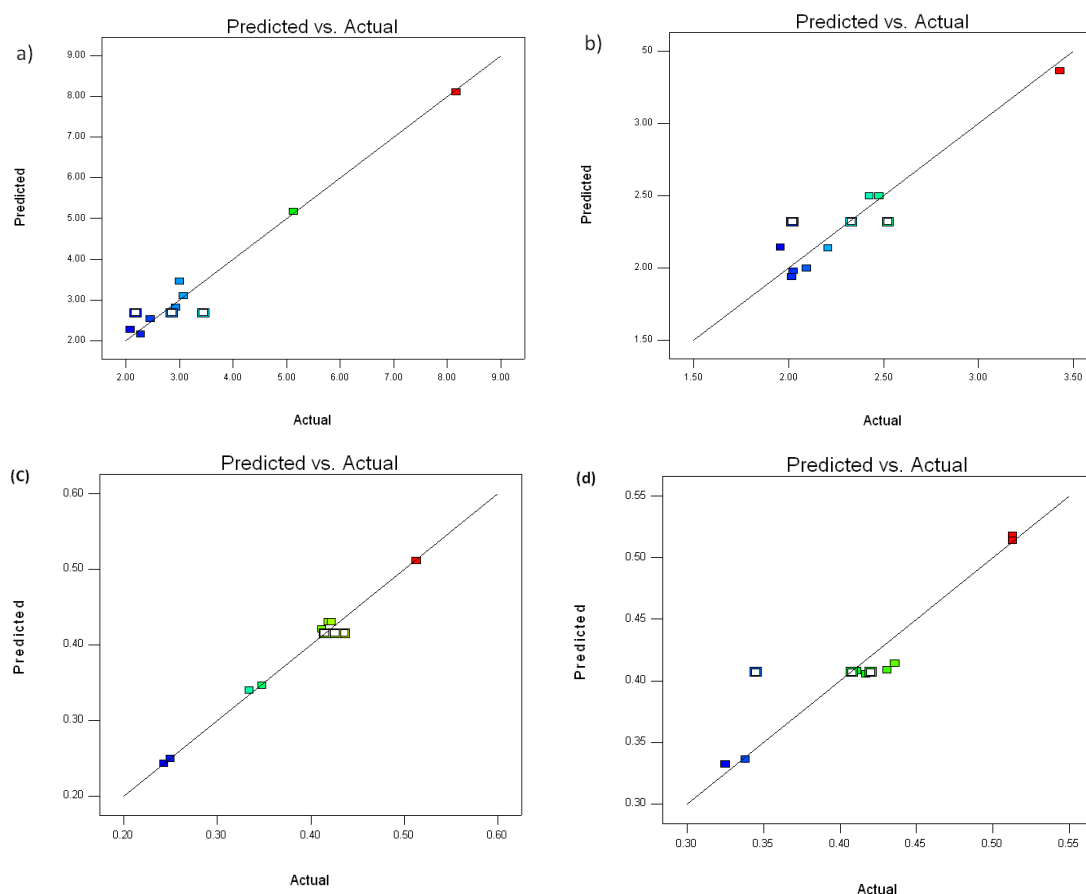


Figure 4- 9 Predicted vs. actual values plot for the UV-vis spectrophotometer absorbance measurement: (a) after one day, (b) after two days, (c) after one week, and (d) after one month

Analytic plots such as the predicted versus actual values help us judge the model satisfactoriness. The plots of predicted versus actual value responses, with respect to the factors, are presented in Figure 4-9. These plots indicate an adequate agreement between the real data and those obtained from the models. Moreover, the AP values higher than four (See Table 4-5) for all the responses confirmed that all models could be

used to navigate the design space defined by the CCD. Based on the data given in Table 4-5, the only model which fails in terms of reproducibility is the model for the response after one month ($CV = 12.77$).

4.2.3 Graph Analysis

Referring to Figs 4-10 and 4-11 as two-dimensional (contour) and three-dimensional (surface) models of the responses, the blue areas indicate the minimum absorbance while the red strips show the maximum amounts of the responses. The four sub-diagrams in these figures demonstrate the absorbance measurements at one day, two days, one week and one month after nanofluid preparation.

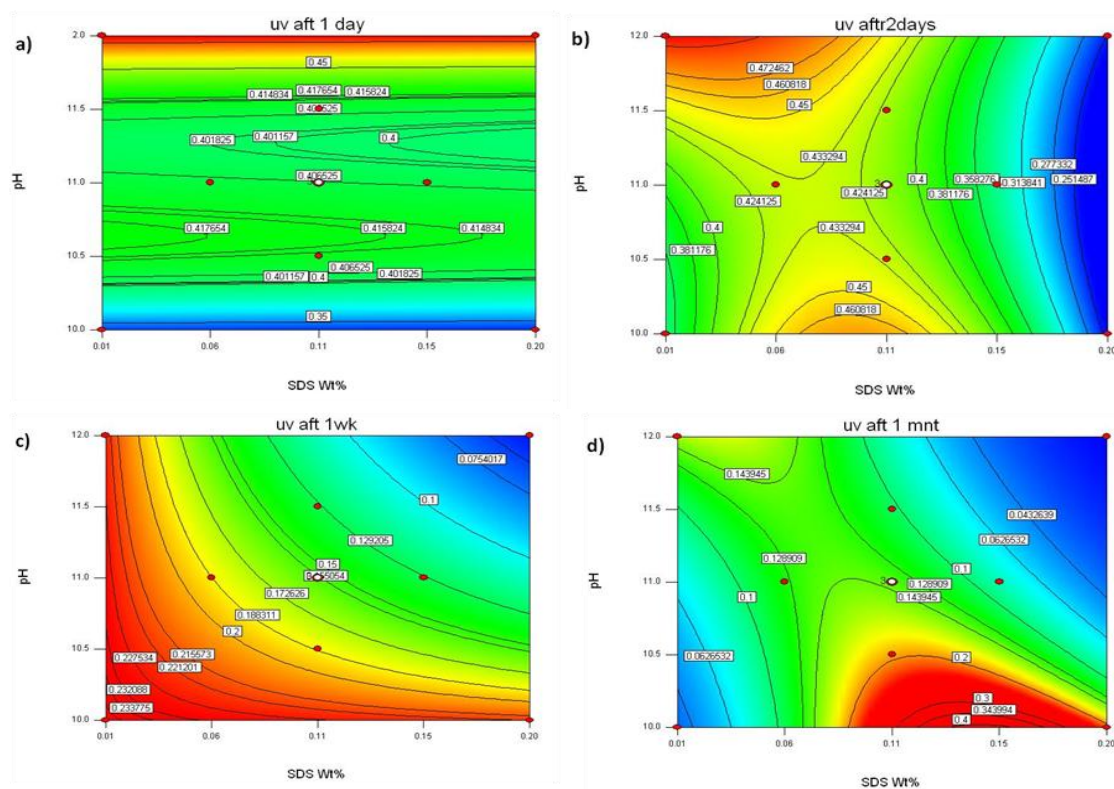


Figure 4- 10 Two-dimensional contour plots for the UV-vis spectrophotometer absorbance measurement; (a) after one day (b) after two days, (c) after one week, and (d) after one month

It can be seen in these figures that the absorbance after one day had not changed by altering pH value. Consequently in comparison with the rest of the graphs, it doesn't show a proper variation. High absorbance after two days came out with high pH values in the low surfactant concentration region. Another noticeable finding is the small area of medium concentration samples which is about to grow for the pH value of 10. Results after one week show that wider range of pH control and SDS concentration could make the nanofluid stable after one week.

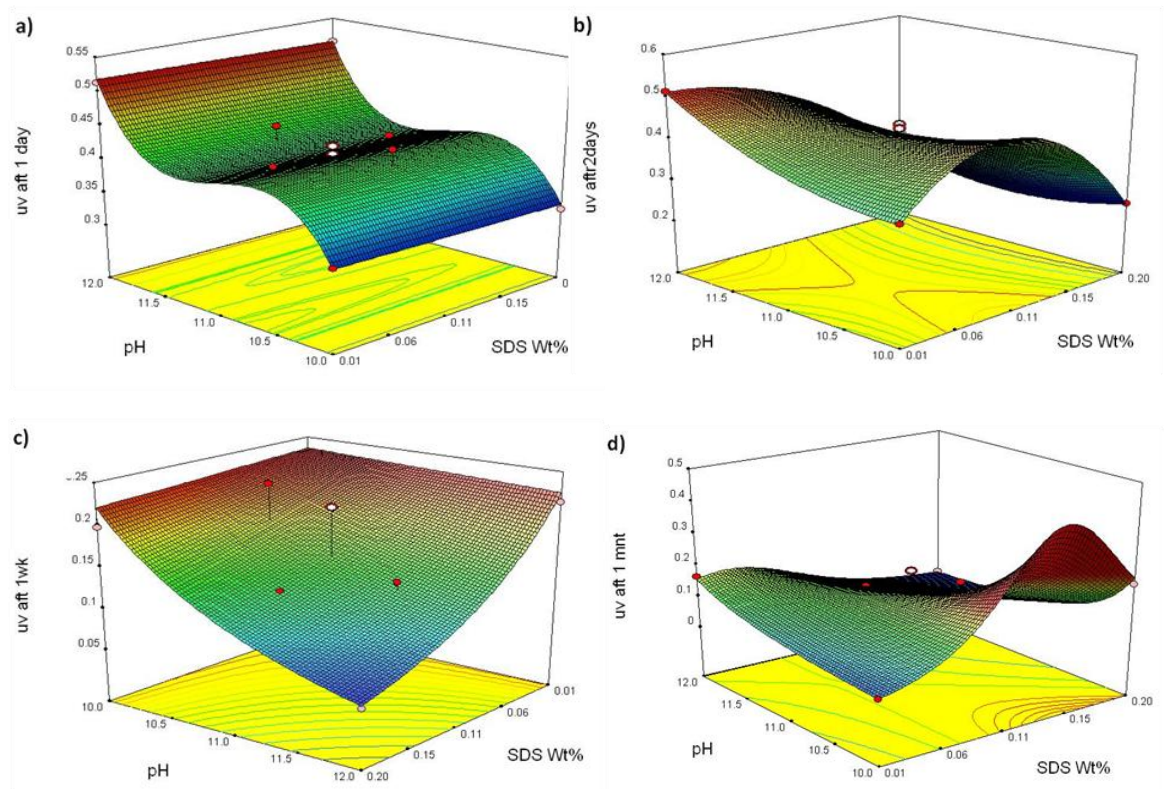


Figure 4- 11 Response surface plot for the UV-vis spectrophotometer absorbance measurement; (a) after one day (b) after two days, (c) after one week, and (d) after one month

This response conveys that high pH values should be accompanied with low concentrations of SDS to reach high stability after one week. Similarly, in order to have low pH values, high SDS concentration should be maintained. These graphs also show that probably a more stable nanofluid could be reached without surfactant at a pH value

of around 9.30. However, this value has not been reported in the literature. Finally, after one month the long term stable nanofluid appeared at pH values of between 10-10.5 and surfactant weight concentration of equal to twice the amount of nanoparticle loading. Due to the sedimentation after long time, the stable region looks smaller.

4.2.4 Optimization

“The goal of optimization is to find a proper set of conditions that will meet all the goals, not to get to a desirability value of 1.0. Desirability is simply a mathematical method to find the optimum“(Stat-Ease, I., 2009).

If all the responses showed high relative stability at the same weight simultaneously, the optimum condition could be achieved. In this case, the maximum desirability of 0.891 in pH value of 12 with minimum surfactant concentration of 0.01 wt. % can be observed in Figure 4-12. However, as discussed in Section 4.2.2, the first sample measurement after one day had insufficient discriminating power. Therefore, the desirability was calculated by removing this response or lowering its weight in the numerical optimization. The point of 0.908 located at pH of 10 with SDS weight percentage of 0.09% (shown in Figure 4-13) can be claimed to have the same loading of nanoparticles.

At one-day interval after preparation, the responses could be observed at all SDS % wt. but only at high pH values. After two days, the measured absorbance showed low SDS concentration as acceptable stability at an area with a high pH controlled nanofluid. In addition, we observed a measurable area of absorbance at a wider range of surfactant weight percentage of about 0.01-0.2. Though, for lower concentrations, the pH value would be confined to a range of 10 to 12. In the case of higher SDS addition, we detected that the stable area occurred only at a pH value of 10. The stability measurement after one month showed that for a long-term application of this suspension, SDS weight percentages of 0.08-0.2 were associated with low pH values.

This result showed that other than this area, our prepared nanofluid would not be applicable after one month.

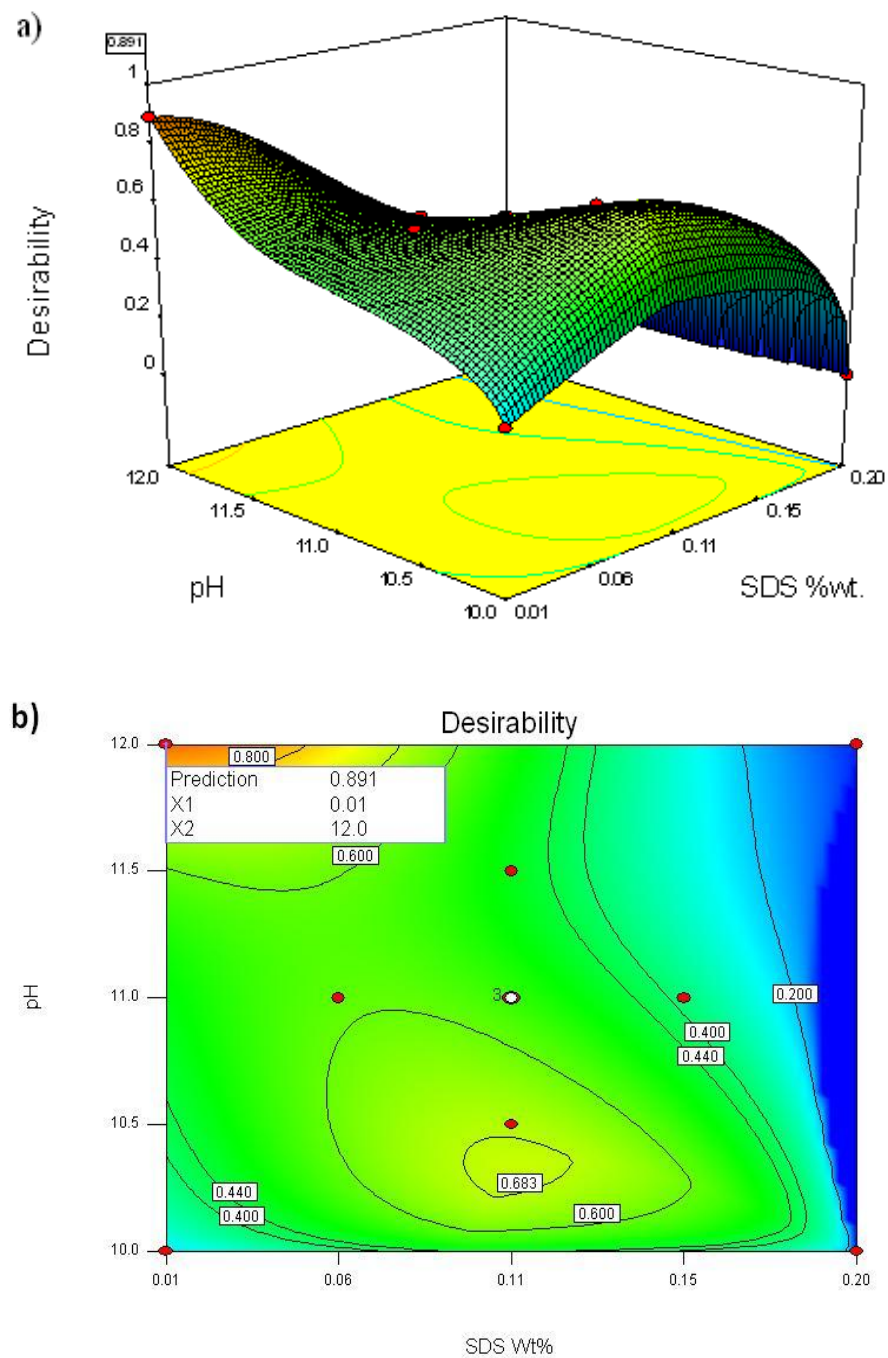


Figure 4- 12 a) 3D surface, b) Contour of desirability with consideration of all four responses for optimum stability area of titania nanofluid

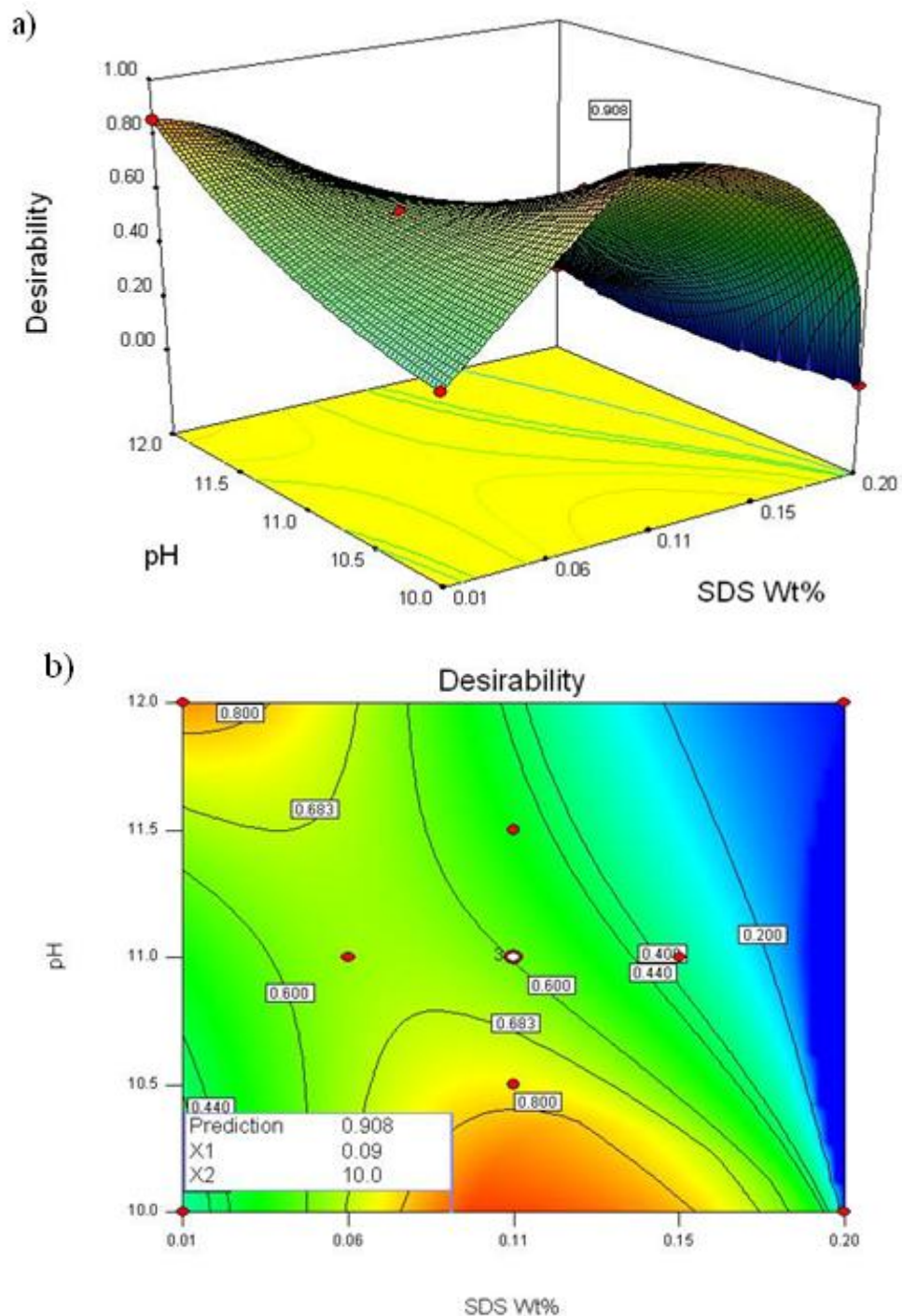


Figure 4- 13 a) 3D surface, b) Contour of desirability of responses for optimum stability area of titania nanofluid without the first response

4.2.4.1 Point Prediction Evaluation

To assess the accuracy of the second order equations, three-additional UV absorption experiments were performed using the SDS concentration and pH value that were prepared under the RSM-predicted optimum conditions. The maximum values of

the repeated experiments and predicted results are presented in Table 4-7. As it is observed in this table, the deviations errors between the experimental and predicted values of UV measurement at experimental intervals of two days, one week and one month after the preparation were 1.2%, 1.1% and 0.7%, respectively. The good agreement between the experimental values and those predicted from the CCD model suggests that the developed model is suitable to simulate variables within 5% of accuracy. The optimization results presented in this section provide background information for detailed process improvement in future researches.

Table 4- 7 Evaluation of experimental and predicted values at optimum condition

Responses of absorbance	Predicted values	Experimental values*	Error (%)
After two days	0.471	0.465	1.2
After one week	0.229	0.232	-1.1
After one month	0.207	0.206	0.7

*represents the maximum value of the experiments

4.3 Experimental design and optimization for the effect of pH value and surfactant concentration on the stability and thermal conductivity of titania nanofluid

Since the optimized values of pH and surfactant concentration in stabilization process of nanofluid are not investigated systematically, and also due to the great influence of these parameters on nanofluid stability and heat transfer, it is taken as a necessity to conduct some systematic experiments on these two parameters. This study aims to optimize the influence of two stabilizing parameters (pH value and surfactant weight percentage) on the stability responses for zeta potential, particle size, and UV absorption accompany with thermal conductivity response of nanofluid. The

optimization process using RSM with CCD method was performed and the obtained results are presented.

The response parameters which determine the samples' properties were zeta potential (in mV), particle size (in nm), thermal conductivity (in W/m.K), and UV absorbance (in g/l). Three repeated runs were carried out at the center of experiment in order to measure the reproducibility at different combinations of the process parameters.

The obtained experimental results were exported to Design Expert (v.8) and the effect of the process parameters including surfactant dosage and the value of pH in the stability of TiO₂ nanofluid and the optimum condition for the stability properties were studied using RSM and CCD.

4.3.1 Data analysis of the effect of pH control and surfactant addition on the stability and thermal conductivity

Table 4-8 shows the coded and real values for designed experiments based on the CCD methodology. The coded values for SDS %wt. (*A*) and pH value (*B*) were set at five levels (−1 (minimum), −0.5, 0 (central), +0.5, and +1 (maximum)). It is worth to mention that the thermal conductivity response is the most important parameter to measure the heat transfer of nanofluid.

ANOVA was used to estimate the effects of main variables and their potential interaction on the stability of considered nanofluid. The experimental results obtained from various homogenization methods of titania nanofluid were analyzed using multiple regression analysis. The statistical results of the four responses including zeta potential (mV), particle size (nm), thermal conductivity (W/m.K), and UV absorbance (g/L) of nanofluid are shown in Table 4-9.

By observing Table 4-9, adequate precision (AP) and coefficient variance (CV) are within the acceptable region which is more than 4 and below 10, respectively, except the zeta potential response which is 15.22 for CV. Lack of fit (LOF) measures

the error due to deficiency of the model. LOF indicates how well the model fits the data. Strong LOF ($P < 0.05$) is an undesirable property, because it indicates that the model does not fit the data well.

It is enviable to have an insignificant LOF ($P > 0.1$). The important outputs of the model are the F-value and associated probability ($P > F$). The higher the F-value, the more likely the model does not adequately fit the data. Similarly, P should be less than 0.05 to demonstrate that the model terms are significant. The F-value and P for all responses are in the acceptable range and therefore, the predicted model is significant (Nosrati, S. et al., 2011a, 2011b).

Table 4- 8 Factors and responses used for CCD in model optimization (coded values)

Exp.	Factor A		Factor B		Response 1	Response 2	Response 3	Response 4
	Code	SDS (%wt.)	Code	pH	Zeta Potential (ZP)	Particle size (PS)	K_{eff}	UV absorbance
					mV	nm		g/l
1	0	0.11	-0.5	10.5	-48	370	0.994	0.223
2	+1	0.20	-1	10.0	-51.6	232.3	1.006	0.193
3	0	0.11	0	11.0	-45	498	1.016	0.229
4	+1	0.20	+1	12.0	-37.2	327	1.006	0.015
5	-1	0.01	-1	10.0	-40	295	0.955	0.039
6	+0.5	0.15	0	11.0	-42.4	409.1	1	0.113
7	0	0.11	0	11.0	-42.9	432.4	1.003	0.154
8	-0.5	0.06	0	11.0	-48	397	1.013	0.125
9	-1	0.01	+1	12.0	-49	350	1.013	0.118
10	0	0.11	+0.5	11.5	-48	450	1.008	0.17
11	0	0.11	0	11.0	-44.8	514.2	1.013	0.108

From Table 4-9, the difference between the adjusted R and predicted R is within the accepted range of 0-0.2. In order to get a quick impression of the overall fit and the prediction power of a constructed model, R, adjusted R and predicted R are very

convenient. Table 4-10 represents the statistical results of ANOVA in terms of coded factors for p-values.

Table 4- 9 Statistical characteristics of optimum models and ANOVA results

Responses	F	P	LOF F	LOF P	R ²	Adj. R ²	Pred. R ²	AP	CV
ZP	60.2	0.0002	2.53	0.2959	0.984	0.967	0.8814	26.02	15.22
PS	15.46	0.0018	1.16	0.5241	0.869	0.812	0.673	10.4	8.44
K _{eff}	18.78	0.003	0.36	0.7911	0.949	0.8989	0.687	14.971	0.54
UV	19.6	0.0014	2.8	0.2804	0.93	0.8815	0.7724	14.613	4.35

The ANOVA results in terms of stability parameters indicate that among the coded parameters, terms A, AB, and A² have considerable effects on the stability of nanofluid in terms of zeta potential as shown in Table 4-10. It means that the zeta potential response is more dependent on the %wt. of surfactant rather than the value of pH. Likewise, the results obtained by ANOVA signify that the terms B and B² have a large influence on the stability of TiO₂ nanofluid in terms of particle size as depicted in Table 4-10. It is concluded that the particle size response completely relies on the %wt. of surfactant instead of the value of pH.

Table 4- 10 P-Value of four responses

	P-Value			
	Zeta potential	Particle size	UV absorbtion	Effective thermal conductivity
	Response 1	Response 2	Response 3	Response 4
Model	0.0002	0.0018	0.0014	0.0030
A-SDS %wt.	0.0015	0.2249	0.0003	0.1443
B- pH	1.0000	0.0270	0.0318	0.0025
AB	< 0.0001	-----	-----	0.0031
A ²	0.0007	-----	0.0153	-----
B ²	-----	0.0005	0.0268	0.0141
A ² B	0.0830	-----	-----	-----
AB ²	-----	-----	-----	0.0299
Lack of Fit	0.2959	0.5241	0.2804	0.7911

Furthermore, the results in Table 4-10 show that among the coded parameters, terms B, AB, B², and AB² have significant effect on the thermophysical properties in terms of the effective thermal conductivity of TiO₂ nanofluid. In other words, any changes in the value of these coded parameters will lead to significant changes in the thermal conductivity of nanofluid. It means that the *K* response is more dependent on the value of pH than on the %wt. of surfactant; however, the interaction between these two factors is a matter of concern in verifying the changes of thermal conductivity even in higher degrees. Compared to the value of pH, the %wt. of surfactant plays a more important role in UV absorbance value; however, no interaction between factors shows up in this last response (UV absorption). After eliminating the insignificant parameters, polynomial equations and response surfaces for a particular response in terms of coded factor were produced using RSM.

For the stability characteristics, an inverse model with constant value set to 35, square root transformation with k set to -150 were required to improve the models for zeta potential, particle size, and UV absorption respectively. For an experimental design with two factors, the model including linear, quadratic, and cross-terms can be expressed in terms of coded factors as given in Table 4-11.

Table 4- 11 The developed models of characteristic and stability responses

Response	Model
ZP	$\frac{1}{(ZP + 35)} = -0.093 - 0.061A - 0.13AB - 0.1A^2 - 0.066A^2B$
PS	$\sqrt{(PS - 150)} = 17.29 - 0.8A + 1.68B - 5.15B^2$
K _{eff}	$K = 1.01 - 0.013A + 0.014B - 0.015AB - 0.013B^2 + 0.025AB^2$
UV	$\frac{1}{UV} = 2.39 + 0.38A - 0.14B + 0.72A^2 - 0.63B^2$

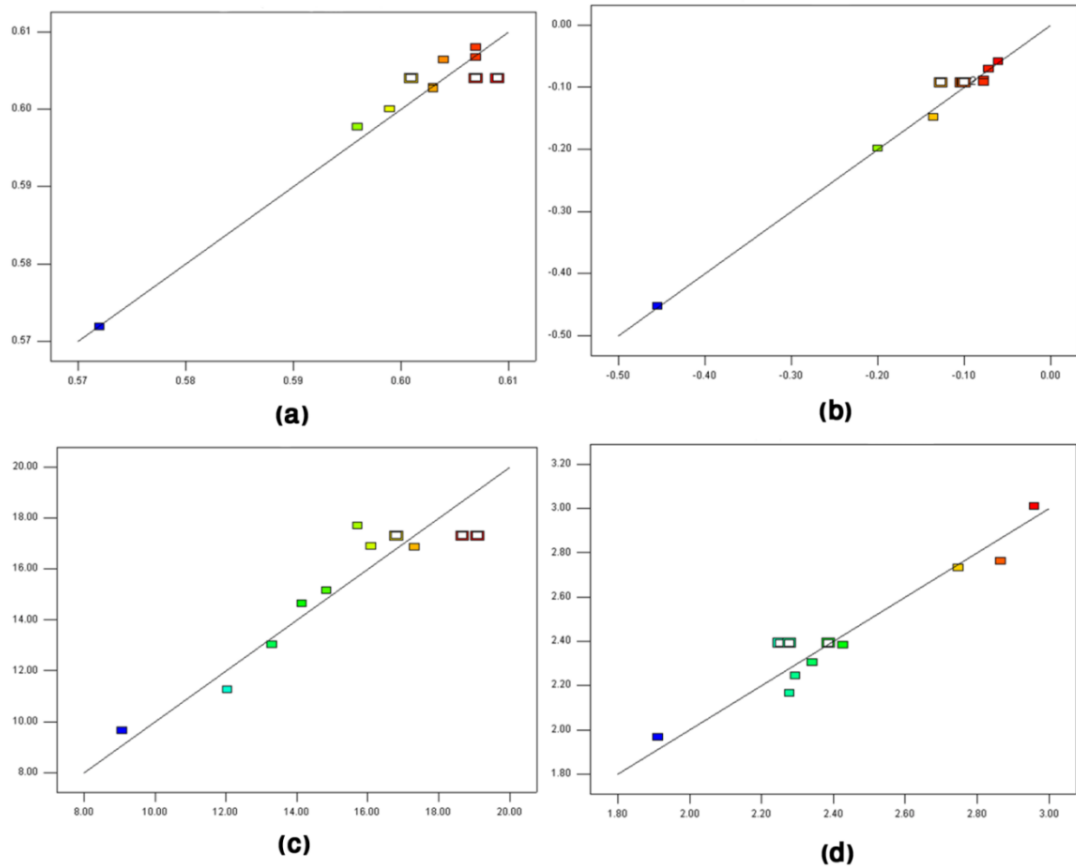


Figure 4- 14 A parity plot between actual experiment and predicted values using RSM for TiO₂ nanofluid: (a) zeta potential, (b) particle size, (c) thermal conductivity, (d) UV absorbance. (The vertical and horizontal axes are predicted output and corresponding targets, respectively)

Therefore, the gained quadratic models represent the actual process of stabilizing nanosuspension. Figure 4-14 represents the linear regression between the predicted and actual experiment results for all considered responses using RSM.

The best linear fit is indicated by a solid line. If there were a perfect fit (outputs exactly equal to targets), the slope would be 1 and the y-intercept would be 0. The correlation coefficient (R-value) between the outputs and targets for all responses are given in Table 4-9. Figure 4-14 indicates that the models were successful in describing the correlation between the factors and the responses (zeta potential, particle size, thermal conductivity, and UV absorption).

4.3.2 Influence of the parameters on responses

In general, the ideal situation may be considered as the maximum value of zeta potential (absolute value), thermal conductivity, and UV absorbance. In contrast, for particle size response, the best condition may be judged as the minimum value for particle dimension. Figures 4-15 and 4-16 illustrate the 2D and 3D plots for predicted response, respectively.

The minimum particle size can be observed at the lowest value of pH (pH=10). In other words, at low surfactant concentration, the particle size increases by pH value increment. This phenomenon can be explained by the significant quadratic term B having a negative influence (see Figure 4-15b and Table 4-11).

As can be seen from Figure 4-15c, the best recipe for high thermal conductivity achievement was obtained at low surfactant concentration along with high value of pH. This can be clarified more by reviewing thermal conductivity model in Table 4-11 in which parameters A and B have significant positive and negative terms for thermal conductivity, respectively. The optimum nanofluid can be resulted at pH value and %wt. of surfactant set to 12 and 0.01, respectively.

Similarly, the high values of UV absorbance were located at two areas of high and low pH value with a wide range of SDS concentration as shown in Figure 4-15d. For further clarification, 3D views of response surface plots are given in Figures 4-16. Regarding the stability measures of zeta potential and UV absorbance, there are mainly two regions which have the most stable nanofluids. Meanwhile, the high thermal conductivity is located at one of these areas.

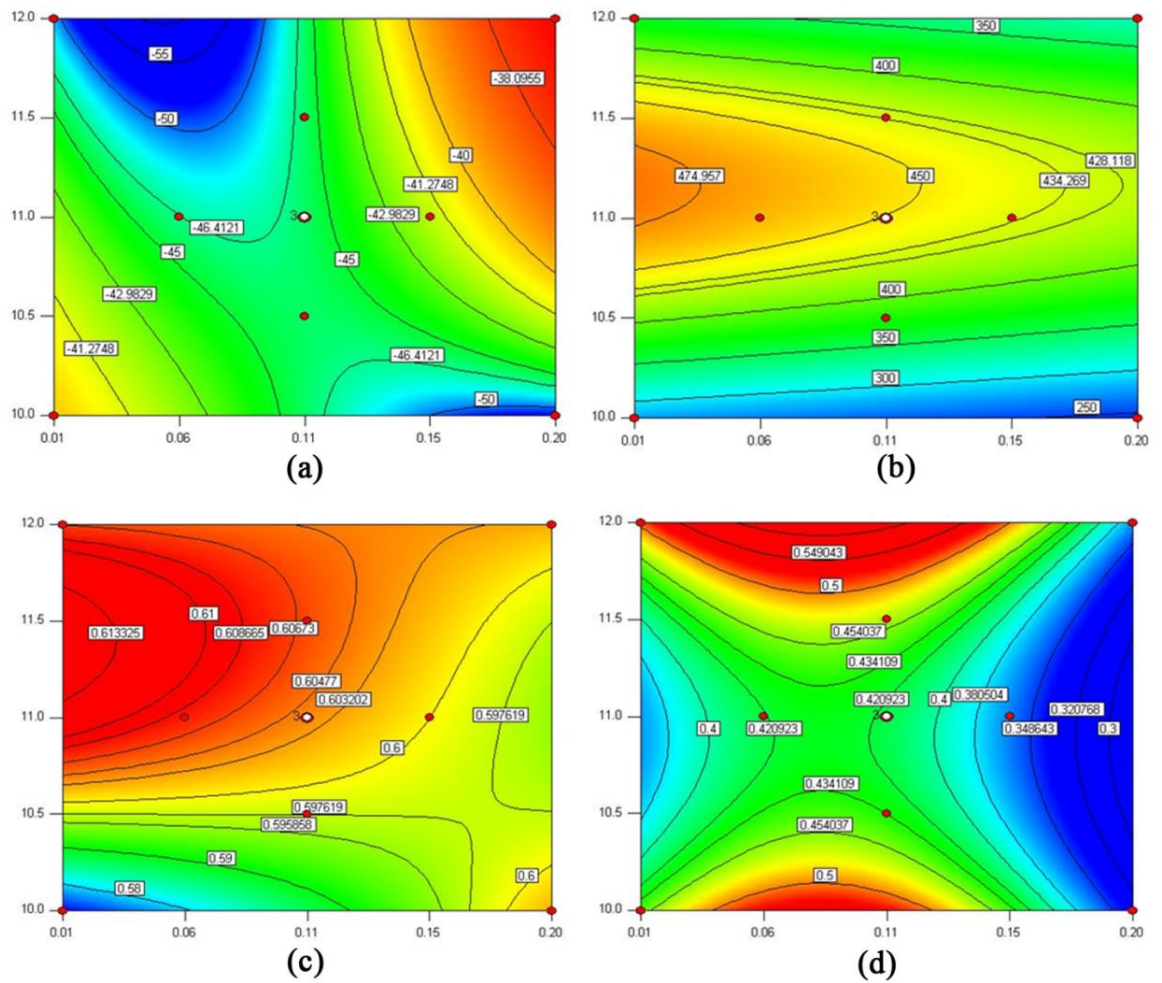


Figure 4- 15 2D representation of the responses for TiO_2 nanofluid: (a) zeta potential, (b) particle size, (c) thermal conductivity, (d) UV absorbance. (Vertical and horizontal axes are the value of pH and the %wt. of surfactant, respectively)

As can be concluded from Figures 4-15b and 4-15c, higher thermal conductivity may not be reached exactly by having higher stability parameters. The most stable nanofluids in terms of having the maximum UV absorption and zeta potential are situated within two different areas (see Figs. 4-15a and 4-15d). These regions exhibit high pH value with low SDS loading and vice versa. However, the particle size does not follow this trend as one of the stability inspectors for a stable nanosuspension. Besides, enhanced thermal conductivity could be reached at high pH value and low surfactant weight percentage. It is worth to mention that almost half of the stable nanofluids show the expected improved thermal conductivity.

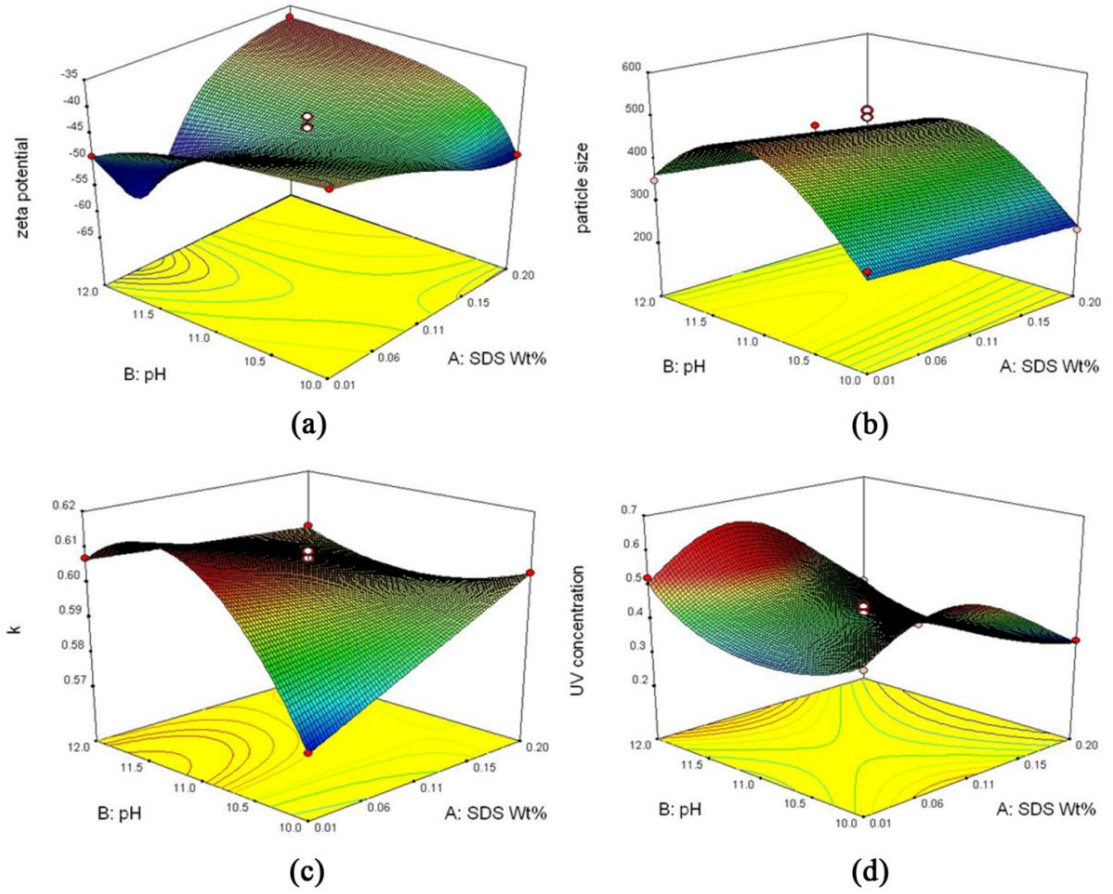


Figure 4- 16 3D response surface plot for TiO₂ nanofluid: (a) zeta potential, (b) particle size, (c) thermal conductivity, (d) UV absorbance.

Since the K response depends on more variables (A , B , AB , B^2 , AB^2) than the agglomerate size, determining the enhancement theory is more complex than the particle size.

Therefore, the agglomerate size can only be a partial parameter for the K effect. Then, since the terms that are shared between the responses (A , B and B^2) have the same sign we can conclude that they are related. Consequently, large particle size may construct a chain shape cluster which increases the heat transfer due to the clustering theory by Evans (2008). Therefore, optimization is necessary to achieve a stable nanofluid with high thermally conductivity.

4.3.3 Nanofluid optimization for thermal conductivity, UV absorbance, zeta potential and particle size responses

The main objective of this study is to determine the optimum TiO₂ nanofluid in terms of pH value and SDS weight concentration. Based on the literature review, the optimization is carried out by setting the absolute zeta potential more than 45 to have good stability (Vandsburger, L., 2009). Therefore, maximum relative UV absorbance and thermal conductivity are assumed to reach the most stable and efficient cooling tool for titania nanofluid. It is a challenging task to define the optimum agglomeration size according to the existing theory of Prasher et al. (2006). As a result, we set all the other parameters to their desired values of maximum thermal conductivity and UV absorbance with minimum particle size and the desirability function will result in the optimum agglomeration size. Figure 4-17 demonstrates the desirability plot for obtained model in 2D and 3D views.

The desirability is a multiple response method with numerical optimization. This response finds a point that maximizes the desirability function. The goal of optimization is to find a good set of conditions that will meet all the goals, not to get to a desirability value of 1.0 (Stat-Ease, I., 2009).

For optimizing these four responses, there are 18 desirability values from 0.388 to 0.972 out of 1. For the maximum amount the values of K , zeta potential, particle size, and UV absorbance are -60.7, 353.048, 1.01 and 0.615, respectively. However, thermal conductivity is not as high as we expected. Subsequently, we selected a desirability value of 0.727 at which all parameters simultaneously meet the desirable amount of -48, 463.562, 1.023 and 0.43 as aforementioned order. The obtained prediction point is located at a pH value of 11.4 and SDS concentration of 0.04 %wt. as shown in Figure 4-17.

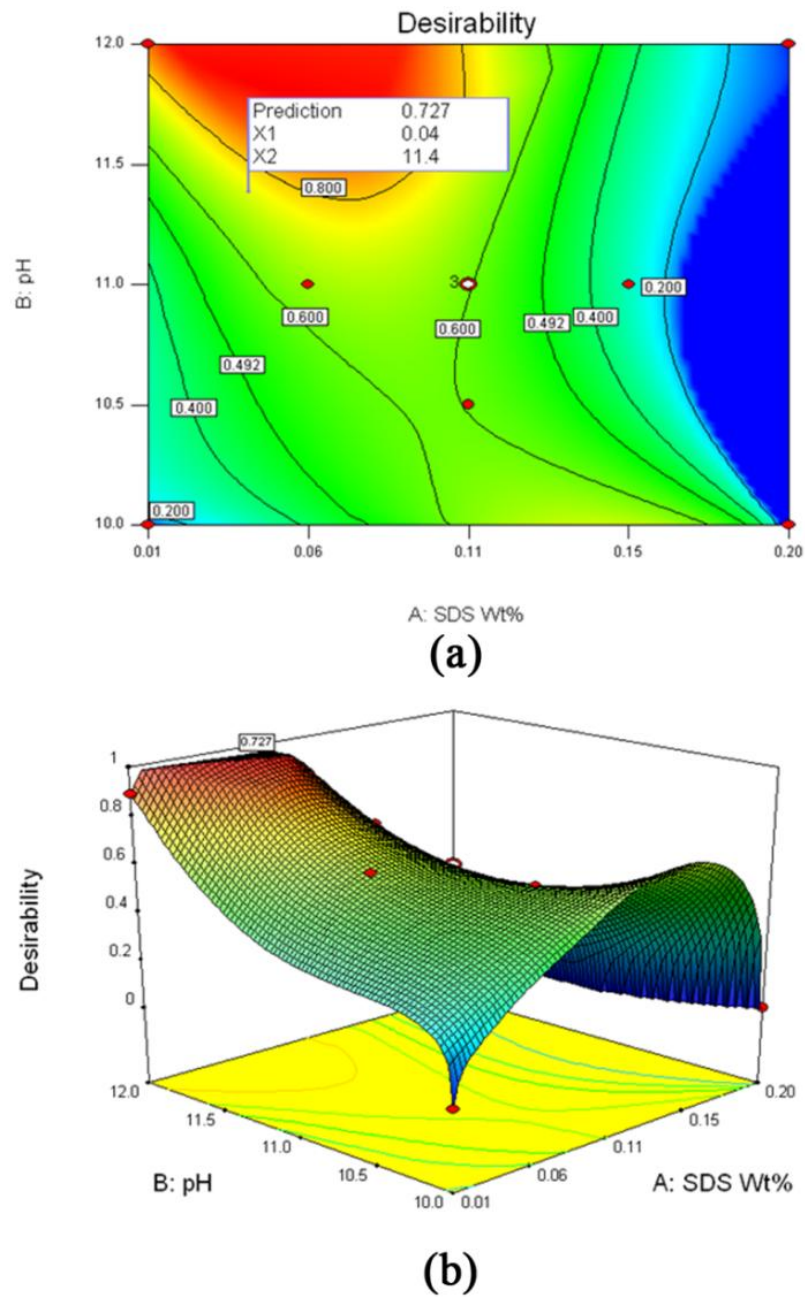


Figure 4- 17 Desirability plot for TiO₂ nanofluid: (a) 2D plot with contours, (b) 3D surface mesh

On the other hand, if we consider thermal conductivity and particle size as an issue of optimization, the obtained prediction points will include 36 points with desirability equal to 1.0. As shown in Figure 4-18, the selected point is placed at pH value of 11.4 and SDS concentration of 0.02%wt. The single limiting condition for this point is maximizing the thermal conductivity. In this case, we have a preparation method in which the enhancement of thermal conductivity will be 2.6%. The

coagulation size in this condition is 471.36 nm. Therefore, larger agglomerate sizes lead to higher thermal conductivity. Due to the experiment limitations, this set of experiments cannot evaluate the clustering and agglomeration theory by Prasher et al.

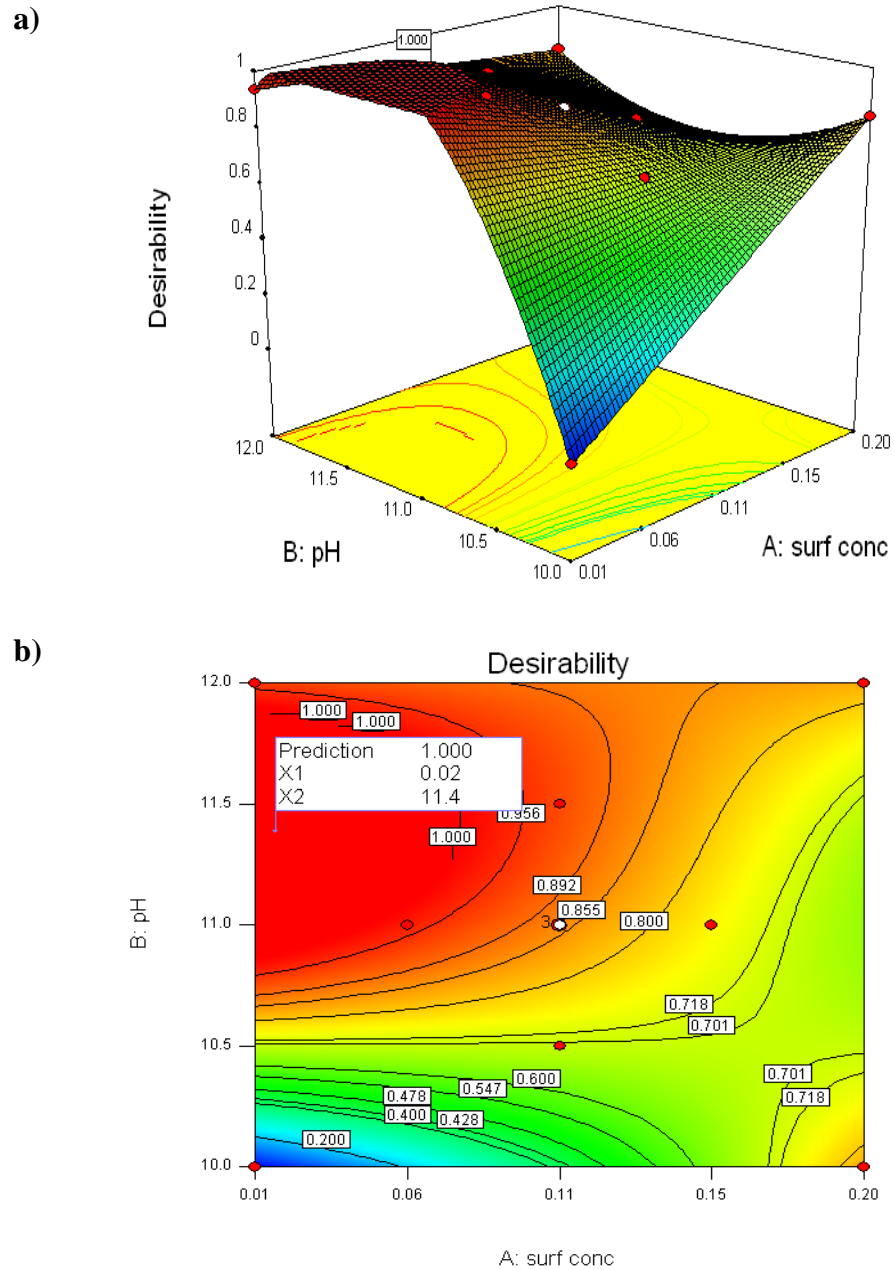


Figure 4- 18 Desirability plot for TiO_2 nanofluid: (a) 3D surface mesh, (b) 2D plot with contours

4.3.3.1 Point Prediction Evaluation

Four additional evaluation runs were carried out to validate the optimization results for the influence of pH value and surfactant concentration on thermal conductivity and stability of TiO₂ nanofluid. The maximum values of the repeated experiments and predicted results are presented in Table 4-12. As it is observed in this table, the deviations errors between the experimental and predicted values of zeta potential, particle size, thermal conductivity and UV absorbance measurement were in a good agreement from the CCD model and these outcomes suggest that the developed model is suitable to simulate variables within 5% of accuracy. The optimization results presented in this thesis provide background information for detailed process improvement in future researches.

Table 4- 12 Evaluation of experimental and predicted values at optimum condition

Responses	Predicted values	Experimental values*	Error (%)
ZP	-48	-46	4.1
PS	463.5	441	5.1
K _{eff}	1.023	1.02	-0.3
UV	0.43	0.444	3.2

*represents the maximum value of the experiments

4.4 Effect of nanoparticle volume concentration, duration and power of ultrasonic on the stability and thermal conductivity of nanofluid by Box Behnken method

The main goal of this study is to investigate the influence of sonication (power and time) on the stability of nanofluids by means of UV-vis spectrophotometer and sediment balance method at different concentrations in short term (after one week) and long term (after one month) intervals. In addition, the magnitude of zeta potential was measured to evaluate the quantity of UV-vis absorbance and sedimentation balance method. Meanwhile, we measured the thermal conductivity of nanofluids right after

preparation to optimize the influence of sonication and TiO₂ volume concentration on the characteristics of nanofluids at 25°C. Moreover, we implemented statistical analysis, RSM method and Box-Behnken to find out the optimum condition for maximum thermal conductivity and high stability of nanofluids (LotfizadehDehkordi, B. et al., 2013).

4.4.1 Experimental design and statistical analysis

The experiment was designed by means of RSM modeling combined with three-level BBD. BBD is an independent quadratic design which needs fewer combinations of the variables to estimate a potentially complex response function than a full factorial design (Yetilmezsoy, K. et al., 2009). In this study, BBD with three independent variables (x_1 : ultrasonic power, x_2 : ultrasonic time, x_3 : TiO₂ volume concentration as shown in Table 4-13) at three-levels was performed. The coded values of the variable for statistical calculation were determined by the following equation:

$$X_i = \frac{x_i - x_0}{\Delta x} \quad (4-1)$$

Where, X_i is a coded value of the variable, x_i is the actual value of the variable and x_0 is the actual value of the i^{th} test variable at the center point. The whole experiment design consisting of 17 experimental runs is shown in Table 4-14. The five replicates at the center point were added to provide a measure of process stability and inherent variability.

Table 4- 13 Independent variables and their levels used in the response surface design

Independent variables	Factor level			References
	-1	0	1	
X_1 : Ultrasonic power (%)	20	50	80	(Lin, C.-Y. et al., 2011)
X_2 : Ultrasonic time (min)	2	11	20	(Amrollahi, A. & et al., 2008)
X_3 : TiO ₂ Volume concentration (%)	0.1	0.55	1	(Chung, S. J. et al., 2009; Hong, K. S. et al., 2006)

In the first step of RSM, a proper approximation is implemented to find the relationship between the dependent variable and the set of independent variables.

4.4.1.1 Thermal conductivity enhancement and stability evaluation by means of UV-vis spectrophotometer at short term and long term application

By applying multiple regression analysis (MRA) on the experimental data, the response and the test variables are given in Table 4-14.

Table 4- 14 Box-Behnken design matrix and experimental record responses

Run	Ultrasonication power (%)	Ultrasonication time (min)	TiO ₂ Vol. concentration (%)	UV after one week	UV after one month	Thermal conductivity (W/m.K)
1	80	11	0.1	0.339	0.201	0.607
2	50	20	1	0.329	0.227	0.613
3	50	20	0.1	0.211	0.208	0.608
4	50	2	1	0.419	0.204	0.611
5	50	11	0.55	0.42	0.333	0.606
6	80	11	1	0.411	0.313	0.616
7	20	11	0.1	0.334	0.318	0.601
8	50	11	0.55	0.424	0.31	0.605
9	20	20	0.55	0.232	0.223	0.604
10	20	2	0.55	0.513	0.328	0.599
11	80	20	0.55	0.331	0.323	0.612
12	20	11	1	0.428	0.196	0.605
13	80	2	0.55	0.418	0.209	0.604
14	50	11	0.55	0.415	0.328	0.603
15	50	2	0.1	0.381	0.219	0.604
16	50	11	0.55	0.339	0.329	0.608
17	50	11	0.55	0.428	0.303	0.607

The following second-order polynomial equations were derived to explain the UV measurements (stability after one week and one month) and thermal conductivity of nanofluids. The developed models for the above-mentioned responses are gathered at Table 4-15.

Table 4- 15 The developed models for stability and characteristic responses

Response	Model
UV after one week	$(Y_1)^{-1} = 2.47 - 0.099 X_1 + 0.72 X_2 - 0.39 X_3 - 0.43 X_{12} - 0.37 X_{23} + 0.47 X_2^2 + 0.23 X_3^2$
UV after one month	$(Y_2)^{-1} = 3.12 + 0.034 X_1 - 0.064 X_2 + 0.014 X_3 - 0.78 X_{12} - 0.93 X_{13} - 0.18 X_{23} + 0.082 X_1^2 + 0.65 X_2^2 + 0.9 X_3^2$
Thermal conductivity	$Y_3 = 0.61 + 3.75E-03 X_1 - 2.375E-03 X_2 + 3.125E-03 X_3 + 7.5E-04 X_{12} + 1.25E-03 X_{13} - 1.382E-03 X_1^2 + 0.2868E-03 X_3^2$

Where, X_1 is the coded power of sonication, X_2 is the time of sonication, X_3 is the TiO₂ volume concentration, X_{12} (X_1X_2) is the interaction between power and time of sonication, X_{13} (X_1X_3) is the interaction between power and volume concentration and X_{23} (X_2X_3) is the interaction between time and volume concentration.

The analysis of variance (ANOVA) is requisite to check the significance of the model (Sen, R. & Swaminathan, T., 2004). Hence, the analysis of variance was implemented to explore the significance and goodness of fit of the models. Table 4-16 shows the ANOVA of the response surface model. According to the ANOVA results, the large F value and the small P-value (<0.05) indicate the validity of the model. In addition, the lack of fit measures the failure of the model to represent data in the experimental domain at points which are not included in the regression (Khajeh, M., 2011). The non-significant value of lack of fit (>0.05) indicates that the quadratic model is statistically significant for the response. The goodness of fit of the model was tested by determination coefficient (R^2). In this case, all the three responses show a very high value of determination coefficient. Furthermore, the values of the adjusted determination coefficient were also very high, which confirms that the models are highly significant (Adinarayana, K. & Ellaiah, P., 2002; Liu, H. L. et al., 2004). At the same time, a high degree of precision and a good deal of reliability of the experimental values were indicated by a low value of the coefficient of variation (CV).

Table 4- 16 ANOVA for response surface quadratic model

Source	Mean of square	F value	P-value	LOF	Std. Dev.	C.V	R ²	Adj.R ²	Pred.R ²
Y ₁	1.14	22.03	<0.0001	0.724	0.23	8.1	0.944	0.902	0.803
Y ₂	1.3	91.88	<0.0001	0.659	0.12	3.05	0.991	0.980	0.950
Y ₃	4.08E-05	14.93	0.0003	0.750	1.65E-03	0.27	0.920	0.859	0.714

Figure 4-19 show that the models were successful in capturing the correlation between the factors and the responses. The points around the diagonal line indicate a satisfactory fit of the model. As it is seen in Figure 4-19, in all the three responses, replications at the center of the design show a very good agreement with each other, which confirms the reliability of the experiments.

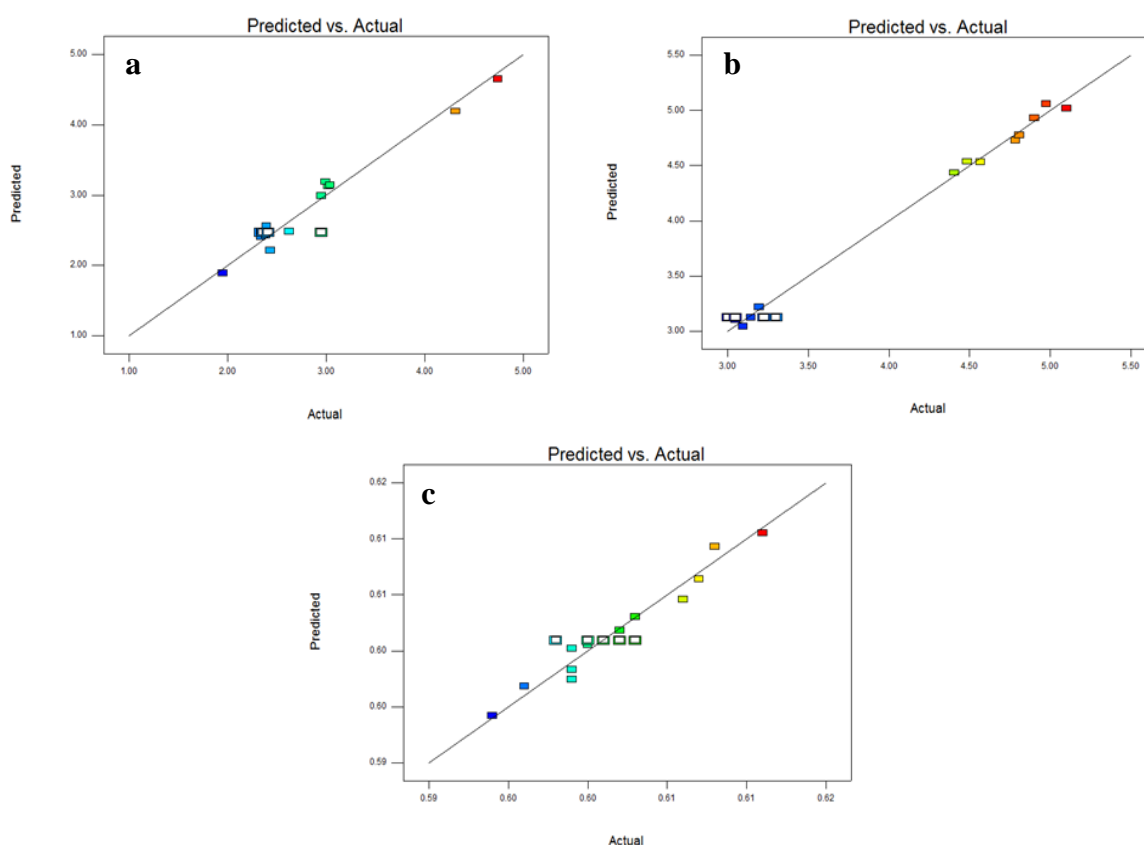


Figure 4- 19 Actual versus predicted values for (a) UV absorbance after one week, (b) UV after one month and (c) thermal conductivity

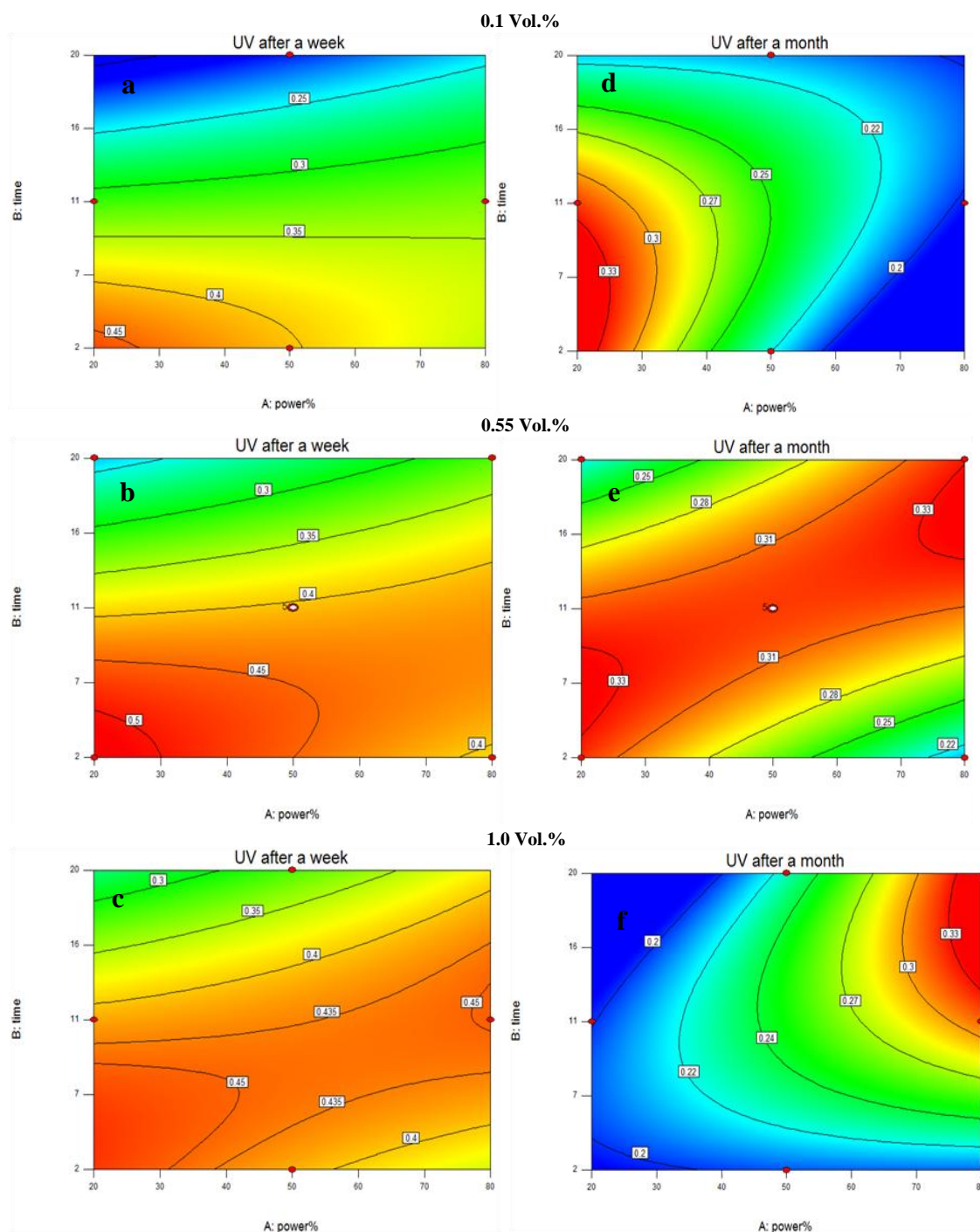


Figure 4- 20 Contour plots showing the effect of time and power of sonication on UV measurements after one week; (a) 0.1, (b) 0.55, (c) 1 % vol., and after one month; (d) 0.1, (e) 0.55 and (f) 1 % vol.

Figure 4-20 show the contour plots for UV measurement after one week and one month, which represent the short term and long term stability of nanofluids at 0.1, 0.55 and 1% TiO_2 volume concentrations. Figure 4-20 illustrate that at low concentration

(0.1 %vol.), after one week and one month, low power and short time of sonication results in the maximum UV values which represent the best stability.

This incident can also be explained by the significant quadratic term of X_{12} in thermal conductivity model of Table 4-15. This effect on stability will continue after one week even by increasing nanoparticle loading. This indicates that at low volume concentration, the nanofluids with short term stability were also stable in long term. It is also clear that increasing the power and time of sonication reduces the UV values. This supports the previous studies, where long time and high power sonication decreased the stability of nanofluids (Lee, J.-H. et al., 2008b; Li, X. et al., 2007).

However, by increasing the particle loading the stability would follow the diagonal direction, which ends up at high power and long time of sonication for 1 %vol. As is shown in Figure 4-20e, the high stability is more significant for UV measurement after one month (long term stability). In fact, at higher concentrations, longer and stronger sonication is needed to breakdown the agglomerated particles and produce a stable nanofluid.

Moreover, the comparison between the UV results after one week and after one month shows that the optimum UV area changes and nanofluids with short term stability may not be stable in long term.

In addition, by comparing the UV trend after one week and one month it can be seen that the short term stability of TiO₂ nanofluids is more dependent on time of sonication, while the long term stability relies more on power of sonication.

Figure 4-21 portray the contour plots for thermal conductivity of TiO₂-water nanofluids. They demonstrate the effect of time and power of ultrasonication on the thermal conductivity of nanofluids by increasing the volume fraction from 0.1 to 1%. As it can be seen from Figure 4-21, all three parameters have a considerable influence

on the thermal conductivity of titania nanofluid. Increasing the power and time will gradually enhance the thermal conductivity of titania nanofluid.

It is possible that stronger and longer ultrasonication of nanofluids increases the Brownian motion which results in the thermal conductivity enhancement. By increasing the time and power of sonication, nanoparticles are agitated and their collisions inside the water increase. This improves the heat transport from one particle to another and the thermal conductivity of nanofluid. Moreover, from the comparison of the three contour plots, it can be observed that a higher loading of TiO_2 nanoparticles augments the thermal conductivity of nanofluids, which is in agreement with the previous studies on thermal conductivity of nanofluids (Duangthongsuk, W. & Wongwises, S., 2009; Murshed, S. et al., 2005; Turgut, A. et al., 2009).

Although stability is essential in preparation and application of nanofluids, comparison between the UV and thermal conductivity data (Figs. 4-20 and 4-21) shows that the nanofluids with higher stability does not necessarily have higher thermal conductivity. Especially, at low volume concentrations, optimizing stability and thermal conductivity follow an opposite trend (Figs. 4-20a, d and 4-21a).

Increased thermal conductivity along with long term stability can be observed by comparing Figs. 4-20e and 4-21b. Furthermore, stability of nanofluid after one month can coexist with enhanced thermal conductivity of TiO_2 nanofluid at 1 %vol. (Figs. 4-21c and 4-20f).

Therefore, it is possible that nanoparticles agglomeration and formation of nanocluster would be responsible for thermal conductivity enhancement at low volume concentrations. In this case, the stability of this nanofluid cannot be guaranteed after one month. Recent studies on the thermal conductivity of nanofluids have also confirmed that the enhancement of thermal conductivity is caused by the growth of nanoparticle size and formation of nanocluster (Evans, W. et al., 2008).

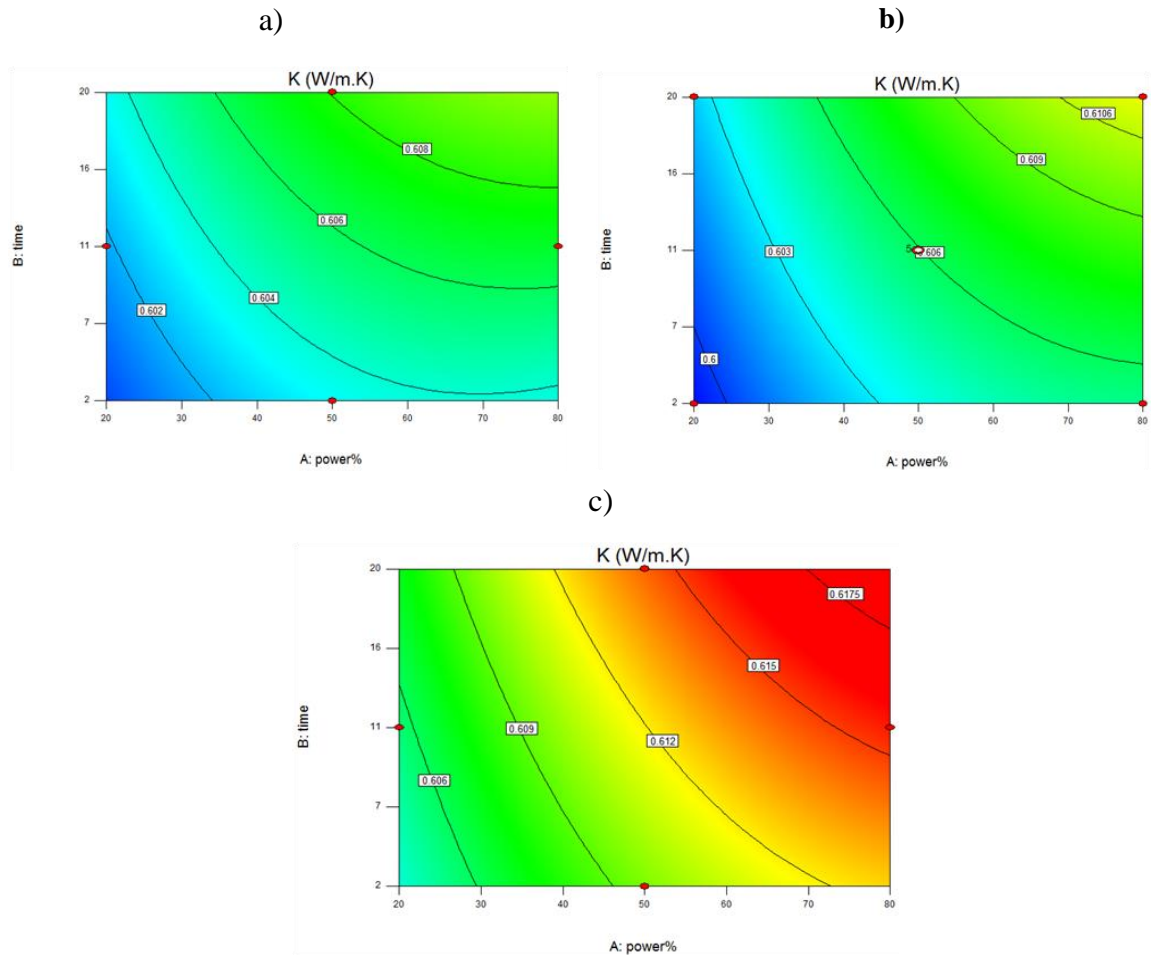


Figure 4- 21 Contour plots showing the effect of time and power of sonication on thermal conductivity of TiO_2 -water nanofluids at (a) 0.1 (b) 0.55 and (c) 1 % vol. concentration

4.4.1.2 The influence of dispersion method on viscosity, thermal conductivity and stability by mean of zeta potential

Experimental data base on the MRA were achieved and the test variables are given in Table 4-17.

From Table 4-18, the difference between the adjusted R and predicted R is within the accepted range of 0-0.2. In addition, AP and CV meet their standards as described in previous sections, which is more than 4 and below 10, respectively. In order to get a quick impression of the overall fit and the prediction power of a constructed model, R , adjusted R^2 and Predicted R^2 are very convenient.

Table 4- 17 Experimental results based on the BBD method

Run	Ultrasonic power (%)	Ultrasonic time (min)	TiO ₂ concentration (%) vol.	Relative Thermal conductivity	Viscosity m.Pa	Zeta potential mV
				K_{eff}	μ	ZP
1	80	11	0.1	1.013	0.9	-15
2	50	20	1	1.023	0.98	-42.8
3	50	20	0.1	1.015	0.9	-15.2
4	50	2	1	1.02	0.98	-22.5
5	50	11	0.55	1.011	0.93	-43.6
6	80	11	1	1.028	1.028	-27.3
7	20	11	0.1	1.003	0.89	-404
8	50	11	0.55	1.010	0.92	-44.4
9	20	20	0.55	1.008	0.9	-42
10	20	2	0.55	1	0.92	-45.2
11	80	20	0.55	1.021	0.97	-41.8
12	20	11	1	1.010	1.02	-21.7
13	80	2	0.55	1.008	0.92	-44.3
14	50	11	0.55	1.006	0.94	-38.9
15	50	2	0.1	1.008	0.89	-48.4
16	50	11	0.55	1.015	0.92	-43.7
17	50	11	0.55	1.013	0.94	-40

Table 4- 18 ANOVA for response surface quadratic models

Responses	R ²	Adj.R ²	Pred.R ²	AP	CV%	Std. Dev.
K _{eff}	0.9207	0.8591	0.7146	13.107	8.1	0.23
μ	0.9334	0.8816	0.6035	0.12	3.05	0.016
ZP	0.9453	0.9028	0.6930	1.65E-03	0.27	3.48

Table 4-19 represents the statistical results of ANOVA in terms of coded factors for P-values. The second-order polynomial equations were derived to explain the characteristics by the means of relative thermal conductivity (Y_3) and viscosity (Y_4) as well as magnitude of zeta potential (Y_5) to evaluate the stability of nanofluids (see Table 4-19). After eliminating the insignificant parameters, polynomial equations and

response surfaces for a particular response in terms of coded factor were produced using RSM. For the viscosity an inverse model were required to improve the models.

Table 4- 19 ANOVA for response surface method

	P-Value		
	Thermal conductivity	Viscosity	Zeta potential
	Y ₃	Y ₄	Y ₅
Model	0.001	0.0001	< 0.0001
X ₁ -power	0.0003	0.0549	0.0624
X ₂ -time	0.0045	0.3636	0.0911
X ₃ -volume conc	0.0009	<0.0001	0.6440
X ₁₂	0.4076	0.0370	-
X ₁₃	0.1833	0.9299	0.0016
X ₂₃	0.5762	-	< 0.0001
X ₁ ²	0.1367	-	-
X ₂ ²	-	0.1512	0.0662
X ₃ ²	0.0089	0.0335	<0.0001
Lack of Fit	0.6878	0.1688	0.1773

Table 4- 20 The developed models of characteristic and stability responses

Response	Final equation in terms of coded factors
K _{eff}	$Y_3 = 0.61 + 3.75 \text{ E-}03 X_1 - 2.375 \text{ E-}03 X_2 + 3.125 \text{ E-}03 X_3 + 7.5 \text{ E-}04 X_{12} + 1.25 \text{ E-}03 X_{13} - 1.382 \text{ E-}03 X_1^2 + 0.2868 \text{ E-}03 X_3^2$
μ	$1/(Y_4) = +1.07 - 0.013 X_1 - 5.545 \text{ E-}03 X_2 - 0.060 X_3 - 0.020 X_{12} + 7.415 \text{ E-}04 X_{13} + 0.013 X_2^2 - 0.02 X_3^2$
ZP	$Y_5 = -41.08 + 2.61 X_1 + 2.32 X_2 + 0.59 X_3 - 7.75 X_{13} - 13.38 X_{23} - 3.54 X_2^2 + 13.69 X_3^2$

The ANOVA results in terms of stability parameter represent that among the coded parameters, terms X₁₃, X₂₃, and X₃² have considerable effects on the stability of nanofluid in terms of zeta potential as shown in Table 4-19. It means that zeta potential response is more dependent on the interactions of nanoparticle loading than the timing and power of ultrasonication.

The results obtained by ANOVA claim that the terms X₃, X₁₂ and X₃² have great influence on viscosity of TiO₂ nanofluid. It is concluded that this characteristic response

relies more on the volume concentration, although the interaction between power and time of ultrasonic horn cannot be ignored.

Furthermore, given results in Table 4-19 show that between the coded parameters, terms X_1 , X_2 , X_3 and X_3^2 have major effect on thermal conductivity of TiO_2 nanofluid. As a result, any changes in the value of these coded parameters will bring momentous change to the thermal conductivity of nanofluid. However, the quadratic form of volume concentration is a matter of concern in verifying the changes of thermal conductivity.

Figures 4-22 show that the models were successful in capturing the correlation between the factors and the responses. The points around the diagonal line indicate a satisfactory fit of the model. As it is seen in Figures 4-22, in all the three responses, replications at the center of the design show a very good agreement with each other, which confirms the reliability of the experiments.

Figures 4-23 (a, c and e) show that viscosity follows a similar trend for all the timing of ultrasonication although altering the power, increases the dispersion and more viscous suspension appears. Growing volume concentration results in higher viscosity as could be expected by the Einstein law.

Meanwhile, at short ultrasonication ($t=1$ min), the most viscous nanofluid accredited to the weakest power (Amplitude= 20%) whereas for the other timings, titania nanosuspension reach to its highest viscosity by the strongest power.

These graphs show that at all ranges of power, short ultrasonication prepares very stable nanofluids (<-40 mV) from 0.1 to 0.72 percent of volume concentration (Figs. 4-23). Increasing volume concentration decreases the stability by the means of zeta potential. This incident can also be proved by the data from Table 4-20 that volume concentration and its interaction by other two factors of time and power does have significant impact on the model but by a negative order. Power has a small effect on

zeta potential increment, which can be found from the small coefficient of term X_2 in zeta potential. Moreover, short ultrasonication at higher volume concentration would not prepare a stable suspension.

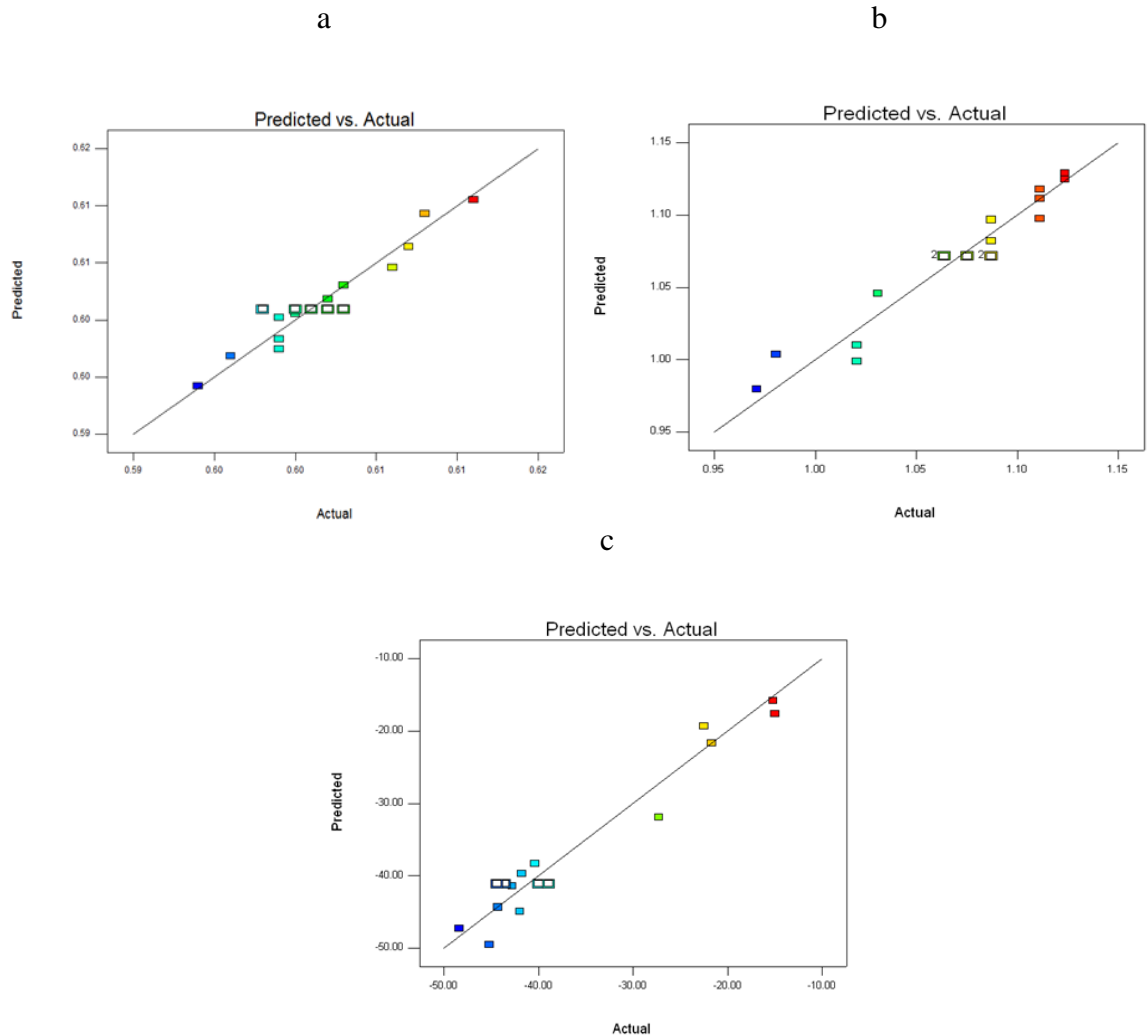


Figure 4- 22 Actual versus predicted values for (a) thermal conductivity, (b) viscosity and (c) zeta potential

Growing ultrasonication time results in fewer stable samples of nanofluids and power increment declines the zeta potential and correspondingly the stability of titania nanosuspension (Figs. 4-23). Longer ultrasonication ($t=20$ min) gives good stability with higher concentration of nanoparticles (above 0.4%) as the duration of ultrasonication has the most significant influence on zeta potential model by positive

order of magnitude. As it can be seen from Figure 4-23, growing power decreases the stability.

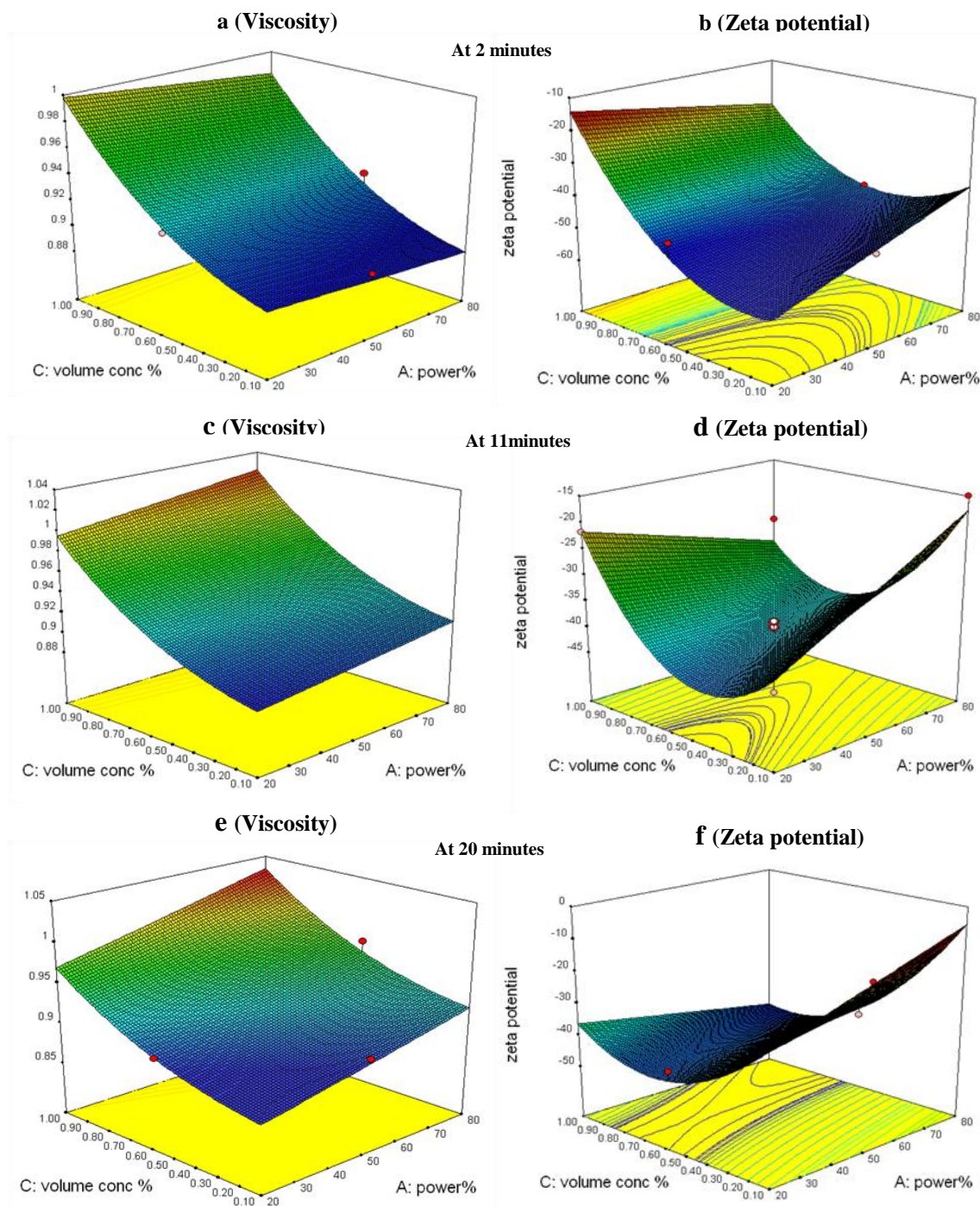


Figure 4- 23 Surface response plots presenting viscosity and zeta potential variation by altering power and volume concentration at different timing (t); (a and b) at t=2; (c and d) at t=11; and (e and f) at t=20 minutes

4.4.1.3 Stability evaluation by sedimentation balance method at intervals of two days, one week and one month

Sedimentation balance method (sedimentation rate measurement by gradient cylinder) which was described briefly in chapter two was nominated as a response for stability measurement in this section.

Multiple regression method by Box-Behnken approach was applied to set the runs in order to get the experimental results (see Table 4-21).

Table 4- 21 Box-Behnken design matrix and experimental record responses

Run	Ultrasonic power (%)	Ultrasonic time (min)	TiO ₂ vol. Concentration (%)	W _s (after two days)	W _s (after one week)	W _s (after one month)
1	80	11	0.1	10	22	68
2	50	20	1	6	16	54
3	50	20	0.1	8	18	76
4	50	2	1	6	13	40
5	50	11	0.55	5	16	45
6	80	11	1	8	14	36
7	20	11	0.1	8	24	48
8	50	11	0.55	5	16	51
9	20	20	0.55	7	19	73
10	20	2	0.55	5	27	68
11	80	20	0.55	6	18	70
12	20	11	1	7	21	58
13	80	2	0.55	5.5	12	60
14	50	11	0.55	5	14	50
15	50	2	0.1	6	22	82
16	50	11	0.55	5.5	17	58
17	50	11	0.55	6	15	60

The developed model for measurements by sedimentation balance method after two days, one week and one month which are presented by Y₆, Y₇ and Y₈ correspondingly, are shown at Table 4-22. These models explain the magnitude of each factor and their interactions on responses.

After eliminating the insignificant parameters, polynomial equations and response surfaces for a particular response in terms of coded factor were produced using RSM.

For the stability characteristics, Y_8 , an inverse model with square root transformation with constant value set to -26, were required to improve the models for sedimentation after one week and one month, respectively.

Table 4- 22 The developed models of W_s responses

Response	Final equation in terms of coded factors
W_s (after 2 days)	$Y_6 = 5.30 + 0.31 X_1 + 0.56 X_2 - 0.63 X_3 - 0.50 X_{23} + 1.16 X_1^2 - 0.59 X_2^2 + 1.79 X_3^2$
W_s (after one week)	$Y_7 = 15.68 - 3.13 X_1 - 0.38 X_2 - 2.75 X_3 + 3.50 X_{12} - 1.25 X_{13} + 1.75 X_{23} + 3.21 X_1^2 + 1.46 X_3^2$
W_s (after one month)	$1/\text{Sqrt}(Y_8 - 26) = 0.19 + 0.013 X_1 - 0.012 X_2 + 0.038 X_3 - 3.076 E-03 X_{12} + 0.050 X_{13} - 0.022 X_{23} - 0.037 X_2^2 + 0.023 X_3^2$

As it is shown in Table 4-23 and discussed earlier in this chapter, coefficient of quadratic R is near to 1 and adjusted R and predicted R are within the accepted range of 0-0.2 which illustrates the models fit the experimental data for all of the responses. In addition, CV and AP meet their requirements of being in the range of more than 10 and below 4, respectively.

Table 4- 23 ANOVA for response surface quadratic models

Responses	R^2	Adj. R^2	Pred. R^2	AP	C.V%	Std. Dev.
Y_6	0.8956	0.8144	0.6145	10.081	9.44	0.61
Y_7	0.9576	0.9151	0.7392	15.111	9.35	1.21
Y_8	0.9112	0.8224	0.6203	12.567	10.76	0.020

Table 4-24 represents the statistical results of ANOVA in terms of coded factors for P-values. The ANOVA results in terms of stability parameters represent that among the coded factors, terms X_2 , X_3 , X_3^2 and X_I^2 have considerable effects on the stability of

nanofluid in terms of sedimentation rate after two days (Y_6) as shown in Table 4-24. It means that the most effective parameter on this response is the volume concentration of nanoparticle which has the lowest p value. In addition, the p-value of power and timing of ultrasonication are below 0.05 and demonstrate the significance of these terms on stability detection after two days.

Table 4- 24 ANOVA for response surface method for sedimentation balance method after intervals of two days, one week and one month

	P-Value		
	W _s (after two days)	W _s (after one week)	W _s (after one month)
	Y ₆	Y ₇	Y ₈
Model	0.0009	0.0001	0.0017
X ₁ -power	0.1784	< 0.0001	0.1105
X ₂ -time	0.0275	0.4045	0.1196
X ₃ -volume conc	0.0170	0.0002	0.0007
X ₁₂	-	0.0004	0.7687
X ₁₃	-	0.0717	0.0012
X ₂₃	0.1330	0.0198	0.0660
X ₁ ²	0.0034	0.0006	-
X ₂ ²	0.0777	-	0.0057
X ₃ ²	0.0002	0.0375	0.0494
Lack of Fit	0.1977	0.4216	0.7354

Similarly, the results obtained by ANOVA shows that the terms X_1 , X_3 , X_1^2 and X_{12} have great influence on the stability of TiO₂ nanofluid for Y_7 response (sedimentation after one week), although the impact of X_3^2 which represents the quadratic coefficient of volume concentration cannot be neglected. It is concluded that sedimentation after one week relies on the power of ultrasonication, volume concentration and the interaction between power and timing of ultrasonication.

Furthermore, given results in Table 4-24 show that among the coded parameters, terms X_3 , X_{13} , X_2^2 and X_3^2 have significant effect on the stability in terms of sedimentation recording after one month. In other words, any changes in the value of these coded parameters will bring significant changes to the long term stability (after

one month) of nanofluid. It means that Y_8 response is more dependent on the amount of nanoparticle loading and its interaction with the power of sonication compared to the time of sonication, however, the quadratic term of timing of ultrasonication is a matter of concern in verifying the precipitation rate.

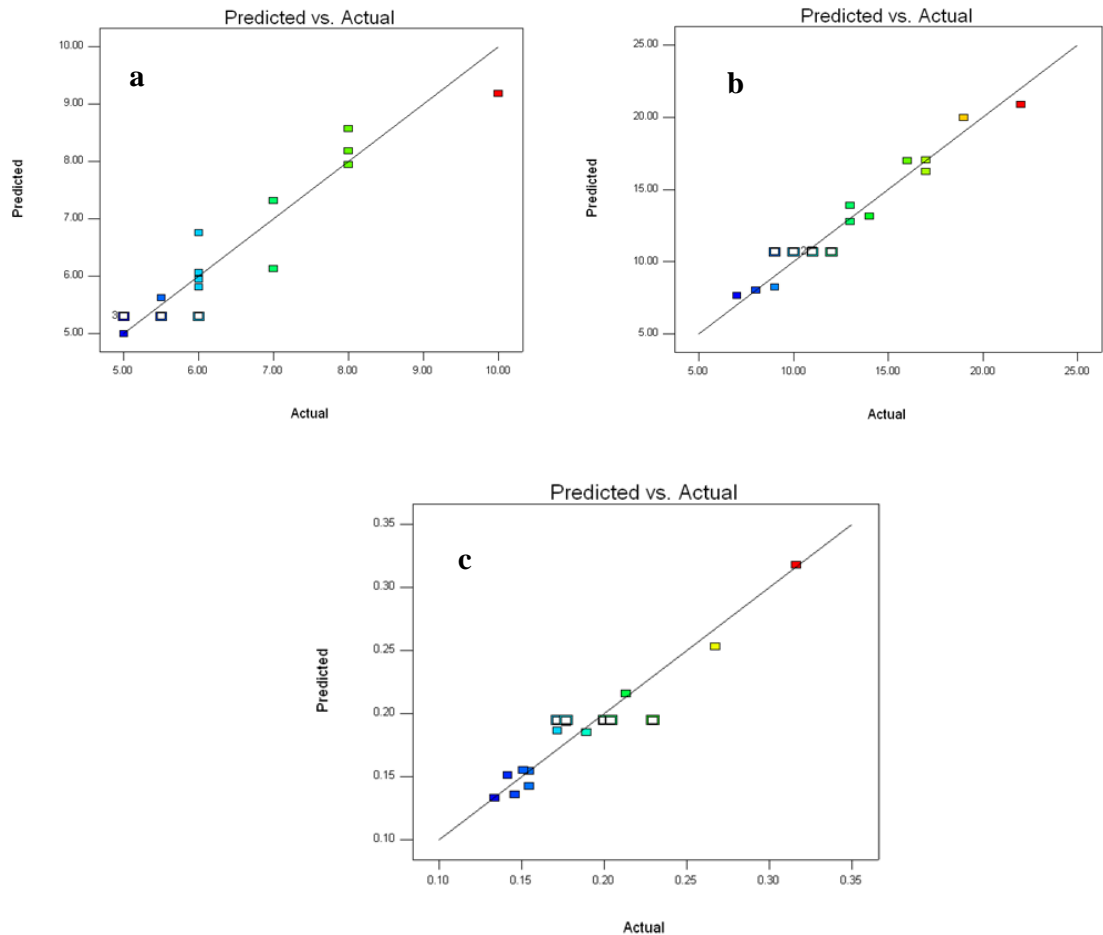


Figure 4- 24 Actual versus predicted plots for TiO_2 nanofluid for the measurement of sedimentation rate: (a) after two days, (b) after one week, (c) after one month

Figs. 4-24 show that the models were successful in capturing the correlation between the factors and the responses. The points around the diagonal line indicate a satisfactory fit of the model. As it is seen in Figs. 4-24, in all the three responses, replications at the center of the design show a very good agreement with each other, which confirms the reliability of the experiments.

The graphs of 4-25 show that by keeping power and time of ultrasonication at its lowest amount, less sedimentation appears in almost all ranges of titania. Surprisingly,

this trend would be repeated by higher powers of 50% and 80% (see Figs. 4-26 and 4-27). This matter demonstrates that weaker or stronger ultrasonication do not have much impact on stability at measurement after two days by sedimentation balance method.

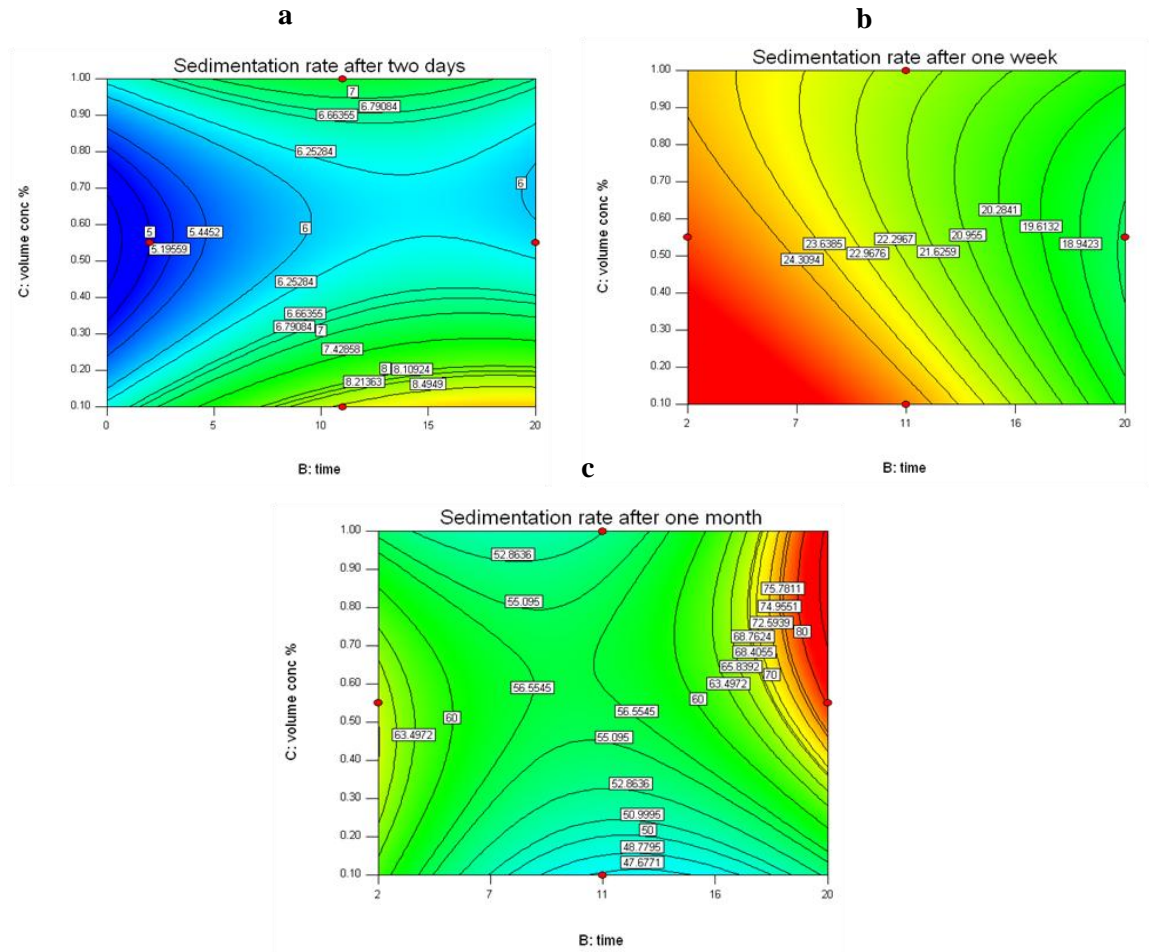


Figure 4- 25 Two dimensional contour plots for sedimentation rate measurement of titania nanofluid at ultrasonic amplitude of 20%; a) after two days; b) after one week; c) after one month

The figure of Ws after one week demonstrates that all the measurements for different concentration follow a routine that longer and weaker ultrasonication produces the most stable nanofluid. Less sedimentation shows up by imposing power more than 50% and sedimentation grows if the time increases.

As is depicted, the area of lowest sedimentation detects by sedimentation rate after one week and still shows up after 30 days (see Figs.4-25). But measurement after

one week demonstrate the highest sedimentation at low sonication time and power at concentrations below 0.6% vol. ,whereas this area shifted to the samples with high power ultrasonication at the measurements after one month. This will prove that shorter and weaker ultrasonication cause sedimentation of the particles after one week but high power and low duration, due to the agglomeration and great Van der Waals force among nanoparticles, persuade the coagulation of nanoparticles to sediment after this period of time.

The most precipitated samples grow between the aforementioned homogenization methods with ultrasonic horn timing of 20 minutes. This plot displays that long ultrasonication is not suitable for most of the samples in order to prepare stable nanofluid. Then they would sediment easily after one month.

Results from Figures 4-25 illustrate that by keeping the amplitude of ultrasonication at 20% of its capacity, short ultrasonication show better result with less sedimentation after two days. But, we identify a change of trend by recording precipitation rate after one week and one month. This shows that low power and time of ultrasonication has short time advantage on stability of nanofluid whereas for having a long time improvement of homogenization, the samples need to be kept at longer ultrasonication with respect to low power. Figure 4-26 shows that increment of volume concentration reduces sedimentation rate whereas longer ultrasonication has better impact on stability of nanofluid after one week.

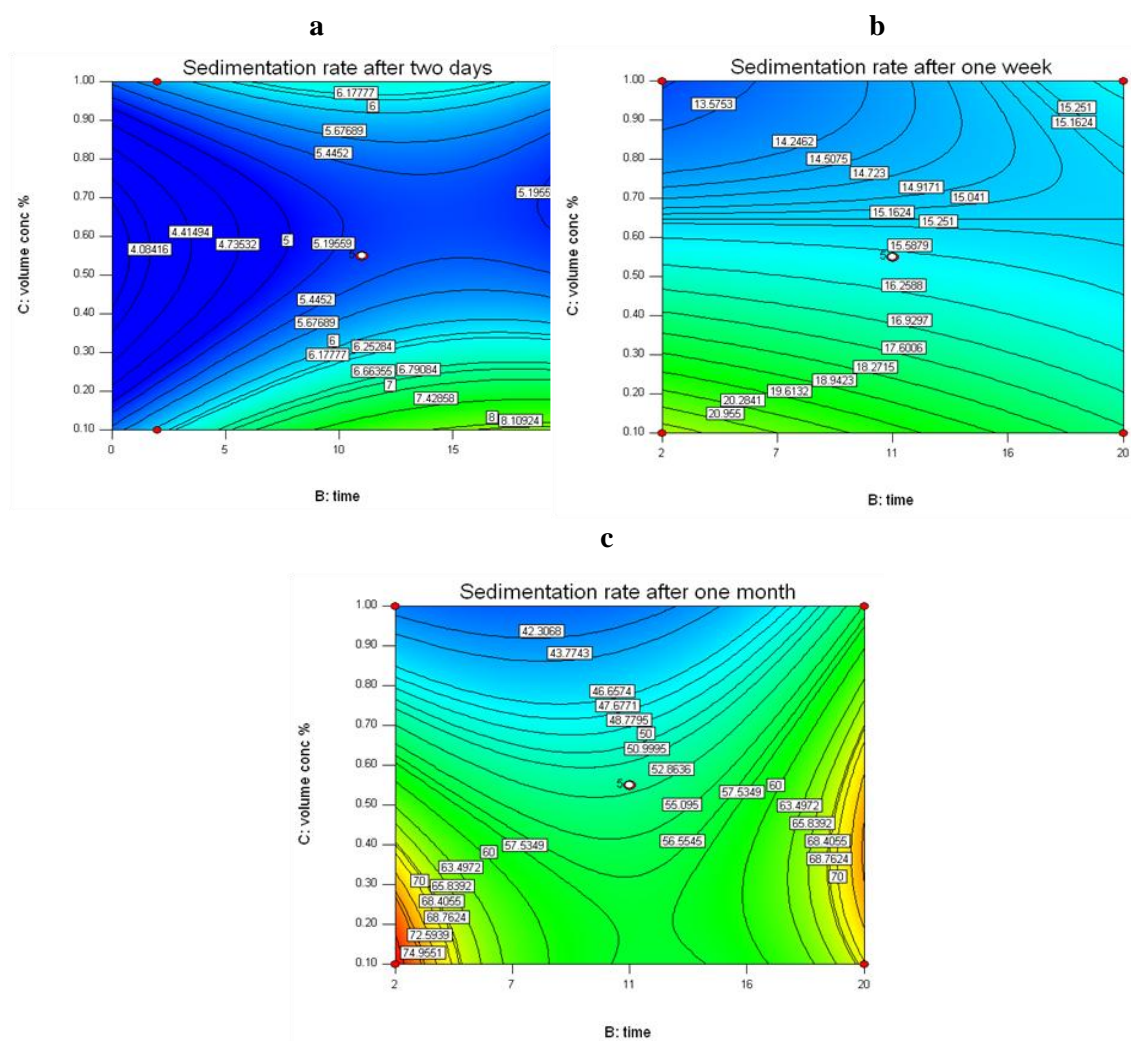


Figure 4- 26 Two dimensional contour plots for sedimentation rate measurement of titania nanofluid at ultrasonic amplitude of 50%; a) after two days; b) after one week; c) after one month

Meanwhile, outcomes from Figures 4-26 reveals that medium amplitude of 50% of ultrasonic horn keeps the samples in a better stability situation even after one month.

Rising volume concentration decreases the sedimentation rate for titania nano-suspensions and this trend is followed by precipitation recording even after one week and one month (see Figs. 4-26). This proves our analytical results (Table 4-24) that coded factor of C (volume concentration) have a significant role on stability of nanofluid for all the above-mentioned intervals. Interestingly, the most stable samples

4.4.2 Optimization

Numerical optimization displays the feasible values in which any combination of one or more goals will meet in the form of factor or responses. The criteria in classifying limits of optimization were set by the values shown in Table 4-25 which shows the acquired maximum thermal conductivity and stability responses. The desirable point was obtained at the ultrasonication amplitude of 75%, duration of 20 minutes and nanoparticle loading of 0.86 %vol.

The results showed that the estimated stability of titania nanofluid considered high regard to the UV absorbance, sedimentation rate and zeta potential of -46.8. Furthermore, within the obtained range of enhanced thermal conductivity, the predicted nanofluid has nearly the maximum value of improvement associated with low viscosity.

The predicted desirable particle size of nanofluid was 411 nm which proves that this optimum point confirms the results from previous sections that clustering and agglomeration would be the reason of heat transfer enhancement for titania nanofluid.

The result in Table 4-25 shows that this modeling and optimization software is able to predict the aforementioned condition of nanofluid preparation successfully up to 6% of accuracy. The precipitation rate measurement by means of sedimentation balance method reaches over 5% of error which may occur due to human reading error. Therefore, there would be no concern for stability monitoring as there are many responses covered by this optimization such as UV absorbance and zeta potential. However, thermal conductivity measurement which is the main concern of nanofluid preparation has the lowest error of 0.29% and shows an excellent uncertainty.

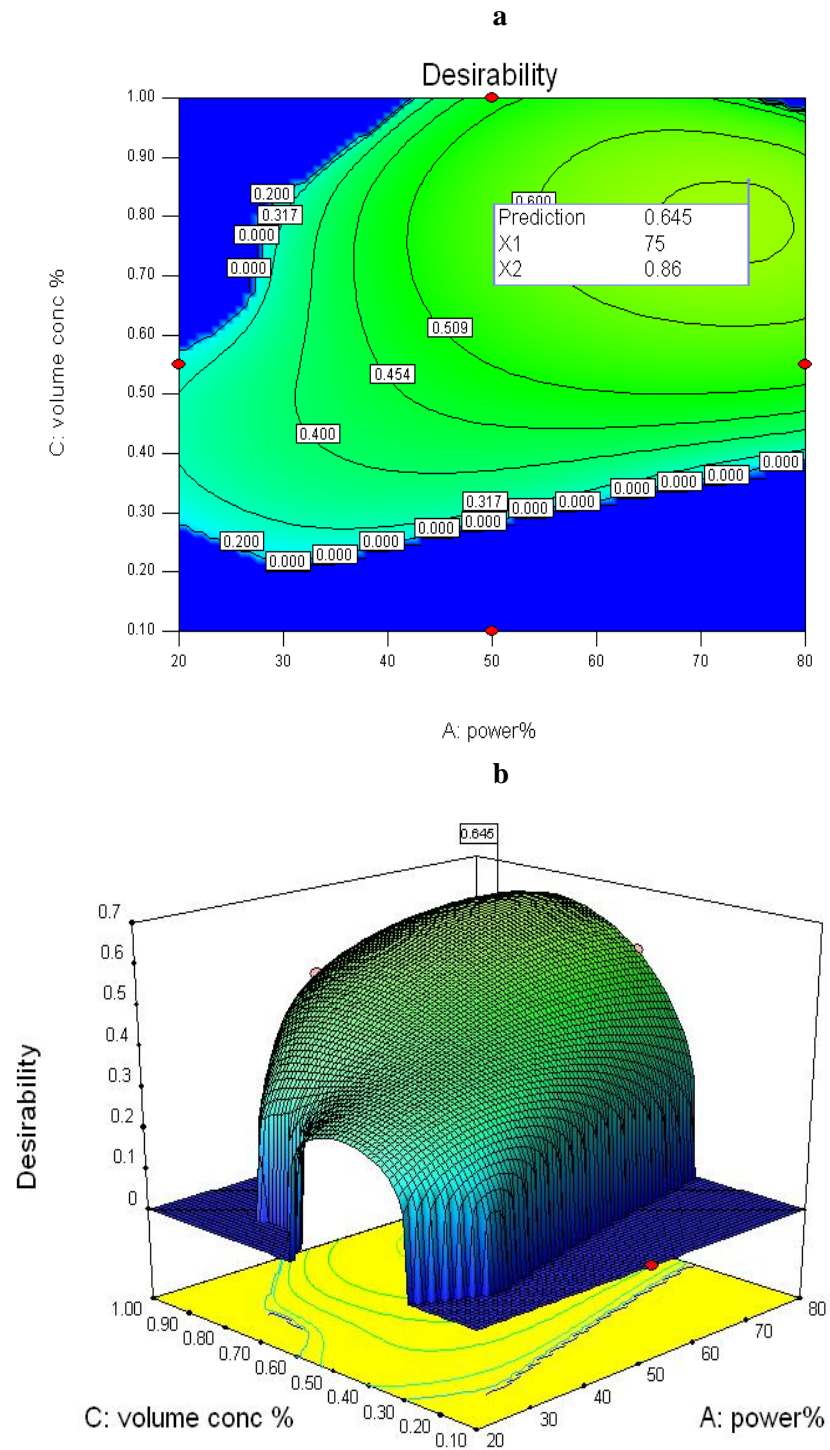


Figure 4- 28 Desirability plot for TiO_2 nanofluid: (a) 2D surface mesh, (b) 3D plot with contours

Table 4- 25 The goals and predicted point for nanofluid characteristics and stability evaluation

Name	Goal	Limit	Limit	Desirable point predicted	Measured	Error (%)
A:power	is in range	20	80	75	75	-
B:time	is in range	2	20	20	20	-
C: volume concentration	is in range	0.1	1	0.86	0.86	-
K_{eff}	maximize	1	1.028	1.027	1.03	0.29
μ	minimize	0.89	1.03	0.998	0.97	-2.8
PS	-	273.8	1515	411.94	390	-5.3
ZP	minimize	-48.4	-30	-46.83	-49	-4.63
W_s after two days	minimize	5	10	6.38	6	-5.9
W_s after one week	minimize	12	27	17.067	16	-6.0
W_s after thirty days	minimize	36	82	50.096	N/A	N/A
UV absorbance after one month	maximize	0.196	0.333	0.327356	0.333	1.83
UV absorbance after one week	maximize	0.211	0.513	0.355093	N/A	N/A

4.5 Comparison of thermal conductivity results

As it was mentioned earlier in the literature review, none of the classical models succeeded in determination of thermal conductivity enhancement of nanofluid. Table 4-26 shows the experimental results in low concentration titania nanofluid compared with some analytical models. The results revealed that although classical models are not able to estimate the experimental results, the models presented by Yu and Choi (2003) and Timofeeva (2007) are capable to predict the experimental results within 1% of error. These two models which are the most applicable models in nanofluid thermal conductivity prediction have different approaches.

Timofeeva et al. (2007) reported that no anomalous enhancements which were reported by some other investigators can be seen by their experiments and evaluations. They declared that agglomeration and clustering by transporting heat rapidly over significant distances and a specific orientation can be the reason of the nanofluid heat transfer enhancement. However, Yu and Choi (2003), predicted the enhancement by exploiting the nanolayer structure to produce nanofluids that are highly thermally conductive. This outcome reveals that thermal conductivity of nanofluid which is stable for over one month can be predicted by the abovementioned models at volume concentrations higher than 0.55 % vol.

Comparing these models with the experimental results, low concentration nanofluids (0.026 and 0.1% vol.) show better enhancement in comparison with higher volume concentrations (0.55 and 1.0% vol.).

Table 4- 26 Models for the evaluation of thermal conductivity of titania nanofluid

%vol.	(Maxwell, C. & Thompson, J. R., 1904)	(Hamilton, R. L. & Crosser, O. K., 1962)	(Jeffrey, D. J., 1973)	(Yu, W. & Choi, S. U. S., 2003)	(Timofeev a, E. V. et al., 2007)	Experimental results
0.026	1.0006	1.0006	1.0006	1.0009	1.0008	1.015
0.1	1.0025	1.0025	1.0025	1.0034	1.003	1.016
0.55	1.0142	1.0142	1.0142	1.0190	1.0165	1.015
1.0	1.0260	1.0260	1.0260	1.0347	1.03	1.028

Conclusion

Chapter five: Conclusion

This thesis work focused on understanding the fundamental basis for the effect of preparative condition on the stability and thermal conductivity of titania nanofluid.

5-1 The influence of homogenization methods on stability and thermal conductivity of titania nanofluid

Based on the experimental investigation, to examine the influence of homogenization methods on stability and thermal conductivity of low concentration nanofluid, addition of SDS as an anionic surfactant increases stability of nano-suspension but the suspension is not durable for more than one month. Ultrasonic processes increase the absorbance of nanofluid which means having more stable suspension. However, the timing should be proportional to the volume concentration if a stable dispersion is needed. Surfactant addition without ultrasonic processing doesn't contribute to stability and in this case titania nanofluid without processing and surfactant addition would have better responses following by increased thermal conductivity. It can be concluded that enhancement of thermal conductivity in low concentration nanofluid (stationary condition), within the same volume fraction of titania in six different samples, ascribes to three-hour ultrasonic bath processing with surfactant, which also proves the notes claimed by Prasher et al. (2006). This theory was concluded from the assumptions of Russel et al. (1989) and Hunter (2001) in which claimed that "the probability of aggregation increases with decreasing particle size, at the constant volume concentration, because the average interparticle distance decrease, making the attractive van der Waals force more important. Aggregation process lessens the Brownian motion effect due to the increase in the mass of the aggregates, whereas it can increase k due to percolation effects in the aggregates, as highly conducting particles touch each other in the aggregate". The UV-vis absorbance, zeta potential and particle size measurements prove this conclusion. For this reason, short term application

of this sample would be a superior idea but in the case of long term, it needs further investigations.

5.2 Suitability of UV-vis spectrophotometer for measuring stability in short and long term

Another objective of this study is to find out whether the UV-vis spectrophotometer is a suitable monitoring tool to quantitatively determine the stability of colloidal suspensions like nanofluid or otherwise. The results revealed that except the UV measurements after one day which were not stable the stability responses for the other three intervals are reliable.

In order to be applied in industry, nanofluid should be stable in long term, for instance one month while for having short term applications in laboratories, this kind of stability simulation for intervals of two days or one week appears essential. Since there is no preferred and suitable standard to accomplish nanofluid preparation with the optimized stability so far, supplementary simulating software like Design of Experiment would be very valuable. The results in this study demonstrated that higher desirability would be achieved if we aspire to include long term stability of nanofluid by excluding the first day measurement of UV-vis spectrophotometer. This validation shows that pH value of 10 with almost the same ratio of surfactant to nanoparticle loading would be a proper combination to homogenize nanofluid in order to keep its stability even after one month with the accuracy of 5%.

5.3 The importance of nanofluid stability by means of zeta potential, UV absorbance and particle size on thermal conductivity enhancement of nanofluid

In order to evaluate the effect of nanoparticle volume concentration, duration and power of ultrasonic on the stability and thermal conductivity of nanofluid, results using RSM showed that the %wt. of surfactant had a significant influence on the zeta

potential and UV absorbance responses of nanofluid. In contrast, the value of pH had a significant effect on the particle size and also thermal conductivity which is the most important parameter to measure the heat transfer of nanofluid. The maximum values (optimum condition) for zeta potential, thermal conductivity and UV absorbance responses achieved at maximum value of pH and almost at minimum quantity of %wt. of surfactant. However, for thermal conductivity, almost half of the stable nanofluids could exhibit the expected improved thermal conductivity. It can be considered that derived from the clustering theory, large particle size may construct a chain shape cluster which increases the heat transfer.

On the other hand, the optimum situation for particle size response occurred at minimum value of pH for the entire values of %wt. of surfactant. The desirability of the constructed model including all responses is 0.727 which is indicated as an acceptable value. The optimum condition considering all responses is pH value of 11.4 and %wt. of the surfactant set to 0.04.

Though we observe a correlation between aggregate size and thermal conductivity, the behavior of the latter is more complex. The model proposed by Prasher et al. (2006) should therefore be improved by adding other factors which it is not clear at the present time. The outcomes reveal that the bigger the radius of gyration the better the enhancement of heat transfer. As the initial average diameter of titanium dioxide was 25 nm and the aggregated nanoparticle size with enhanced thermal conductivity of 2.6% was 463 nm (at 0.1% wt.), it seems that clustering theory can be one of the reasons to describe the increasing thermal conductivity.

5.4 The influence of nanoparticle volume concentration, duration and power of ultrasonic on the stability and thermal conductivity of nanofluid

Another part of this study focused on the influence of duration and power of sonication on stability and thermal conductivity of TiO₂ - water nanofluids in different

nanoparticle loadings. UV-vis spectrophotometer, zeta potential and sedimentation balance method were employed to determine the relative stability of nanofluids after one week and one month. Implementing the contour plots in response surface methodology (RSM) based on the Box-Behnken design (BBD) was helpful to study the effect of time of sonication, power of sonication, and TiO_2 volume concentration as three independent variables. The UV-vis spectrophotometer measurements revealed that nanofluids with short term stability may not be stable in long term. Results explain that the stability of nanofluids after one week relies more on the time of sonication, while the power of sonication was found more significant for stability after one month. In addition, at low volume concentration, short time and low power sonication established the highest stability without any increase in the thermal conductivity. However, increasing the power and time of sonication at low volume concentration deteriorated the stability. On the other hand, by increasing the volume concentration, higher stability was more likely to be obtained at longer and stronger sonication.

Thermal conductivity enhancement was monitored with increasing the time and power of sonication as well as increasing TiO_2 volume concentration. It is possible that, increasing the sonication time and power enhances the Brownian motion of TiO_2 nanoparticles, which improves the thermal conductivity of nanofluids.

We have also observed that, higher thermal conductivity of TiO_2 -water nanofluids was not necessarily obtained at higher stability. Hence, authors suggest that, other factors such as clustering effect due to aggregation and growth of nanoparticle size are responsible for thermal conductivity enhancement.

Finally, we suggest that, stability and thermal conductivity enhancement of nanofluid should be pursued together in optimization of heat transfer characteristic. The discrepancies among the reported results in this area may be stemmed from the lack of

attention to the interaction between the maximum thermal conductivity and stability in the optimization of nanofluid preparation.

5-5 Future works and recommendations

This work focused on understanding the effect of stability on thermal conductivity of low concentration titania nanofluid. It is determined that aggregation and clustering are the cause of the enhanced thermal conductivity reported by many researchers.

Thermal conductivity and stability researches in stationary condition in this study showed that not all the stable nanofluids lead to high thermal conductivity and vice versa. Therefore, the exact situation and option in this thesis should be moved to the flowing condition in order to get the span of vision for heat transfer coefficient and enhanced thermal conductivity in flowing condition. A circular, rectangular with straight or opaque set up should be prepared consisted of thermometer and pressure gauges to check the thermal conductivity and pressure loss by data logger. Finalizing these results combined with stationary condition would comprehensively demonstrate the correct situation in which industry would follow in the near future.

Appendix A

Table A- 1 Specification of equipment in this research

ID	Brand	Specifications	Accuracy
Horn ultrasonic	Sonic Vibra	Ti-horn, 20 kHz, and 130	-
	Cell	W/cm ² (6 mm) probe	
Ultrasonic bath	Branson	47 khz, System 000092,	-
	3210	bath size approx. 12 x 6 x	
		6 with cover	
Zeta potential			±0.1mV
DLS	Malvern	100-260 v 50-60Hz	±0.1nm
	3000HSA		
UV-vis	Varian	Cary-50 probe	± 0.5 at 541.94
spectrophotometer			
XRD	Philips	Cu-K _α with a wavelength	± 0.5
	X'pert MPD	of 0.1542 nm	
	PW3040		
Thermal conductivity	KD2 pro	Transient hot needle	± 5% from 0.2-
meter			2W/(m.K)
Viscometer	A&D	Vibration method	1% of Reading
			(Full Range
pH meter	Eutech	Auto-Buffer Recognition	±0.01 pH
Water Distiller	Favorit	WCS4L	-

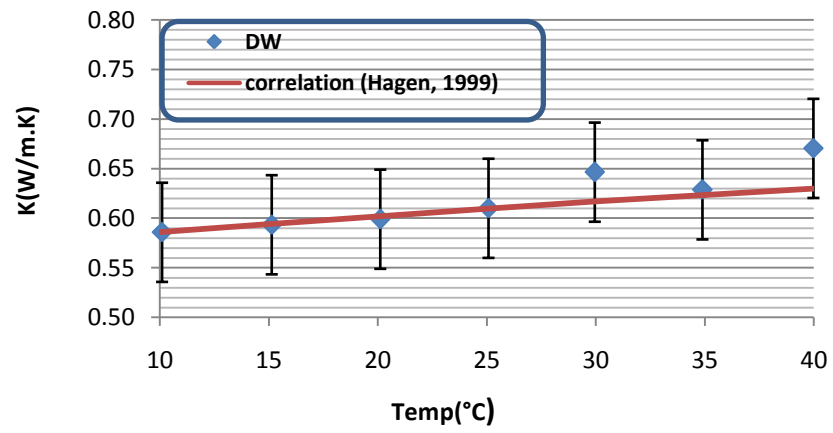


Figure A- 1 Comparison between distilled water data from KD2 pro and correlation

Certificate of Analysis

SIGMA-ALDRICH

Product Name	Titanium(IV) oxide, anatase, nanopowder, <25 nm particle size, 99.7% trace metals basis
Product Number	637254
Product Brand	ALDRICH
CAS Number	1317-70-0
Molecular Formula	TiO ₂
Molecular Weight	79.87

TEST

Appearance (Color)
Appearance (Form)
Particle Size
X-Ray Diffraction
ICP: Confirms Titanium Component
Trace Metal Analysis
Aluminum (Al)
Arsenic (As)
Boron (B)
Barium (Ba)
Calcium (Ca)
Copper (Cu)
Iron (Fe)
Potassium (K)
Magnesium (Mg)
Manganese (Mn)
Sodium (Na)
Lead (Pb)
Tin (Sn)
Vanadium (V)
Zinc (Zn)
Purity

SPECIFICATION

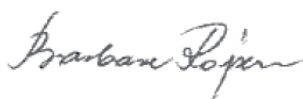
White
Powder
≤25.0 nm
Conforms to Structure
Confirmed
≤4000.0 ppm
ppm
ppm
ppm
ppm
ppm
ppm
ppm
ppm
ppm
ppm
ppm
ppm
ppm
ppm
ppm
ppm
Conforms
99.7% Based On Trace Metals Analysis

LOT MKBC4889 RESULTS

White
Powder
< 25.0 nm
Conforms
Conforms
2088.7 ppm
650.8 ppm
10.8 ppm
1.5 ppm
1.2 ppm
361.1 ppm
17.7 ppm
20.6 ppm
228.6 ppm
89.3 ppm
1.5 ppm
590.7 ppm
60.2 ppm
32.8 ppm
9.4 ppm
12.6 ppm
Conforms

Specification Date:
Date of QC Release:
Print Date:

JAN 2009
NOV 2009
NOV 03 2009



Barbara Rajzer, Supervisor
Quality Control
Milwaukee, Wisconsin USA

References

- Abareshi, M., Goharshadi, E.K., Mojtaba Zebarjad, S., Khandan Fadafan, H., & Youssefi, A. (2010). Fabrication, characterization and measurement of thermal conductivity of Fe_3O_4 nanofluids. *Journal of Magnetism and Magnetic Materials*, 322(24), 3895-3901.
- Adinarayana, K., & Ellaiah, P. (2002). Response surface optimization of the critical medium components for the production of alkaline protease by a newly isolated *Bacillus* sp. *Journal of Pharmacy and Pharmaceutical Sciences*, 5(3), 272-278.
- Altekar, M., Homon, C.A., Kashem, M.A., Mason, S.W., Nelson, R.M., Patnaude, L.A., . . . Taylor, P.B. (2006). Assay optimization: a statistical design of experiments approach *A Tutorial from the Journal of the Association for Laboratory Automation*, 11, 33-41.
- Amrollahi, A., & et al. (2008). The effects of temperature, volume fraction and vibration time on the thermo-physical properties of a carbon nanotube suspension (carbon nanofluid). *Nanotechnology*, 19(31), 315701.
- Asirvatham, L.G., Vishal, N., Gangatharan, S.K., & Lal, D.M. (2009). Experimental study on forced convective heat transfer with low volume fraction of CuO/water nanofluid. *Energies*, 2(1), 97-119.
- Assael, M.J., Metaxa, I.N., Arvanitidis, J., Christofilos, D., & Lioutas, C. (2005). Thermal conductivity enhancement in aqueous suspensions of carbon multi-walled and double-walled nanotubes in the presence of two different dispersants. *International Journal of Thermophysics*, 26(3), 647-664.
- Beck, M.P. (2008). *Thermal conductivity of metal oxide nanofluids*. (PhD), Georgia Institute of Technology, Georgia.
- Chandrasekar, M., & Suresh, S. (2009). A Review on the mechanisms of heat transport in nanofluids. *Heat Transfer Engineering*, 30(14), 1136-1150.
- Chandrasekar, M., Suresh, S., & Chandra Bose, A. (2010). Experimental investigations and theoretical determination of thermal conductivity and viscosity of Al_2O_3 /water nanofluid. *Experimental Thermal and Fluid Science*, 34(2), 210-216.
- Chang, H., Jwo, C., Fan, P., & Pai, S. (2007). Process optimization and material properties for nanofluid manufacturing. *The International Journal of Advanced Manufacturing Technology*, 34(3), 300-306.

Chang, H., Wu, Y.C., Chen, X.Q., & Kao, M.J. (2006). Fabrication of Cu based nanofluid with superior dispersion. [www.ntut.edu.tw. http://www.ntut.edu.tw/~wwwwoaa/download/phd/std/12/paper_01.pdf](http://www.ntut.edu.tw/~wwwwoaa/download/phd/std/12/paper_01.pdf)

Chen, H., Ding, Y., & Lapkin, A. (2009). Rheological behaviour of nanofluids containing tube / rod-like nanoparticles. *Powder Technology*, 194(1-2), 132-141.

Chen, H., Ding, Y., & Tan, C. (2007). Rheological behaviour of nanofluids. *New Journal of Physics*, 9, 367-361–367-324.

Chen, H., Yang, W., He, Y., Ding, Y., Zhang, L., Tan, C., . . . Bavykin, D.V. (2008). Heat transfer and flow behaviour of aqueous suspensions of titanate nanotubes (nanofluids). *Powder Technology*, 183(1), 63-72.

Chen, L., & Xie, H. (2010). Properties of carbon nanotube nanofluids stabilized by cationic gemini surfactant. *Thermochimica Acta*, 506, 62-66.

Choi, S.U.S., & Eastman, J.A. (1995). *Enhancing thermal conductivity of fluids with nanoparticles*. Paper presented at the Conference: 1995 International mechanical engineering congress and exhibition, San Francisco CA (United States), 12-17 Nov 1995, San Francisco. <http://www.osti.gov/energycitations/servlets/purl/196525-Xh0J02/webviewable/>

Chon, C.H., Kihm, K.D., Lee, S.P., & Choi, S.U.S. (2005). Empirical correlation finding the role of temperature and particle size for nanofluid (Al_2O_3) thermal conductivity enhancement. *Applied Physics Letters*, 87(15), 153107-153103.

Chou, J.-C., & Liao, L.P. (2005). Study on pH at the point of zero charge of TiO_2 pH ion-sensitive field effect transistor made by the sputtering method. *Thin Solid Films*, 476(1), 157-161.

Chung, S.J., Leonard, J.P., Nettleship, I., Lee, J.K., Soong, Y., Martello, D.V., & Chyu, M.K. (2009). Characterization of ZnO nanoparticle suspension in water: Effectiveness of ultrasonic dispersion. *Powder Technology*, 194(1-2), 75-80.

Das, K., Putra, N., Thiesen, P., & Roetzel, W. (2003). Temperature dependence of thermal conductivity enhancement for nanofluids. *Journal of Heat Transfer-Transactions of the ASME*, 125(4), 567-574.

Das, S.K., Choi, S.U.S., & Patel, H.E. (2006). Heat transfer in nanofluids; a review. *Heat Transfer Engineering*, 27(10), 3-19.

Das, S.K., Choi, S.U.S., Yu, W.H., & Pradeep, T. (2007). *Nanofluid: science and technology*. Hoboken, New Jersey, USA: John Wiley & Sons Inc.

Daungthongsuk, W., & Wongwises, S. (2007). A critical review of convective heat transfer of nanofluids. *Renewable and Sustainable Energy Reviews*, 11(5), 797-817.

Duangthongsuk, W., & Wongwises, S. (2008). Effect of thermophysical properties models on the predicting of the convective heat transfer coefficient for low concentration nanofluid. *International Communications in Heat and Mass Transfer*, 35(10), 1320-1326.

Duangthongsuk, W., & Wongwises, S. (2009). Measurement of temperature-dependent thermal conductivity and viscosity of TiO₂ - water nanofluids. *Experimental Thermal and Fluid Science*, 33(4), 706-714.

Duangthongsuk, W., & Wongwises, S. (2010a). Comparison of the effects of measured and computed thermophysical properties of nanofluids on heat transfer performance. *Experimental Thermal and Fluid Science*, 34(5), 616-624.

Eastman, J.A., Choi, U.S., S. Li, L.J.T., & Lee, S. (1996). *Enhanced thermal conductivity through the development of nanofluids*. Paper presented at the MRS Proceedings.

Eastman, J.A., Phillpot, S.R., Choi, S.U.S., & Keblinski, P. (2004). Thermal transport in nanofluids 1. *Annual Review of Materials Research*, 34(1), 219-246.

Evans, W., Prasher, R., Fish, J., Meakin, P., Phelan, P., & Keblinski, P. (2008). Effect of aggregation and interfacial thermal resistance on thermal conductivity of nanocomposites and colloidal nanofluids. *International Journal of Heat and Mass Transfer*, 51(5-6), 1431-1438.

Fovet, Y., Gal, J.-Y., & Toumelin-Chemla, F. (2001). Influence of pH and fluoride concentration on titanium passivating layer: stability of titanium dioxide. *Talanta*, 53(5), 1053-1063.

Gao, L., & Zhou, X.F. (2006). Differential effective medium theory for thermal conductivity in nanofluids. *Physics Letters A*, 348, 355-360.

Garg, P., Alvarado, J.L., Marsh, C., Carlson, T.A., Kessler, D.A., & Annamalai, K. (2009). An experimental study on the effect of ultrasonication on viscosity and heat transfer performance of multi-wall carbon nanotube-based aqueous nanofluids. *International Journal of Heat and Mass Transfer*, 52, 5090-5101.

Ghadimi, A., Saidur, R., & Metselaar, H.S.C. (2011). A review of nanofluid stability properties and characterization in stationary conditions. *International Journal of Heat and Mass Transfer*, 54(17-18), 4051-4068.

Ghafari, S., Aziz, H.A., Isa, M.H., & Zinatizadeh, A.A. (2009). Application of response surface methodology (RSM) to optimize coagulation “floculation treatment of leachate using poly-aluminum chloride (PAC) and alum. *Journal of Hazardous Materials*, 163(2-3), 650-656.

Gharagozloo, P., & Goodson, K.E. (2010). Characterization and modeling of thermal diffusion and aggregation in nanofluids (pp. 140). California: Sandia National Laboratories.

Gharagozloo, P.E., Eaton, J.K., & Goodson, K.E. (2008). Diffusion, aggregation, and the thermal conductivity of nanofluids. *Applied Physics Letters*, 93(10), 103110-103113.

Gharagozloo, P.E., & Goodson, K.E. (2010). Aggregate fractal dimensions and thermal conduction in nanofluids. *Journal of Applied Physics*, 108(7), 074309-074307.

Godson, L., Raja, B., Mohan Lal, D., & Wongwises, S. (2010). Enhancement of heat transfer using nanofluids--An overview. *Renewable and Sustainable Energy Reviews*, 14(2), 629-641.

Goldstein, R.J., Joseph, D.D., & Pui, D.H. (2000). Convective Heat Transport in Nanofluids. Faculty of Aerospace Engineering and Mechanics, University of Minnesota.

Habibzadeh, S., Khodadadi, A.A., Kazami, A., Hosseinpour, N., & Mortazavi, Y. (2010). Colloidal stability of nanofluids of tin oxide synthesized via microwave-induced combustion route.

Hadjov, K.B. (2009). Modified self-consistent scheme to predict the thermal conductivity of nanofluids. *International Journal of Thermal Sciences*, 48(12), 2249-2254.

Hamilton, R.L., & Crosser, O.K. (1962). Thermal conductivity of heterogeneous two-component systems. *Industrial & Engineering Chemistry Fundamentals*, 1(3), 187-191.

He, Y., Jin, Y., Chen, H., Ding, Y., Cang, D., & Lu, H. (2007). Heat transfer and flow behavior of aqueous suspensions of TiO₂ nanoparticles (nanofluids) flowing upward through a vertical pipe. *International Journal of Heat and Mass Transfer*, 50(11-12), 2272-2281.

Henderson, J.R., & van Swol, F. (1984). On the interface between a fluid and a planar wall. *Molecular Physics*, 51(4), 991-1010.

Hiemenz, P.C., & Dekker, M. (1986). *Principles of colloid and surface chemistry* (Second ed.). New York: Dekkar.

Hong, K.S., Hong, T.K., & Yang, H.S. (2006). Thermal conductivity of Fe nanofluids depending on the cluster size of nanoparticles. *Applied Physics Letters*, 88(3), 031901-031903.

Hong, S.W., Kang, Y.-T., Kleinstreuer, C., & Koo, J. (2011). Impact analysis of natural convection on thermal conductivity measurements of nanofluids using the transient hot-wire method. *International Journal of Heat and Mass Transfer*, 54(15–16), 3448-3456.

Hong, T.K., & Yang, H.S. (2005). Nanoparticle-dispersion-dependent thermal conductivity in nanofluids. *Journal of the korean physical society* 321-324.

Hunter, R.J. (2001). *Foundations of Colloid Science*. New York: Oxford University Press.

Hwang, K.S., Jang, S.P., & Choi, S.U.S. (2009). Flow and convective heat transfer characteristics of water-based Al₂O₃ nanofluids in fully developed laminar flow regime. *International Journal of Heat and Mass Transfer*, 52(1-2), 193-199.

Hwang, Y., Lee, J.-K., Lee, J.-K., Jeong, Y.-M., Cheong, S.-i., Ahn, Y.-C., & Kim, S.H. (2008). Production and dispersion stability of nanoparticles in nanofluids. *Powder Technology*, 186(2), 145-153.

Hwang, Y., Lee, J.K., Lee, C.H., Jung, Y.M., Cheong, S.I., Lee, C.G., . . . Jang, S.P. (2007). Stability and thermal conductivity characteristics of nanofluids. *Thermochimica Acta*, 455(1-2), 70-74.

Hwang, Y., Park, H.S., Lee, J.K., & Jung, W.H. (2006). Thermal conductivity and lubrication characteristics of nanofluids. *Current Applied Physics*, 6(s1), e67-e71.

Hwang, Y.J., Ahn, Y.C., Shin, H.S., Lee, C.G., Kim, G.T., Park, H.S., & Lee, J.K. (2006). Investigation on characteristics of thermal conductivity enhancement of nanofluids. *Current Applied Physics*, 6(6), 1068-1071.

Jeffrey, D.J. (1973). *Proceedings of the Royal Society A: Mathematical, Physical and Engineering Sciences* 355-367.

Jiang, L., Gao, L., & Sun, J. (2003). Production of aqueous colloidal dispersions of carbon nanotubes. *Journal of Colloid and Interface Science*, 260(1), 89-94.

Jin, H., Xianju, W., Qiong, L., Xueyi, W., Yunjin, Z., & Liming, L. (2009, 14-16 Aug. 2009). *Influence of pH on the stability characteristics of nanofluids*. Paper presented at the Photonics and Optoelectronics, 2009. SOPO 2009. Symposium on.

Kang, H.U., Kim, S.H., & Oh, J.M. (2006). Estimation of thermal conductivity of nanofluid using experimental effective particle volume. *Experimental Heat Transfer*, 19(3), 181 - 191.

Karthikeyan, N.R., Philip, J., & Raj, B. (2008). Effect of clustering on the thermal conductivity of nanofluids. *Materials Chemistry and Physics*, 109(1), 50-55.

Kebllinski, P., Eastman, J.A., & Cahill, D.G. (2005). Nanofluids for thermal transport. *Materials Today*, 8(6), 36-44.

Kebllinski, P., Phillpot, S.R., Choi, S.U.S., & Eastman, J.A. (2002). Mechanisms of heat flow in suspensions of nano-sized particles (nanofluids). *International Journal of Heat and Mass Transfer*, 45(4), 855-863.

Khajeh, M. (2011). Response surface modelling of lead pre-concentration from food samples by miniaturised homogenous liquid-liquid solvent extraction: Box-Behnken design. *Food Chemistry*, 129(4), 1832-1838.

Kim, H., & Kim, M. (2009). Experimental study of the characteristics and mechanism of pool boiling CHF enhancement using nanofluids. *Heat and Mass Transfer*, 45(7), 991-998.

Kim, S.H., Choi, S.R., & Kim, D. (2007). Thermal conductivity of metal-oxide nanofluids: particle size dependence and effect of laser irradiation. *Journal of Heat Transfer-Transactions of the ASME*, 129(3), 298-307.

Koo, J., & Kleinstreuer, C. (2005). Impact analysis of nanoparticle motion mechanisms on the thermal conductivity of nanofluids. *International Communications in Heat and Mass Transfer*, 32(9), 1111-1118.

Kreibig, U., & Genzel, L. (1985). Optical absorption of small metallic particles. *Surface Science*, 156(Part 2), 678-700.

Kreibig, U., & Vollmer, M. (1995). *Optical Properties of Metal Clusters*.

Kumar, R., & Milanova, D. (2009). Effect of surface tension on nanotube nanofluids. *Applied Physics Letters*, 94(7), 073107-073103.

Kwak, K., & Kim, C. (2005). Viscosity and thermal conductivity of copper oxide nanofluid dispersed in ethylene glycol. *Korea Australia Rheology Journal*, 17(2), 35-40.

Lee, D., Kim, J.-W., & Kim, B.G. (2006). A new parameter to control heat transport in nanofluids: surface charge state of the particle in suspension. *Journal of Physical Chemistry B*, 4323-4328.

Lee, J.-H., Hwang, K.S., Jang, S.P., Lee, B.H., Kim, J.H., Choi, S.U.S., & Choi, C.J. (2008a). Effective viscosities and thermal conductivities of aqueous nanofluids containing low volume concentrations of Al_2O_3 nanoparticles. *International Journal of Heat and Mass Transfer*, 51(11-12), 2651-2656.

Lee, J.H. (2009). *Convection performance of nanofluids for electronics cooling*. (Ph.D), Stanford University.

Lee, K., Hwang, Y., Cheong, S., Kwon, L., Kim, S., & Lee, J. (2009). Performance evaluation of nano-lubricants of fullerene nanoparticles in refrigeration mineral oil. *Current Applied Physics*, 9 (2, Supplement 1), e128-e131.

Lee, S., Choi, S.U.S., Li, S., & Eastman, J.A. (1999). Measuring thermal conductivity of fluids containing oxide nanoparticles. *Journal of Heat Transfer-Transactions of the ASME*, 121(2), 280-289.

Leong, K.Y., Saidur, R., Kazi, S.N., & Mamun, A.H. (2010). Performance investigation of an automotive car radiator operated with nanofluid-based coolants (nanofluid as a coolant in a radiator). *Applied Thermal Engineering*, 30 (17-18), 2685-2692.

Li, C.H., & Peterson, G.P. (2007). The effect of particle size on the effective thermal conductivity of water nanofluids. *Journal of Applied Physics*, 101(4), 044312-044312-044315.

Li, L., Zhang, Y., Ma, H., & Yang, M. (2008). An investigation of molecular layering at the liquid-solid interface in nanofluids by molecular dynamics simulation. *Physics Letters A*, 372(25), 4541-4544.

Li, X., Zhu, D., & Wang, X. (2007). Evaluation on dispersion behavior of the aqueous copper nano-suspensions. *Journal of Colloid and Interface Science*, 310(2), 456-463.

Li, X.F., Zhu, D.S., Wang, X.J., Gao, J.W., & Li, H. (2006). *Proceedings of the International Symposium on Biophotonics, Nanophotonics and Metamaterials*.

Li, X.F., Zhu, D.S., Wang, X.J., Wang, N., Gao, J.W., & Li, H. (2008). Thermal conductivity enhancement dependent pH and chemical surfactant for Cu-H₂O nanofluids. *Thermochimica Acta*, 469(1-2), 98-103.

Li, Y., Zhou, J.e., Tung, S., Schneider, E., & Xi, S. (2009). A review on development of nanofluid preparation and characterization. *Powder Technology*, 196(2), 89-101.

Lin, C.-Y., Wang, J.-C., & Chen, T.-C. (2011). Analysis of suspension and heat transfer characteristics of Al₂O₃ nanofluids prepared through ultrasonic vibration. *Applied Energy*, 88(12), 4527-4533.

Link, S., & El-Sayed, M.A. (2003). Optical properties and ultrafast dynamics of metallic nanocrystals. *Annual Review of Physical Chemistry*, 54(1), 331-366.

Liu, H.L., Lan, Y.W., & Cheng, Y.C. (2004). Optimal production of sulphuric acid by *Thiobacillus thiooxidans* using response surface methodology. *Process Biochemistry*, 39(12), 1953-1961.

Liu, M.S., Lin, M.C.C., Tsai, C.Y., & Wang, C.C. (2006). Enhancement of thermal conductivity with Cu for nanofluids using chemical reduction method. *International Journal of Heat and Mass Transfer*, 49(17-18), 3028-3033.

Liu, S., McDonald, T., & Wang, Y. (2010). Producing biodiesel from high free fatty acids waste cooking oil assisted by radio frequency heating. *Fuel*, 89(10), 2735-2740.

Liu, Z.-Q., Ma, J., & Cui, Y.-H. (2008). Carbon nanotube supported platinum catalysts for the ozonation of oxalic acid in aqueous solutions. *Carbon*, 46(6), 890-897.

LotfizadehDehkordi, B., Ghadimi, A., & Metselaar, H.C. (2013). Box–Behnken experimental design for investigation of stability and thermal conductivity of TiO₂ nanofluids. *Journal of Nanoparticle Research*, 15(1), 1-9.

Low, K.L., Tan, S.H., Zein, S.H.S., McPhail, D.S., & Boccaccini, A.R. (2011). Optimization of the mechanical properties of calcium phosphate/multi-walled carbon nanotubes/bovine serum albumin composites using response surface methodology. *Material design*, 32(6), 3312-3319.

Madni, I., Hwang, C.-Y., Park, S.-D., Choa, Y.-H., & Kim, H.-T. (2010). Mixed surfactant system for stable suspension of multiwalled carbon nanotubes. *Colloids and Surfaces A: Physicochemical and Engineering Aspects*, 358, 101-107.

Masuda, H., Ebata, A., Teramae, K., & Hishinuma, N. (1993). Alteration of thermal conductivity and viscosity of liquid by dispersing ultra-fine particles (dispersion of Al_2O_3 , SiO_2 and TiO_2 ultra-fine particles). *Netsu Bussei (Japan)*, 7, 227–233.

Maxwell, C., & Thompson, J.R. (1904). *A treatise on electricity and magnetism* (Vol. 1). Oxford: Clarendon Press.

Meibodi, M.E., Vafaie-Sefti, M., Rashidi, A.M., Amrollahi, A., Tabasi, M., & Kalal, H.S. (2010a). The role of different parameters on the stability and thermal conductivity of carbon nanotube/water nanofluids. *International Communications in Heat and Mass Transfer*, 37(3), 319-323.

Meibodi, M.E., Vafaie-Sefti, M., Rashidi, A.M., Amrollahi, A., Tabasi, M., & Kalal, H.S. (2010b). Simple model for thermal conductivity of nanofluids using resistance model approach. *International Communication Heat and Mass Transfer*, In Press, *Uncorrected Proof*.

Mintsa, H.A., Roy, G., Nguyen, C.T., & Doucet, D. (2009). New temperature dependent thermal conductivity data for water-based nanofluids. *International Journal of Thermal Sciences*, 48(2), 363-371.

Moosavi, M., Goharshadi, E.K., & Youssefi, A. (2010). Fabrication, characterization, and measurement of some physicochemical properties of ZnO nanofluids. *International Journal of Heat and Fluid Flow*, 31(4), 599-605.

Munson, B.R., Young, D.F., & Okiishi, T.H. (1998). *Fundamentals of Fluid Mechanics*: John Wiley & Sons Inc.

Murshed, S.M.S., Leong, K.C., & Yang, C. (2005). Enhanced thermal conductivity of TiO_2 - water based nanofluids. *International Journal of Thermal Sciences*, 44(4), 367-373.

Murshed, S.M.S., Leong, K.C., & Yang, C. (2008). Investigations of thermal conductivity and viscosity of nanofluids. *International Journal of Thermal Sciences*, 47, 560-568.

Murshed, S.M.S., Leong, K.C., & Yang, C. (2008). Thermophysical and electrokinetic properties of nanofluids – A critical review. *Applied Thermal Engineering* 28, 2109–2125.

Namburu, P.K., Kulkarni, D.P., Misra, D., & Das, D.K. (2007). Viscosity of copper oxide nanoparticles dispersed in ethylene glycol and water mixture. *Experimental Thermal and Fluid Science*, 32(2), 397-402.

Naphon, P., Thongkum, D., & Assadamongkol, P. (2009). Heat pipe efficiency enhancement with refrigerant-nanoparticles mixtures. *Energy Conversion and Management*, 50(3), 772-776.

Nasiri, A., Shariaty-Niasar, M., Rashidi, A., Amrollahi, A., & Khodafarin, R. (2011). Effect of dispersion method on thermal conductivity and stability of nanofluid. *Experimental Thermal and Fluid Science*, 35(4), 717-723.

Nguyen, C.T., Desgranges, F., Galanis, N., Roy, G., Maré, T., Boucher, S., & Angue Mintsas, H. (2008). Viscosity data for Al₂O₃-water nanofluid -hysteresis: is heat transfer enhancement using nanofluids reliable? *International Journal of Thermal Sciences*, 47(2), 103-111.

Nguyen, C.T., Desgranges, F., Roy, G., Galanis, N., Maré, T., Boucher, S., & Angue Mintsas, H. (2007). Temperature and particle-size dependent viscosity data for water-based nanofluids - Hysteresis phenomenon. *International Journal of Heat and Fluid Flow*, 28(6), 1492-1506.

Nield, D.A., & Kuznetsov, A.V. (2010). The onset of double-diffusive convection in a nanofluid layer. *International Journal of Heat and Fluid Flow*, 32(4), 771-776.

Nosrati, S., Jayakumar, N.S., & Hashim, M.A. (2011a). Extraction performance of chromium (VI) with emulsion liquid membrane by Cyanex 923 as carrier using response surface methodology. *Desalination*, 266(1-3), 286-290.

Nosrati, S., Jayakumar, N.S., & Hashim, M.A. (2011b). Performance evaluation of supported ionic liquid membrane for removal of phenol. *Journal of Hazardous Materials*, 192(3), 1283-1290.

Oh, D.-W., Jain, A., Eaton, J.K., Goodson, K.E., & Lee, J.S. (2006). *Thermal conductivity measurement of aluminum oxide nanofluids using the 3-omega method*. Paper presented at the ASME Conference Proceedings.

Oh, D.-W., Jain, A., Eaton, J.K., Goodson, K.E., & Lee, J.S. (2008). Thermal conductivity measurement and sedimentation detection of aluminum oxide nanofluids by using the 3omega method. *International Journal of Heat and Fluid Flow*, 29(5), 1456-1461.

Ozerinc, S., Yaz, x, oğlu, A., la, G., & Kakac, S. (2010). Convective heat transfer enhancement with nanofluids: the effect of temperature-variable thermal conductivity. *ASME Conference Proceedings*, 2010(49163), 719-731.

Pak, B.C., & Cho, Y.I. (1998). Hydrodynamic and heat transfer study of dispersed fluids with submicron metallic oxide particles. *Experimental Heat Transfer*, 11(2), 151 - 170.

Pantzali, M.N., Kanaris, A.G., Antoniadis, K.D., Mouza, A.A., & Paras, S.V. (2009). Effect of nanofluids on the performance of a miniature plate heat exchanger with modulated surface. *International Journal of Heat and Fluid Flow*, 30(4), 691-699.

Pantzali, M.N., Mouza, A.A., & Paras, S.V. (2009). Investigating the efficacy of nanofluids as coolants in plate heat exchangers (PHE). *Chemical Engineering Science*, 64(14), 3290-3300.

Patel, H., Sundararajan, T., Pradeep, T., Dasgupta, A., Dasgupta, N., & Das, S. (2005). A micro-convection model for thermal conductivity of nanofluids. *Pramana*, 65(5), 863-869.

Paul, G., Chopkar, M., Manna, I., & Das, P.K. (2010). Techniques for measuring the thermal conductivity of nanofluids: A review. *Renewable and Sustainable Energy Reviews*, 14(7), 1913-1924.

Peng, H., Ding, G., & Hu, H. (2011). Effect of surfactant additives on nucleate pool boiling heat transfer of refrigerant-based nanofluid. *Experimental Thermal and Fluid Science*, 35(6), 960-970.

Penkavova, V., Tihon, J., & Wein, O. (2011b). Stability and rheology of dilute TiO₂ - water nanofluids. *Nanoscale Research Letters*, 6(1), 1-7.

Peterson, G.P., & Li, C.H. (2006). Heat and mass transfer in fluids with nanoparticle. *Adv. Heat Transfer suspensions*, 39, 257-376.

Philip, J., Shima, P.D., & Raj, B. (2007). Enhancement of thermal conductivity in magnetite based nanofluid due to chainlike structures. *Applied Physics Letters*, 91(20), 203108-203103.

Prasher, R., Phelan, P.E., & Bhattacharya, P. (2006). Effect of aggregation kinetics on the thermal conductivity of nanoscale colloidal solutions (nanofluid). *Nano Letters*, 6(7), 1529-1534.

Prasher, R., Song, D., Wang, J., & Phelan P.E. (2006). Measurements of nanofluid viscosity and its implications for thermal applications. *Applied Physics Letters*, 89.

Quaresma, J.o.N.N., Macedo, E.N., da Fonseca, H.M., Orlande, H.R.B., & Cotta, R.M. (2010). An analysis of heat conduction models for nanofluids. *Heat Transfer Engineering*, 31(14), 1125-1136.

Russel, W.B., Saville, D.A., & Schowaltes, W.R. (1989). *Colloidal Dispersion*. Cambridge, U.K.: Cambridge University Press.

Sastry, N.N.V., Bhunia, A., Sundararajan, T., & Das, S.K. (2008). *Nanotechnology*, 19, 055704.

Sato, M., Abe, Y., Urita, Y., Di Paola, R., Cecere, A., & Savino, R. (2009). *Thermal performance of self-rewetting fluid heat pipe containing dilute solutions of polymer-capped silver nanoparticles synthesized by microwave- polyol process* Paper presented at the Proceedings of ITP2009.

Sen, R., & Swaminathan, T. (2004). Response surface modeling and optimization to elucidate and analyze the effects of inoculum age and size on surfactin production. *Biochemical Engineering Journal*, 21(2), 141-148.

Sommers, A., & Yerkes, K. (2009). Experimental investigation into the convective heat transfer and system-level effects of Al₂O₃–propanol nanofluid, . *Journal of Nanoparticle Research*, 12 (3), 1003-1014.

Stat-Ease, I. (2009). Design-Expert (Version v8.0 CD-11102009).

Swanson, E.J., Tavares, J., & Coulombe, S. (2008). Improved dual-plasma process for the synthesis of coated or functionalized metal nanoparticles. *Plasma Science, IEEE Transactions on*, 36(4), 886-887.

Tavman, S., & Tavman, I.H. (1998). Measurement of effective thermal conductivity of wheat as a function of moisture content. *International Communications in Heat and Mass Transfer*, 25(5), 733-741.

Tillman, P., & Hill, J.M. (2007). Determination of nanolayer thickness for a nanofluid. *International Communications in Heat and Mass Transfer*, 34(4), 399-407.

Timofeeva, E.V., Gavrilov, A.N., McCloskey, J.M., Tolmachev, Y.V., Sprunt, S., Lopatina, L.M., & Selinger, J.V. (2007). Thermal conductivity and particle agglomeration in alumina nanofluids: Experiment and theory. *Physical Review E*, 76(6), 061203.

Trisaksri, V., & Wongwises, S. (2007). Critical review of heat transfer characteristics of the nanofluids. *Renewable and Sustainable Energy Reviews*, 11 512-523.

Truong, B., Hu, L.-w., Buongiorno, J., & McKrell, T. (2010). Modification of sandblasted plate heaters using nanofluids to enhance pool boiling critical heat flux. *International Journal of Heat and Mass Transfer*, 53(1-3), 85-94.

Tsai, C.Y., Chien, H.T., Ding, P.P., Chan, B., Luh, T.Y., & Chen, P.H. (2004). Effect of structural character of gold nanoparticles in nanofluid on heat pipe thermal performance. *Materials Letters*, 58(9), 1461-1465.

Turgut, A., Tavman, I., Chirtoc, M., Schuchmann, H., Sauter, C., & Tavman, S. (2009). Thermal conductivity and viscosity measurements of water-based TiO₂ nanofluids. *International Journal of Thermophysics*, 30(4), 1213-1226.

Vadasz, P. (2006). Heat conduction in nanofluid suspensions. *Journal of Heat Transfer-Transactions of the ASME*, 128(5), 465-477.

Vadász, P. (2008). Nanofluid suspensions and bi-composite media as derivatives of interface heat transfer modeling in porous media *Emerging Topics in Heat and Mass Transfer in Porous Media* (pp. 283-326).

Vajjha, R.S., & Das, D.K. (2009). Experimental determination of thermal conductivity of three nanofluids and development of new correlations. *International Journal of Heat and Mass Transfer*, 52(21-22), 4675-4682.

Vandsburger, L. (2009). *Synthesis and covalent surface modification of carbon nanotubes for preparation of stabilized nanofluid suspensions*. (Master), McGill University, Montreal, Quebec, Canada.

Wang, B.-X., Zhou, L.-P., & Peng, X.-F. (2003). A fractal model for predicting the effective thermal conductivity of liquid with suspension of nanoparticles. *International Journal of Heat and Mass Transfer*, 46(14), 2665-2672.

Wang, H., & Sen, M. (2008). Analysis of 3 omega method for thermal conductivity measurement: University of Notre Dame.

Wang, X.-J., & Li, X.-F. (2009). Influence of pH on nanofluids' viscosity and thermal conductivity. *Chemical Physics Letters*, 26(5), 056601.

Wang, X.-j., Zhu, D.-s., & yang, S. (2009). Investigation of pH and SDBS on enhancement of thermal conductivity in nanofluids. *Chemical Physics Letters*, 470(1-3), 107-111.

Wang, X.-Q., & Mujumdar, A.S. (2007). Heat transfer characteristics of nanofluids: a review. *International Journal of Thermal Sciences*, 46(1), 1-19.

Wang, X., Xu, X., & Choi, S.U.S. (1999). Thermal conductivity of nanoparticles–fluid mixture,. *Journal of Thermophys and Heat Transfer*, 4, 474–480.

Weber, H.F. (1880). *Wiedermann's Annual Physical Chemistry*., 10, 103.

Wei, X., Kong, T., Zhu, H., & Wang, L. (2010). CuS/Cu₂S nanofluids: Synthesis and thermal conductivity. *International Journal of Heat and Mass Transfer*, 53(9-10), 1841-1843.

Wei, X., Zhu, H., Kong, T., & Wang, L. (2009). Synthesis and thermal conductivity of Cu₂O nanofluids. *International Journal of Heat and Mass Transfer*, 52(19-20), 4371-4374.

Wen, D., & Ding, Y. (2004). Experimental investigation into convective heat transfer of nanofluids at the entrance region under laminar flow conditions. *International Journal of Heat and Mass Transfer*, 47(24), 5181-5188.

Wen, D., & Ding, Y. (2005). Formulation of nanofluids for natural convective heat transfer applications. *International Journal of Heat and Fluid Flow*, 26(6), 855-864.

Wen, D., Lin, G., Vafaei, S., & Zhang, K. (2009). Review of nanofluids for heat transfer applications. *Particuology*, 7(2), 141-150.

Wu, D., Zhu, H., Wang, L., & Liua, L. (2009). Critical issues in nanofluids preparation, characterization and thermal conductivity. *Current Nanoscience*, 5, 103-112.

Xie, H., Chen, L., & Wu, Q. (2008). Measurements of the viscosity of suspensions (nanofluids) containing nanosized Al₂O₃ particles. *High Temperature-High Pressure*, 37, 127–135.

Xie, H., Fujii, M., & Zhang, X. (2005). Effect of interfacial nanolayer on the effective thermal conductivity of nanoparticle-fluid mixture. *International Journal of Heat and Mass Transfer*, 48(14), 2926-2932.

Xie, H., Lee, H., Youn, W., & Choi, M. (2003). Nanofluids containing multiwalled carbon nanotubes and their enhanced thermal conductivities. *Journal of Applied Physics*, 94(8), 4967-4971.

Xuan, Y., Li, Q., & Hu, W. (2003). Aggregation structure and thermal conductivity of nanofluids. *AIChE Journal*, 49(4), 1038-1043.

Xue, Q., & Xu, W.-M. (2005). A model of thermal conductivity of nanofluids with interfacial shells. *Materials Chemistry and Physics*, 90(2-3), 298-301.

Yajie, R., & et al. (2005). Effective thermal conductivity of nanofluids containing spherical nanoparticles. *Journal of Physics D: Applied Physics*, 38(21), 3958.

Yeganeh, M., Shahtahmasebi, N., Kompany, A., Goharshadi, E.K., Youssefi, A., & Siller, L. (2010). Volume fraction and temperature variations of the effective thermal conductivity of nanodiamond fluids in deionized water. *International Journal of Heat and Mass Transfer*, 53(15-16), 3186-3192.

Yetilmezsoy, K., Demirel, S., & Vanderbei, R.J. (2009). Response surface modeling of Pb(II) removal from aqueous solution by Pistacia vera L.: Box–Behnken experimental design. *Journal of Hazardous Materials*, 171(1–3), 551-562.

Yoo, D.-H., Hong, K.S., & Yang, H.-S. (2007). Study of thermal conductivity of nanofluids for the application of heat transfer fluids. *Thermochimica Acta*, 455(1-2), 66-69.

Yu, W., & Choi, S.U.S. (2003). The role of interfacial layers in the enhanced thermal conductivity of nanofluids: A renovated Maxwell model. *Journal of Nanoparticle Research* 5, 167–171.

Yu, W., Xie, H., Chen, L., & Li, Y. (2009). Investigation of thermal conductivity and viscosity of ethylene glycol based ZnO nanofluid. *Thermochimica Acta*, 491(1-2), 92-96.

Yu, W., Xie, H., Chen, L., & Li, Y. (2010). Enhancement of thermal conductivity of kerosene-based Fe₃O₄ nanofluids prepared via phase-transfer method. *Colloids and Surfaces A: Physicochemical and Engineering Aspects*, 355(1-3), 109-113.

Zabeti, M., Daud, W.M.A.W., & Aroua, M.K. (2009). Optimization of the activity of CaO/Al₂O₃ catalyst for biodiesel production using response surface methodology. *Applied Catalysis A: General*, 366(1), 154-159.

Zhang, X., Gu, H., & Fujii, M. (2006). Experimental study on the effective thermal conductivity and thermal diffusivity of nanofluids. *International Journal of Thermophysics*, 27(2), 569-580.

Zhang, X., Gu, H., & Fujii, M. (2007). Effective thermal conductivity and thermal diffusivity of nanofluids containing spherical and cylindrical nanoparticles. *Experimental Thermal and Fluid Science*, 31(6), 593-599.

Zhou, X.F., & Gao, L. (2006). Effective thermal conductivity in nanofluids of nonspherical particles with interfacial thermal resistance: Differential effective medium theory. *Journal of Applied Physics*, 100(2), 024913-024916.

Zhu, D., Li, X., Wang, N., Wang, X., Gao, J., & Li, H. (2009). Dispersion behavior and thermal conductivity characteristics of $\text{Al}_2\text{O}_3\text{-H}_2\text{O}$ nanofluids. *Current Applied Physics*, 9(1), 131-139.

Zhu, H., Zhang, C., Liu, S., Tang, Y., & Yin, Y. (2006). Effects of nanoparticle clustering and alignment on thermal conductivities of Fe_3O_4 aqueous nanofluids. *Applied Physics Letters*, 89(2).

Zhu, H., Zhang, C., Tang, Y., Wang, J., Ren, B., & Yin, Y. (2007). Preparation and thermal conductivity of suspensions of graphite nanoparticles. *Letters to the Editor*, 45, 203–228.